

**ASSESSING CYTOTOXIC T LYMPHOCYTE RESPONSE DURING SIMIAN
IMMUNODEFICIENCY VIRUS INFECTION IN RHESUS MACAQUES**

by

Benjamin Bruno Policichio

B.S., University of Pittsburgh at Johnstown, 2012

Submitted to the Graduate Faculty of
the Department of Infectious Diseases and Microbiology
Graduate School of Public Health in partial fulfillment
of the requirements for the degree of
Doctor of Philosophy

University of Pittsburgh

2017

UNIVERSITY OF PITTSBURGH
GRADUATE SCHOOL OF PUBLIC HEALTH

This dissertation was presented

by

Benjamin Bruno Policicchio

It was defended on

December 07, 2017

and approved by

Charles R. Rinaldo, Jr., Ph.D.

Professor

Department of Infectious Diseases and Microbiology,
Graduate School of Public Health, University of Pittsburgh

Velpandi Ayyavoo, Ph.D.

Professor

Department of Infectious Diseases and Microbiology,
Graduate School of Public Health, University of Pittsburgh

Bernard J.C. Macatangay, M.D.

Assistant Professor

Department of Medicine
School of Medicine, University of Pittsburgh

Cristian Apetrei, M.D., Ph.D.

Professor

Department of Microbiology and Molecular Genetics
School of Medicine, University of Pittsburgh

Ruy M. Ribeiro, Ph.D.

Professor

Laboratório de Biomatemática
Faculdade de Medicina, Universidade de Lisboa, Lisbon, Portugal

Dissertation Advisor: Ivona V. Pandrea, M.D., Ph.D.

Professor

Department of Pathology
School of Medicine, University of Pittsburgh

Copyright © by Benjamin Bruno Policchio

2017

**ASSESSING CYTOTOXIC T LYMPHOCYTE RESPONSE DURING SIMIAN
IMMUNODEFICIENCY VIRUS INFECTION IN RHESUS MACAQUES**

Benjamin Policicchio, Ph.D.

University of Pittsburgh, 2017

ABSTRACT

The host immune response against human immunodeficiency virus (HIV) infection is multifaceted, with the cytotoxic T lymphocyte (CTL) response playing a significant role in controlling the virus. However, it is uncertain what mechanism(s) these CTLs utilize to suppress virus replication. Previous research utilizing mathematical modeling and nucleoside reverse transcriptase inhibitors (NRTIs) showed that CTLs most likely have a non-cytolytic effect against infected cells, but these data are not universally accepted in the field. I **hypothesized** that CTLs exert the majority of their cytolytic function against infected cells containing virus that has yet to be integrated, due to minimal viral cytopathic effects at this stage. To test this hypothesis, I modeled the impact of CD8⁺ T cells through experimental CD8⁺ cell depletion on the pre- and post-integration stages of simian immunodeficiency virus (SIV) infection on both plasma viral load and 2-LTR circles. Model predictions were tested in the pathogenic SIVmac251-infected rhesus macaques (RMs) receiving the integrase inhibitor raltegravir (RAL) monotherapy with or without CD8⁺ T cells. CD8⁺ T cell depletion was profound and lasted throughout RAL therapy, with administration resulting in an immediate and sustained suppression of CD8⁺ cells. CD4⁺ cells recovered slightly during RAL treatment. The estimated efficacy of RAL in preventing integration was 97%. We next calculated the loss rate of infected cells prior to integration and determined that this loss rate was reduced by 82% in the CD8⁺ cell depletion with RAL treatment group compared to the RAL monotherapy group, but also that viral production increased 2.5 times in the absence of CD8⁺ cells. Further, we observed that CD8⁺ cell depletion

by itself increases 2-LTR circles, RAL monotherapy does not affect 2-LTR circle levels, and combination treatment increases 2-LTR circle levels faster than CD8 depletion alone. Upon fitting an extended viral dynamics model to the 2-LTR data, we conclude that the data best matches the hypothesis that CD8⁺ cells exert a killing effect on infected cells prior to integration, supporting our hypothesis. We attempted to analyze the effects of RAL intensification on 2-LTR circle dynamics, but we were unable to due to the development of resistance mutations, reinforcing the fact that in suboptimally ART-treated RMs, mutations do, indeed, occur, resulting in viral rebound during treatment. The public health significance of this dissertation is that by showing CD8⁺ cells kill cells containing virus prior to integration, we are aiding in the hunt for an elusive vaccine and/or cure against HIV.

TABLE OF CONTENTS

PREFACE.....	XIII
1.0 INTRODUCTION.....	1
1.1 THE HIV/AIDS PANDEMIC.....	1
1.2 SIV NONHUMAN PRIMATE MODEL OF HIV	2
1.3 HIV/SIV INFECTION AND ART	4
1.3.1 Replication cycle, virus dissemination and disease progression.....	4
1.3.2 ART and virus suppression	7
1.3.3 Viral decay under ART.....	8
1.3.4 Development and impact of 2-LTR circles.....	10
1.4 CELLULAR IMMUNE RESPONSES TO HIV/SIV	11
1.4.1 Roles of cytotoxic cells during infection	12
1.4.2 Noncytotoxic effects of cytotoxic cells.....	14
1.5 HIV/SIV RESISTANCE TO ART	16
1.5.1 Establishment of resistance.....	17
1.5.2 Known resistance mutations.....	18
2.0 HYPOTHESIS AND SPECIFIC AIMS.....	22

3.0	CHAPTER ONE: CD8⁺ T-CELL DEPLETION LEADS TO A DIFFERENT PROFILE OF SIV VIRAL DECAY UNDER INTEGRASE INHIBITOR MONOTHERAPY	24
3.1	PREFACE	25
3.2	ABSTRACT.....	26
3.3	INTRODUCTION	27
3.4	MATERIALS AND METHODS	29
3.4.1	Ethics statement.....	29
3.4.2	Animals, infections, and treatments.....	30
3.4.3	Sample and sample processing	30
3.4.4	Plasma viral load (pVL) quantification	31
3.4.5	Flow cytometry	31
3.4.6	Mathematical modeling.....	31
3.4.7	Data Fitting	32
3.5	RESULTS	34
3.5.1	M-T807R1 effectively depletes CD8⁺ cells from blood and induces an increase in pVL.....	34
3.5.2	RAL monotherapy in CD8⁺ cell-depleted macaques results in a small decline in pVL.....	37
3.5.3	RAL monotherapy induces peripheral CD4⁺ T- cell recovery and a strong decline in pVL.....	39
3.5.4	Modeling indicates that CD8⁺ cells exert an effect in removing cells before integration and in reducing viral production from infected cells.....	41

3.6	DISCUSSION.....	42
4.0	CHAPTER TWO: THE DYNAMICS OF SIV 2-LTR CIRCLES IN SIV- INFECTED RHESUS MACAQUES.....	50
4.1	PREFACE	51
4.2	ABSTRACT.....	52
4.3	INTRODUCTION	53
4.4	MATERIALS AND METHODS	55
4.4.1	Ethics statement.....	55
4.4.2	Animals, infections and treatments.....	55
4.4.3	Sampling and sample processing.....	56
4.4.4	Plasma viral load quantification	56
4.4.5	Flow cytometry	57
4.4.6	2-LTR circle extraction and quantification.....	57
4.4.7	Statistics.....	59
4.4.8	Modeling 2-LTR dynamics	59
4.5	RESULTS	61
4.5.1	CD8 ⁺ cell depletion increases the levels of pVL and of the 2-LTR circles in the periphery but it has minimal impact on 2-LTR levels in the LNs.....	61
4.5.2	RAL monotherapy decreases pVL but does not impact the 2-LTR circles	62
4.5.3	Combined RAL monotherapy and CD8 ⁺ cell depletion results in a slight decline of plasma VLs associated with a sustained increase in 2-LTR circles	62

4.5.4	What effector mechanism of CD8 ⁺ cells is responsible for the observed 2-LTR dynamics?	65
4.6	DISCUSSION.....	68
5.0	CHAPTER THREE: EMERGENCE OF RESISTANCE MUTATIONS IN SIMIAN IMMUNODEFICIENCY VIRUS (SIV)-INFECTED RHESUS MACAQUES RECEIVING NON-SUPPRESSIVE ANTIRETROVIRAL THERAPY (ART)	71
5.1	PREFACE	72
5.2	ABSTRACT.....	73
5.3	INTRODUCTION	74
5.4	MATERIALS AND METHODS	74
5.4.1	Ethics Statement	74
5.4.2	Animals, infections and treatments.....	75
5.4.3	Sample and sample processing	75
5.4.4	Plasma viral load quantification	76
5.4.5	Flow cytometry	76
5.4.6	Assessment of the occurrence of resistance mutations.....	76
5.5	RESULTS AND DISCUSSION	77
6.0	OVERALL DISCUSSION	81
7.0	PUBLIC HEALTH SIGNIFICANCE	86
	APPENDIX A: ABBREVIATIONS	88
	APPENDIX B: PUBLICATIONS	92
	BIBLIOGRAPHY	108

LIST OF TABLES

Table 1. Model estimates obtained from fitting the viral dynamics model to the data.....	47
--	----

LIST OF FIGURES

Figure 1. Decay dynamics of plasma HIV-1 RNA during ART.....	9
Figure 2. The effects of CD8 ⁺ cell depletion of CD4/CD8 dynamics and proliferation.	35
Figure 3. The effects of CD8 ⁺ cell depletion in the presence and absence of RAL on peripheral NK cells.	36
Figure 4. The effects of CD8 cell depletion in the presence and absence of RAL on pVL.....	37
Figure 5. The effects of CD8 ⁺ cell depletion and RAL treatment on CD4/CD8 dynamics and proliferation.....	38
Figure 6. The effects of RAL monotherapy on CD4/CD8 dynamics and proliferation.	40
Figure 7. Virus dynamics when CD8 ⁺ cells affect death rate of infected cells prior to integration and virus production rate.	43
Figure 8. Model fit of individual macaque pVL data in the CD8 ⁺ cell depletion group.	44
Figure 9. Model fit of individual macaque pVL data in the CD8 ⁺ cell depletion and RAL treatment group.	45
Figure 10. Model fit of individual macaque pVL data in the RAL monotherapy group.....	46
Figure 11. Effects of CD8 ⁺ cell depletion alone.	63
Figure 12 Effects of CD8 depletion with or without RAL monotherapy on 2-LTR circles in blood and LNs.	64
Figure 13. Effects of RAL monotherapy alone.....	66

Figure 14. Effects of CD8⁺ cell depletion and RAL monotherapy..... 67

Figure 15. CD8⁺ cells affect death rate of infected cells prior to integration. 69

Figure 16. Administration of nonsuppressive ART to two SIVmac251-infected rhesus macaques resulted in development of resistance mutations and treatment failure..... 79

PREFACE

I would like to thank my committee members, Dr. Charles Rinaldo, Dr. Velpandi Ayyavoo, Dr. Bernard Macatangay, Dr. Cristian Apetrei and Dr. Ruy Ribeiro. I appreciate your willingness to serve on my committee, your insightful guidance and your help in keeping my dissertation on track. I would further like to thank my dissertation advisor, Dr. Ivona Pandrea, for providing me with the priceless opportunities I have had during my time as a Ph.D. candidate, they have been instrumental in shaping who I am currently and who I will become in the future. I would also like to thank all those members of the Pandrea lab, both past and present, who have helped me through this process. Your friendship has been invaluable to me and I will never forget you. I would like to thank God for providing me with such a blessing as this. Most importantly, I thank my wife, Shauna, and my family for providing me with endless love, patience and support throughout all steps of this program. Thank you all.

1.0 INTRODUCTION

1.1 THE HIV/AIDS PANDEMIC

Human immunodeficiency virus 1 (HIV) remains the most important modern pandemic, with an estimated 36.7 million infected people worldwide (1.8 million of which are children), an average 2.1 million new infections annually [down from 3.1 million in 2001 (1)] and 1.1 million HIV/acquired immunodeficiency syndrome (AIDS)-related deaths occurring during 2015 (2). HIV is transmitted through several routes, including: direct blood-to-blood via syringe or needle sharing, sexual intercourse (both horizontal transmissions), and mother-to-infant transmission (vertical transmission) that occurs during both pregnancy and breastfeeding (3). Without treatment, the average survival time of the HIV-infected patient ranges between 9 to 11 years (4), with variations represented by either rapid AIDS progressors or long-term nonprogressors and elite controllers, in which infection may progress to AIDS in less than 2 years or more than 20 years, respectively. With the advent of antiretroviral (ARV) therapy (ART), the lifespan of the infected individuals increases to 59 years, resulting in a nearly normal lifespan of the HIV-infected subjects on ART (5). ART has improved in recent years, with optimal treatment resulting in complete or near complete suppression of circulating virus. Unfortunately, treatment must be maintained indefinitely to maintain virus suppression, with ART interruption resulting in rebound of virus (6). This is attributed to the fact that HIV integrates into the host genome and persists there indefinitely. As such, neither a cure nor a vaccine for HIV exists, furthering the financial and health strains already associated with long-term ART treatment. As such, it is imperative to further understand the host immune responses against HIV to aid in these research endeavors. Cytotoxic T lymphocytes (CTLs) are associated with control of the virus at multiple

points post-infection and in different disease models (7), suggesting that CTLs may be necessary for developing a way to combat HIV.

1.2 SIV NONHUMAN PRIMATE MODEL OF HIV

HIV is the etiologic agent of AIDS and is a single-stranded positive sense RNA virus belonging to the *Retroviridae* family, which preferentially infects CD4⁺ T cells, macrophages and dendritic cells (8-10). Upon infection of a susceptible cell, HIV reverse transcribes its RNA into linear complementary DNA, followed by integration into the host cells' genome and utilization of the host cellular machinery to produce progeny virus (11, 12). A vast amount of data collected about HIV has come from the use of the simian immunodeficiency virus (SIV)-infected nonhuman primate (NHP) model of HIV research. HIV and SIV are closely related lentiviruses that cause AIDS in humans and macaques, respectively (13-15). The SIV/NHP model is the most widely used animal model for AIDS research as the infection of different NHP species with different SIV strains results in a variety of disease states like those observed in HIV-infected humans. In particular, SIV infection of multiple macaque species typically results in a persistent pathogenic infection, culminating in progression to AIDS in a similar fashion as HIV (16). Further, NHPs allow both the active manipulation of treatments and the collection of large volumes of samples and invasive tissues that otherwise cannot ethically be performed in humans. As such, the use of NHPs help define key paradigms of HIV infection pathogenesis and are essential for studies targeting a cure or a vaccine for HIV (17).

Of the wide variety of macaque species present, three species are most commonly used in HIV-1 research: rhesus macaque (*Macaca mulatta*), pigtailed macaque (*Macaca nemestrina*) and cynomolgus macaque (*Macaca fascicularis*). Infection of these species with different SIV strains and HIV/SIV chimeras results in different disease states useful for a variety of studies (18, 19).

Of the three species, the rhesus macaque (RM), particularly of Indian origin, is the best characterized and most commonly used.

The Indian origin RM infected with either the reference swarm SIVmac251 or the infectious molecular clone SIVmac239 represents the most common SIV NHP model, accurately reproducing several aspects of HIV infections, including sustained, high viral loads (VLs), immediate and progressive depletion of mucosal CD4⁺ T cells, and chronic immune activation (20, 21). SIVmac251 infection can have several disease outcomes, depending on the immune genotype of the individual macaques and the route of viral inoculation, ranging from AIDS progression in a few months to natural control of virus replication (22, 23).

Another model, useful especially for HIV cure-related studies is the SIVSAB-infected RM. In this model, SIV infection is spontaneously controlled (i.e., functionally cured) in the absence of ART (24). As with the SIVmac251/RM model, infection with SIVSAB results in robust, acute viral replication and massive CD4⁺ T cell depletion. However, unlike the SIVmac251/RM model, control of SIVSAB occurs between 2-3 months postinfection and is maintained indefinitely (24), residual immune activation returns to preinfection levels following virus control, and mucosal CD4⁺ T cells return to near preinfection levels after 4 years of control (24). Experimental depletion of CD8⁺ cells with anti-CD8-depleting antibodies reverts virus control, resulting in significant virus rebound. Rebounding virus is controlled again upon CD8⁺ cell restoration, suggesting that functional immune responses (particularly the cytotoxic response) are responsible for the virus control (discussed further in section 3.0).

For the purposes of this dissertation, from this point forward (unless otherwise noted), all discussion of NHPs will refer to SIVmac251-infected Indian origin RMs.

1.3 HIV/SIV INFECTION AND ART

HIV and SIV share key features of virus persistence: (a) HIV/SIV DNA are similarly integrated in the target cell genome (25-27); (b) response to interferons results in transcriptional control of LTRs through a bias of histone acetylation favoring HIV/SIV DNA persistence (28); (c) costimulatory signals induce latent HIV/SIV without coengagement of T cell receptors (29); (d) distribution of cells containing HIV/SIV DNA and RNA sequences in blood, lymph nodes (LNs) and at mucosal sites are similar in humans and RMs (30-32). SIVmac infection of RMs reproduces all the stages of HIV infection in a condensed time frame. These characteristics underline similar reservoir dynamics during HIV and SIV infections. Historically, SIVmac was difficult to control with ART, requiring complex and expensive drug combinations (33). More recently, emergence of new integrase inhibitors and use of coformulated drugs allowed a better control of SIVmac with ART regimens that are like those used in HIV infection (34). As such, unless otherwise mentioned, discussion of HIV characteristics is representative of SIV and vice-versa.

1.3.1 Replication cycle, virus dissemination and disease progression

Upon virus transmission to an uninfected host (mucosally or intravenously), HIV will bind to the target cell to initiate infection. Binding requires a combination of two surface cellular receptors: CD4 and a chemokine receptor, either CCR5 or CXCR4 (this coreceptor usage pattern leading to the terms R5-tropic and X4-tropic strains, respectively) (35). Once HIV/SIV binding occurs, fusion of the viral envelope with the host membrane allows entry of the viral capsid into the cellular cytoplasm, where both capsid uncoating and reverse transcription of the viral RNA strands occur to form the preintegration complex (PIC), consisting of viral integrase, viral DNA, viral capsid and cellular proteins (36, 37). The PIC migrates through the cytoplasm and translocates into the nucleus, where it contributes to the integration of the viral genome into the host genome (38). Integration does not always occur, resulting in the production of the

extrachromosomal episomes 2-long terminal repeat (LTR) and 1-LTR circles. These episomes are generally considered to be dead-end products of viral replication, but 2-LTR circles can aid in transcription of other integrated virus and can occasionally decircularize and integrate to become a productively infected cell (39-42). Following integration, the now productively infected cell will either transition to a resting, memory state, forcing the integrated virus into a latent state, or start to actively produce viral RNA transcripts. HIV RNA transcription occurs in multiple steps, with transcripts for “early genes” (*i.e.*, *tat* and *rev*) being transcribed first to aid in the transcription and export of longer spliced and unspliced viral RNA strands (43-45). Translation of exported RNA transcripts (spliced and unspliced) occurs to produce accessory proteins and structural proteins, with the eventual joining of proteins and two full-length, unspliced viral RNA transcripts to form a viral capsid. The end result is the budding of a new cell-free virion into the extracellular environment to maintain infection (46). 24 hours is the time needed from binding of a virion to a CD4⁺ T cell’s surface to release of new virions, with overlap present at the different stages, emphasizing the rapidity of viral replication (47).

A severe genetic bottleneck occurs upon mucosal transmission at the site of virus entry, with active infection arising by a single virion (48, 49). That one successful infection is enough to disseminate the virus throughout the body, as one infected cell can produce up to 5×10^4 virions during its life span (50). Virus from various fluids exchanged during sex migrate across the epithelial barrier via M cells, microtears in the epithelia and dendritic cells (DCs) present at the sites of entry (51-53). At the mucosal level, the virus is exposed to local lymphocytes and macrophages, which can eliminate the virus (at which point is at its most vulnerable state). On the other hand, cellular activation in response to infection contributes to an increase in target cells at the site of entry, which may facilitate infection. This, combined with the rapid replication cycle of HIV/SIV, results in the virus rapidly infecting most of the target cells present at the site of entry. Infected cells rapidly migrate to the draining lymph nodes, where at the infection is amplified and is rapidly spread systemically (51, 54, 55). Upon systemic spread, HIV/SIV

reaches the main sites of viral replication, the mucosal surfaces, particularly the gastrointestinal mucosa and lymphoid organs. These are the main sites where CD4⁺ T cell depletion occurs, leading to massive mucosal damage, microbial translocation, persistent immune activation and inflammation and eventually disease progression (56). In contrast to mucosal transmission, in which windows of opportunities for prevention of systemic infection have been postulated by numerous authors, the direct, intravenous (I.V.) transmission from infected needles allows for the immediate dissemination of infectious virus throughout the body, where multiple foci of infection are established. As a result, acute infection is achieved earlier after I.V. transmission than upon mucosal transmission, with peak VL occurring between 10-14 days postinfection (dpi) in I.V. transmission compared to between 12-28 dpi in mucosal transmission (57, 58). Acute infection produces an enormous amount of virus that directly damages the target memory CD4⁺ T cell population and indirectly depletes the overall CD4⁺ T cell population through bystander mechanisms (i.e. apoptosis). This leads to a massive depletion of CD4⁺ T cells, particularly at the mucosal sites within 3 weeks of infection (59-67). Conversely, the levels of CD8⁺ cells expand during acute HIV infection due to massive antigenic stimulation, triggering immense cellular immune responses. The increase in SIV-specific CD8⁺ T cells is associated with a decrease in the levels of viral replication, which is partially controlled to a set-point amount of replication (65, 68-72). The setpoint VL levels, which are defintory for the chronic HIV/SIV infection, are maintained for years. Upon the partial control of viremia, the levels of CD4⁺ cells in blood recover to near preinfection levels, but decline resumes if the infection is left untreated (65, 71, 72). Following the acute infection, CD8⁺ T cell levels decrease and fluctuate throughout the chronic infection (corresponding to HIV developing resistance mutations to the CD8⁺ CTL response and the CTLs mounting a new response to the virus), but will eventually succumb to cellular exhaustion and their effectiveness decrease (73, 74). AIDS occurs when levels of CD4⁺ T cells decrease below 200 cells/ μ L blood and opportunistic infections start to appear (75).

1.3.2 ART and virus suppression

ART is currently the only way to effectively suppress viral replication and extend the lifespan of those infected. The development of antiretroviral therapy is the most important accomplishment of the modern medicine in the 20th century. There are numerous different FDA-approved ARVs available, split into several classes based on the stage of HIV replication cycle the drugs act against. These classes (and examples of drugs within said classes) include: entry/fusion inhibitors (maraviroc [MVC], enfuvirtide [T20]), nucleoside/nucleotide reverse transcriptase inhibitors (NRTIs) (tenofovir disoproxil fumarate [TDF], emtricitabine [FTC], abacavir [ABC], zidovudine [AZT]), non-nucleoside reverse transcriptase inhibitors (NNRTIs) (efavirenz [EFV], nevirapine [NVP], rilpivirine [RPV], etravirine [ETR]), integrase strand-transfer inhibitors (InSTIs) (raltegravir [RAL], elvitegravir [EVG], dolutegravir [DTG]), protease inhibitors (PIs) (saquinavir [SQV], ritonavir [RTV], indinavir [IDV], darunavir [DRV], lopinavir [LPV]).

Those who become infected are now started on combination ART, preferably with each ARV belonging to a different drug class. Combining different classes of drugs together allows: 1) for a more robust suppression of virus; 2) minimizes the development of drug-resistant mutations; 3) allows for restoration of CD4⁺ cells; 4) improves the quality and length of life or those infected (76, 77). Compared to monotherapy, combination ART has resulted in a larger percentage of completely suppressed virus in those treated, improved CD4⁺ cell counts and an overall decrease in HIV-related events while increasing the quality of life (78, 79). Last, but not least, combination ART extends the lifespan of HIV-infected subjects to nearly normal levels, with an expected death age of 78 years, the same as the general, uninfected male population in the US (80). Patient adherence to ART is a major barrier to achieving and maintaining complete suppression of virus (81, 82). Unlike other diseases, interrupting HIV treatment is not forgiving, with even a few missed doses resulting in the development of drug-resistant virus (82, 83). Upon identification of infection, established first-line regimens are given, as these drug combinations have been shown to be effective in suppressing virus quickly and maintaining suppression with

minimal chance of developing resistance mutations, if proper adherence is maintained (84). If first-line ART regimen is unable to suppress virus to <200 copies/mL (termed drug failure), second-line ARVs are given normally alongside the first-line drugs, with the drawbacks being increased price of treatment and increased risk of drug-related toxicities (85). Mega-ART is the final resort given to those who have developed extremely resistant virus, consisting of 6+ different ARVs (86, 87).

1.3.3 Viral decay under ART

Initiation of ART results in a rapid decrease in circulating virus, as ART acts to prevent new infections, while the host naturally clears free virus and kills productively infected cells. This virus decay occurs in separate phases, each corresponding to specific events, which can change depending on the ARVs administered (88-90). The primary phase is very rapid, with an approximate 2 log decrease in plasma viremia, has a half-life of 6 hours to 1.6 days and is representative of the rapid clearance of free virus from plasma and the decay of productively infected cells (88, 91); the secondary decay phase has a half-life of 1-4 weeks and corresponds with the decay of chronically-infected, longer-lived cells (macrophages and CD4⁺ T cells in a lower activation state) and the release of virus from tissues reservoirs (an example being follicular dendritic cells) (92-94); the tertiary decay phase has a half-life of 39-63 weeks and is believed to occur due to the release of virus from latently-infected, resting memory CD4⁺ T cells that become activated (95, 96); the quaternary phase is still under debate as to its existence and lacks a decay rate due to no observable decay in viremia (95) (Figure 1). Even though the tertiary and quaternary phases look at virus only detectable using the highly sensitive single copy assay, the interruption of treatment will result in a rebound of the virus. This emphasizes that ART is not curative and life-long treatment is necessary to, in theory, reduce the size of the reservoir using ART by itself. This is something not easily achievable by the HIV-infected subjects in which treatment was initiated during the terminal stages of infection (97-100). Conversely, in

patients in which ART is initiated early, a nonnegligible fraction of posttreatment controllers was described to occur (101).

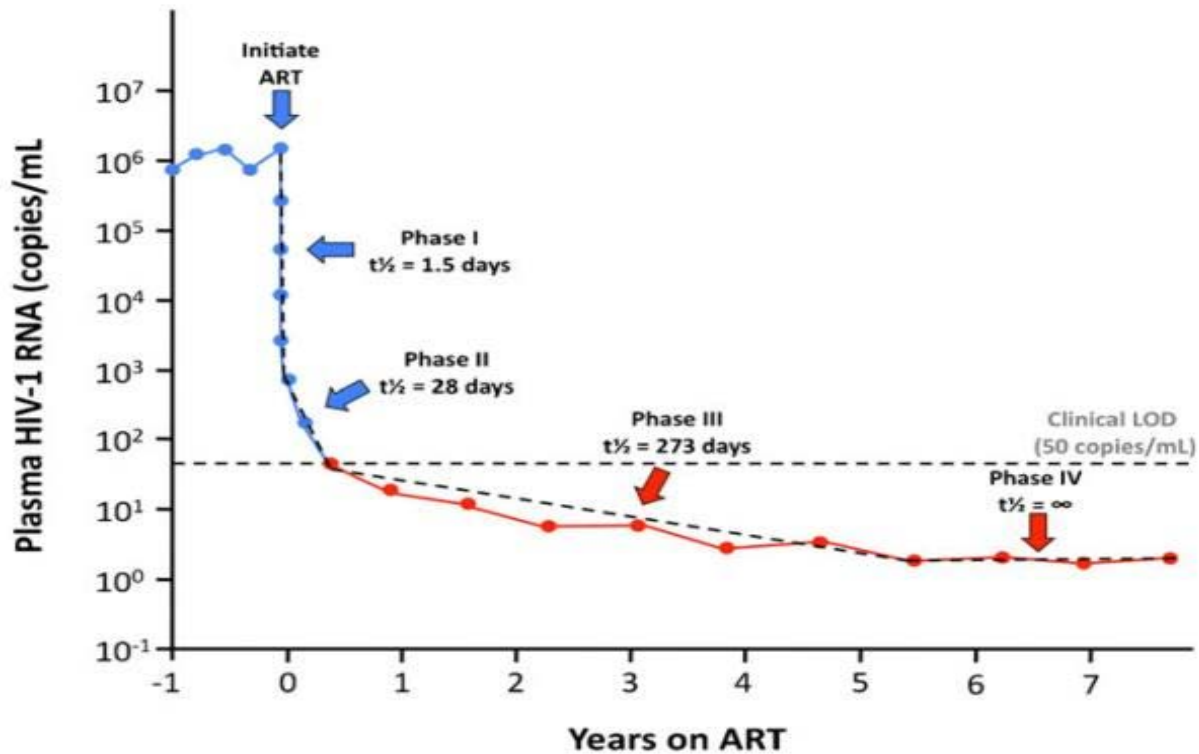


Figure 1. Decay dynamics of plasma HIV-1 RNA during ART.

Upon initiation of ART, viremia decays in multiple overlapping phases, which reflects the turnover of cells infected prior to ART with different half-lives. The first phase of decay has a half-life of approximately 1.5 days and represents the turnover of free virus and productively infected T cells (88, 102, 103). The second phase of decay, with a half-life of approximately 28 days, represents the attrition of cells more resistant to HIV cytopathicity, such as partially activated T cells and cells of the monocyte-macrophage lineage (91, 104). The third phase of decay, which has a half-life of approximately 273 days, levels off to a stable set point that represents a fourth phase showing no evidence of further decay (105). Viremia persists at this stable set point for at least 7 years following the initiation of ART and reflects the remarkable stability of the long-lived cellular reservoirs that maintain residual viremia (95). Blue = above clinical limit of detection (LOD). Red = below clinical LOD (ie, detectable by SCA). Dotted lines = theoretical decay slopes. Adapted from Hilldorfer *et al.*, 2012.

Newer, stronger ARVs are being investigated to help both minimize ART-associated toxicities and improve virus suppression, which, in turn, can aid in the decay of the reservoir. InSTIs have been investigated as potentially able to aid in the reservoir reduction when given as intensification drugs to already established regimens (106). In one study, TDF and FTC with

either RAL or EFV were given to a cohort of HIV-infected subjects, followed by measuring the primary and secondary stages of virus decay. The RAL group experienced longer primary and secondary phases compared to the EFV group. The RAL group also experienced a faster time to undetectable virus, suggesting that InSTIs are the more effective ARV compared to NNRTIs (94, 107, 108).

1.3.4 Development and impact of 2-LTR circles

Optimal infection of a susceptible cell by HIV/SIV results in integration of the reverse-transcribed viral genome into the host genome. However, this is often not the scenario, with the viral DNA either digested within the host nucleus or wrapping on itself to form the extrachromosomal episomes 2-LTR and 1-LTR circles, named for the number of LTR regions present. These episomes form due to the poor efficacy of viral integration and can be promoted by the presence of InSTIs. Upon blocking of integration, the viral genomes are either circularized by host DNA repair enzymes or undergo recombination on themselves.

2-LTR circles have been reported to be useful as surrogate markers of viral replication (109). However, some studies have shown that 2-LTR circles have a short half-life while others have shown that 2-LTR circles can be detected by qPCR in some patients with undetectable plasma viremia (109-111). Though 2-LTR circles form due to failed integration, it has been shown that these episomes can re-linearize as a result of cleaving the palindromic site at the LTR-LTR junction by the viral integrase protein (112, 113). This now linear viral genome can act as the substrate for integration, upon which a productive infection can occur. As such, understanding the mechanisms and dynamics of 2-LTR forms during infection is relevant and essential for cure research.

The development of InSTIs made 2-LTR circles more relevant, especially in studies utilizing an InSTI as an intensifying agent in an already effective ART regimen. These studies have consistently shown that upon addition of an InSTI (RAL in these cases), viral integration is

blocked, plasma viremia is almost not affected and 2-LTR circle levels immediately increase. However, 2-LTR levels do not remain elevated, as most patients will exhibit 2-LTR levels return to pre-RAL treatment values (114-116). This transient increase in 2-LTR levels has been attributed to the RAL inducing increased 2-LTR circle levels while simultaneously preventing *de novo* infection events (117). However, several studies have shown contradictory results whereby they were not able detect changes (or not significant changes) in 2-LTR levels following RAL intensification (118-121). It is reasoned that this lack of change in 2-LTR levels may be attributed to the presence of ongoing viral replication in compartments with limited communication with plasma, such as LNs (122, 123). These anatomical reservoirs must exist in such a way to limit the amount of antiviral drugs present, limit the ability of replicating virus to enter the blood, but be sufficiently connected to allow cells containing 2-LTR circles to enter into the blood (124-126). LNs sufficiently satisfy these requirements, making them an important replication site to study when investigating InSTI treatments.

Though much research has investigated the effects of InSTIs as an intensifying treatment, not much is known about the effects of InSTIs used as a monotherapy. Further, the specific mechanisms CD8⁺ cells utilize to target cells during HIV/SIV infection are not well understood. As such, we investigated the dynamics of 2-LTR circles and modeled the data to interpret if CD8⁺ cells preferentially target cells containing 2-LTR circles either prior to integration or in a productively (integrated) cell. This will be discussed in section 4.0.

1.4 CELLULAR IMMUNE RESPONSES TO HIV/SIV

Like with all pathogens, the host utilizes multiple avenues of defense to eradicate (or attempt to eradicate) the invading pathogen before it kills the host. Thus, the immune response to HIV/SIV infection include innate responses (127), humoral responses (128) and cell-mediated immune responses (129). The CD8⁺ CTL response particularly is important, and its role in HIV/SIV

infection is supported by the following arguments: (i) a strong association between specific host MHC-I alleles and HIV/SIV disease progression exists (130); (ii) a temporal association between the post-peak decline in plasma viremia and the increase in virus-specific CD8⁺ CTL responses (68, 70); (iii) virus escape mutations consistently arise in the face of host cytotoxic responses during all stages of infection (131-135); (iv) CD8⁺ cell depletion *in vivo* results in a rapid and sustained increase in plasma viremia, which then returns to predepletion levels following rebound of CD8⁺ cells (24, 136-147). Further, it was shown that CD8⁺ T cells suppress HIV infection *in vitro* (148, 149). However, the role of CTLs *in vivo* is more difficult to assess, as those infected still progress to AIDS without treatment regardless of the quantity of HIV epitopes CTLs are targeting (150). As such, continued research into the mechanisms of CTL responses against HIV is of utmost importance for cure and vaccine research.

1.4.1 Roles of cytotoxic cells during infection

CD8⁺ CTLs are antigen-specific and will react in a cytotoxic manner when the T cell receptor (TCR) on their surface binds to and recognizes a foreign antigen presented on major histocompatibility type I (MHC-I) (151, 152). CTLs have multiple cytotoxic responses against infected cells, including: the secretion of granzymes/perforin and the binding of Fas ligand (FasL) with Fas. These responses have been observed in the control of several infections, including cytomegalovirus (153), hepatitis B virus (154), hepatitis C virus (155) and Epstein-Barr virus (156). It has been shown that the cytotoxic responses are very important during acute infection and may play a role during chronic infection (74, 157-159).

CTL release of granzyme/perforin initially requires the binding of the TCR with its cognate antigen presented on MHC-I of an infected cell; this results in the formation a synaptic cleft between the CTL and the infected cell. Lytic granules containing granzymes and perforin present within the CTL near the cell surface will release their contents into the cleft. Perforin binds within the infected cell's membrane to form a pore that most likely destabilizes the

membrane through the passive diffusion of Ca^{2+} ions into the infected cell. This diffusion triggers the intake of both perforin and granzymes into the infected cell (160). At this point, granzymes act to stimulate multiple death pathways within the cell, including the cleavage of caspases 3 and 7; the release of cytochrome C from within mitochondria (resulting in further caspase activation) by granzyme B; the induction of single-stranded nicks in chromosomal DNA by granzyme A and other, lesser known functions by the remaining granzyme proteins (161-167). These processes culminate in forced apoptosis of the infected cell. The different granzyme classes have been shown to act independently of each other to ensure cell death if one or more of the granzyme classes are inhibited (168).

The second cytotoxic response CTLs use is the binding of the FasL (CD95L) on their surface with the Fas receptor (CD95) expressed on the surface of infected cells (169). FasL expression is upregulated when a CTL recognizes a foreign antigen (again, through the binding of TCR and MHC-I) and becomes activated. Upon cross-linking of FasL with Fas, the death-inducing signaling complex (DISC) forms within the infected cell. The DISC rapidly cleaves apoptotic procaspases 8 and 10 and c-FLIP into their activated forms, forcing the cell to undergo apoptosis (170, 171). This pathway is triggered by binding of membrane-bound FasL only, whereas soluble FasL induces nonapoptotic pathways, such as NF- κ B, and promotes autoimmunity and tumorigenesis (172).

During the HIV/SIV infection, both perforin/granzymes and FasL binding are utilized by CTLs (173). However, it has been shown that the granzyme/perforin is the preferential mechanism used, regardless of FasL expression on CTLs (157, 173). Further, the FasL/Fas pathway was shown to not play a role in killing bystander, uninfected cells, as was expected in early studies (173, 174).

1.4.2 Noncytotoxic effects of cytotoxic cells

In addition to the direct cytotoxic effects of CTLs against infected cells, CTLs also exert indirect, noncytotoxic effects. As such, the life-span of the infected cell is not affected by noncytotoxic effects, unlike cytotoxic ones. Most noncytotoxic responses involve the release of various chemokines and cytokines that directly affect the replication cycle of the infecting pathogen (175). These chemokines and cytokines include, but are not limited to: β -chemokines macrophage inflammatory protein-1 α (MIP-1 α) and MIP-1 β ; regulated upon activation, normal T-cell expressed and secreted (RANTES); T-cell antiviral factor (CAF); interferon (IFN)- γ and tumor necrosis factor (TNF)- α (159, 176-178).

MIP-1 α , MIP-1 β and RANTES have been shown to directly inhibit HIV-1 replication by binding and occupying their cognate receptor CCR5, which prevents the binding of HIV virions and subsequent infection (179, 180). Further, it is believed that the binding of these proteins to CCR5 results in internalization of CD4, further limiting HIV binding potential (181). However, these proteins do not prevent infection of monocytes and macrophages (182). Additionally, oligomerization of RANTES alone has been shown to increase HIV infectivity by cross-linking the membranes of HIV with a target cell and by making a target cell more permissive to infection by HIV (183). β -chemokines are naturally inflammatory and their release results in leukocyte recruitment, which may provide more susceptible cells for infection (184). As such, β -chemokines may act to both limit and help HIV replication, most likely dependent on chemokine concentration (184).

CAF was first identified in the context of HIV infection, but little is known about this protein, as it lacks identity with all chemokines associated with dampening HIV-1 replication (185, 186). CAF has not been shown to block HIV entry (187), is not MHC I restricted (188), does not prevent proviral integration (189) nor reverse transcription (189, 190). Rather, CAF acts to prevent HIV LTR gene expression (187). CAF has been shown to be produced by non-HIV-specific CD8⁺ CTLs, but still acts to limit HIV replication. This shows that CAF production is

not limited to HIV-specific CTLs, and suggests that CAF may be part of an innate response rather than an adaptive one (191). Regardless of the exact classification, CAF remains an important protein produced during HIV infection.

IFN- γ is a type II interferon and is most commonly used when analyzing CD8⁺ T cell responses. It acts nonspecifically against all viral pathogens by: (i) upregulating expression of TAP transporter proteins to increase the transportation of viral peptides from the cytosol into the endoplasmic reticulum for MHC-I presentation (192, 193); (ii) increasing the production and stability of MHC-I for presentation of foreign peptides (194, 195); (iii) converting the normal cellular proteasome into an immunoproteasome to specifically prepare foreign viral peptides for presentation by MHC-I (196); (iv) increasing the expression of TNF- α and Fas receptors to make virally-infected cells more susceptible to apoptosis (197-199). However, IFN- γ has also been shown to induce HIV production in infected monocytes, underlining that IFN- γ is both beneficial and detrimental in preventing HIV replication (200).

TNF- α is an important antiviral factor as it can trigger apoptosis in virally-infected cells (201, 202). Upon binding of TNF receptor (TNFR) 1 or 2, NF- κ B production is stimulated, apoptotic pathways are initiated and p38 mitogen-activated protein kinase (MAPK), extracellular signal-regulated kinase (ERK), and c-Jun N-terminal kinase (JNK) activation occurs (203). NF- κ B production and migration into the nucleus stimulates the production of inflammation mediators, such as chemokines, IL-6, IL-8 and IL-18 (204). TNFR binding triggers recruitment of TNFR-associated death domain (TRADD) and Fas-associated death domain (FADD) to trigger apoptosis *via* caspase 3, 8, and 9 cascades (205). TNF- α expression prevents HIV infection of macrophages, most likely through downregulation of CD4 and CCR5 expression on the cell surface (206). Further, TNF- α binding promotes expression of MIP- α , MIP-1 β and RANTES, further suppressing HIV replication (180, 207, 208). However, like IFN- γ , TNF- α has been shown to activate HIV transcription through production of NF- κ B and activation of the HIV LTR (209-211).

It is uncertain whether cytolytic or noncytolytic effects are preponderant in controlling HIV infection. Two papers published in 2010 attempted to answer this question by utilizing CD8⁺ T cell depletion with NRTI therapy in SIV-infected RMs (141, 142). Both studies looked at the effect of CD8⁺ T cells on the lifespan of productively infected cells by comparing the decay rates between CD8 depletion and CD8 depletion with ART. They observed no difference in decay between the groups, indicating that CD8⁺ CTL cytolytic activity does not account for the CD8⁺-mediated virus control during chronic infection. The authors concluded that noncytolytic mechanisms must represent a large portion of the effect CD8⁺ T cells have on the virus. However, this conclusion has been refuted by multiple papers (212, 213), with one of the more notable points being that NRTI treatment precludes the ability to measure the effect of CD8⁺ T cells on all stages of the HIV/SIV life cycle, particularly cells containing virus but prior to viral integration. Further, the frequency of measurements used in the papers may not have been frequent enough to observe a difference between the two groups. These aspects will be further addressed in section 3.0.

1.5 HIV/SIV RESISTANCE TO ART

ART is administered to HIV-infected subjects to suppress virus replication and delay the onset of AIDS. However, the development of viral resistance against ARVs limits the use of these drugs, resulting in adjustment of the ART regimen used. These adjustments typically involve adding ARVs presumed to be effective on strains with viral resistance mutations. However, such drugs are not always able to suppress virus replication. Improper adherence to a given ART regimen is the typical cause of drug resistance, but this is only one part of the issue.

1.5.1 Establishment of resistance

Upon infection by a single virion, HIV rapidly replicates and infects up to 10^8 cells within a few weeks (214). A combination of factors such as the rapid rate of mutation per base pair [$4.3 \pm 1.7 \times 10^{-3}$ (215)], the extremely rapid turnover rate of virion production [$10^8 - 10^9$ virions per day (88, 102, 103)] and frequent recombination events (216) results in a very diverse virus quasispecies present at any one point (217). This is how HIV is able to accommodate and overcome environmental stressors, such as ARVs, to minimize the effect of fidelity on replication (218). Most of the resistance mutations occur during the reverse transcription step of HIV replication, as the viral reverse transcriptase (RT) enzyme lacks a 5'→3' exonucleolytic proofreading mechanism (219, 220). It is believed that the host RNA polymerase II may also contribute to this mutagenesis, but its contribution is minimal compared to that of the viral RT (221).

The host cell has several innate defenses against viral replication, one of which is apolipoprotein B mRNA-editing, enzyme-catalytic, polypeptide-like 3G (APOBEC3G). This enzyme acts during HIV reverse transcription to induce guanine-to-adenine hypermutations by deaminating cytosines into uracils (222-224). These uracils appear in the negative-strand viral cDNA, which can trigger the host cellular uracil-DNA glycolase protein to prevent HIV from integrating and replicating (225). HIV counters this defensive tactic by encoding Vif, a protein that will bind APOBEC3G to cause polyubiquitination and degradation (226). This allows HIV to minimize forced hypermutations and allow for viral integration to occur.

Recombination between genetically different viral genomes present within a heterozygous virion or between genomes from different virions present with a cell is common (227). It has been shown that one cell can be infected by multiple HIV virions simultaneously, all of which will undergo reverse transcription (216). It is during reverse transcription that these viral genomes will recombine with each other, with an average of 3 crossovers occurring per genome (228-230). Viral recombination allows the virus to increase overall variation in the virus

population by dispersing the acquired mutations between genomes (231). Further, it allows the rapid spread of acquired drug-resistant mutations to further overcome the ARV regimen (232-234).

1.5.2 Known resistance mutations

Every ARV has at least one known resistance mutation that limits drug efficacy; knowing these mutations is relevant when conducting experiments that utilize ARVs to suppress virus replication, especially if there is any risk of improper dosing, drug monotherapy or improper adherence. I will discuss each ARV class and the known resistance mutations present against each of the main drugs present in their respective classes.

Viral entry inhibitors are split into two classes, with each class containing one FDA-approved drug: CCR5-antagonists (MVC) and fusion inhibitors (T20). Unlike other ARVs that target the virus itself, MVC targets CCR5 on the host cell surface to prevent the interaction of viral gp120 with it after the binding of host CD4 (235). MVC achieves this by binding an allosteric hydrophobic pocket of CCR5, altering the conformation of CCR5 and preventing its recognition by gp120 (236). Due to the variations in HIV-1 tropism, MVC only prevents infection by R5-tropic viruses, and as such, one way the virus can overcome MVC is to switch to a X4 tropism and utilize the CXCR4 receptor for viral entry instead of the CCR5 receptor (237). Resistance mutations against MVC can occur, allowing gp120 to bind CCR5, even if MVC is already bound (238). These mutations occur on gp120 and include: T199K, T275M and a series of associated mutations (239).

Comparatively, T20 targets the fusion activity of viral gp41, which acts to bring the viral envelope and the host membrane into proximity and assist in their fusion (240). T20 is a synthetic peptide segment of gp41 that binds to a different region of gp41 to prevent fusion (241). Resistance against T20 occurs in the binding region of gp41, effectively allowing the virus

to fuse properly with the host cellular membrane (242). The specific resistance mutations are: G36D, I37M/N, V38A/E/L/N and Q41R, each associated with a secondary mutation (243-245).

NRTIs are extensively used, being included in various ART regimens designed to suppress HIV, and as such, their resistance profile has been thoroughly investigated. NRTIs directly compete with host dNTPs for incorporation into the viral genome during reverse transcription, with the key difference between NRTIs and deoxyribose nucleoside triphosphates (dNTPs) being that NRTIs lack a 3' hydroxyl group, preventing the addition of the next nucleotide (246). The most commonly used NRTIs include TDF, FTC and ABC, with others reserved for when primary ART regimens fail. Two resistance mechanisms exist against NRTIs: mutations that weaken the binding efficacy of NRTIs while maintaining the binding efficacy of natural dNTPs, and mutations that allow the excision of incorporated NRTIs followed by proper dNTP addition *via* ATP manipulation (247, 248). Specific mutations within HIV RT for weakening the binding efficacy of NRTIs are: K65R, L74V, Q151M and M184V/I, with these mutations affecting most, but not all, NRTIs (249-251). Comparatively, mutations specific for the nucleotide excision pathway are: M41L, D67N, K70R, L210W, T215F/Y and K219E/Q, again, with these mutations affecting most NRTIs in different degrees (252, 253). Specific RT mutations associated with any given NRTI have been described and are actively updated (254).

NNRTIs are different from NRTIs, as they do not bind within the active site of viral RT. Rather, they bind noncompetitively to an allosteric hydrophobic pocket located on RT away from the active site (255, 256). NNRTI binding induces a conformational change in the RT active site, preventing the binding of necessary substrates for reverse transcription to occur (257-259). NNRTIs are valuable to use in treatment of HIV-1 infections as they have minimal side effects and overall less toxicity compared to NRTIs (260). Due a larger hydrophobic pocket on HIV-2, SIV and HIV-1 group O, these strains are naturally resistant to NNRTIs.

The most prescribed NNRTI is EFV, with ETR and RPV being prescribed when primary ART fails. A single dose of NVP administered in peripartum used to be the recommended

treatment to prevent mother-to-infant transmission (MTIT), but has since been updated to include AZT during and following pregnancy with NVP administered at onset of labor or triple ARV during pregnancy and while breastfeeding (261, 262). Resistance mutations against EFV are K103N, Y181C and G190A and, when introduced, cause clinical failure against HIV (263). ETR and RPV have an increased genetic barrier against resistance, as their binding pocket conformation is different compared to EFV and is flexible in the face of resistance mutations (264-266). Both ETR and RPV require multiple mutations to reduce efficacy of these drugs (263, 267). The individual mutations are: L100I, K101E, K103N, V179F/I, Y181C, G190E, M230L, Y318F for ETR and V90I, L100I, K101E/P, V106A/I, V108I, E138A/G/K/Q/R/V, V179L/F/I, Y181C/I/V, Y188L, V189I, G190E, H221Y, F227C, M230I/L for RPV (263, 267-270).

InSTIs target one of three major steps for integration, the strand transfer event. During this step, exposed 3'-hydroxyl viral DNA is ligated to the 5' DNA phosphate in the host genome resulting in integration (271). InSTIs bind within the catalytic core of the integrase enzyme and chelate the two divalent metal ions present within the integrase active site, effectively preventing integration from occurring (272, 273). However, InSTI binding is reversible, necessitating the continual presence of InSTI to have long-lasting effects (272). There are three major InSTIs currently in use: RAL, EVG and DTG. Resistance mutations that develop against InSTIs affect the binding of InSTIs within the catalytic core by altering the integrase shape, resulting in ejection of the InSTI from the integrase active site. RAL and EVG share similar resistance mutations: Q148H/K/R, N155H, with each of these major mutations associated with other mutations in their vicinity (274-277). Y143C/H/R is found to cause resistance against RAL, but not EVG while T66I/A/K and E92Q cause higher resistance to EVG (275, 278). DTG is believed to have a higher genetic barrier to resistance, as it is effective against RAL and EVG resistant isolates (279). This is due to DTG's slower dissociation rate from the integrase/viral DNA complex (280). However, resistance mutations against DTG can appear and include R263K and G118R (281, 282). It was reported that the HIV strains carrying the resistance mutations to DTG

have an impaired fitness and are unable to evade drug pressure nor develop secondary resistance mutations to overcome this replication deficiency (283).

PIs act to bind competitively within the viral protease active site to prevent the cleaving of Gag and Gag-Pol polyproteins and viral budding (284, 285). PIs play a key role in ART regimens as they block a different step of the replication cycle compared the NRTIs and NNRTIs, allowing for a lower risk of resistance. The most commonly prescribed PIs include: DRV, SQV, LPV and RTV. RTV is given in combination with specific PIs as it is a potent inhibitor of cytochrome P450 3A4 (CYP3A4), which, in turn, increases the plasma concentrations of proteases that are normally degraded by CYP3A4 (286). Resistance mutations against PIs act to reduce the binding affinity of the PIs within the protease active site while not affecting the binding of the intended substrates (287, 288). The known resistance mutations against PIs are: D30N, V32I, L33F, M46I/L, I47A/V, G48V, I50L/V, V82A/F/T/S/L, I84V and L90M, with some mutations occurring against specific PIs and others, such as I84V, that affect all PIs (288-290).

2.0 HYPOTHESIS AND SPECIFIC AIMS

Hypothesis

H1: Despite decades of research, there is no vaccine nor cure for HIV. Long-term ART suppresses virus replication, resulting in improved quality and length of life, but interruption of ART almost invariably leads to virus rebound. This is due to the establishment of a latent reservoir in resting CD4⁺ T cells with an extremely long half-life, necessitating life-long treatment. To effectively produce a vaccine or cure for HIV, the immune responses that act against HIV must be understood. CD8⁺ T cells are an important aspect of the host immune response against HIV, as evidenced by several factors, most importantly that depletion of CD8⁺ cells results in a sustained increase in plasma viremia that decreases upon CD8⁺ T cell restoration. However, the specific effector mechanism(s) exerted by these cells is not known. Two papers in 2010 independently concluded that CD8⁺ cells are not killing infected cells; rather, they suggested that CD8⁺ T cells control viral replication *via* a non-cytolytic mechanism. However, this conclusion is not entirely accepted by the field. The authors' use of NRTI only allows the measure of CD8⁺ T cells effect against productively infected cells, even though it is known viral-induced cytopathicity occurs upon viral integration, thus obscuring the data. Further, the first wave of antigen presentation occurs 3 hours postinfection, corresponding to the time following viral reverse transcription, but prior to integration. As such, **we hypothesized that CD8⁺ T cells exert a cytotoxic effect against infected cells prior to becoming productively infected.** This effector mechanism will be observable in the context of CD8⁺ cell depletion

experiments during integrase inhibitor therapy. This hypothesis is supported by viral dynamics modeling/simulations.

Specific Aims

To test the hypothesis above, we designed a set of experiments and established the following specific aims:

1. To determine the effector mechanism of CD8⁺ T cells by depleting CD8⁺ cells in RAL-treated rhesus macaques, comparing them with two control groups: (i) CD8⁺ cell depletion without RAL; (ii) RAL monotherapy. We will analyze the viral dynamics between the groups to ascertain the effector mechanism.

2. To analyze 2-LTR dynamics in the above-mentioned groups from SA1, which modeling predicted would add more information to the analyses of viral dynamics.

3. To better characterize the parameters of 2-LTR dynamics in the context of RAL intensification experiments.

**3.0 CHAPTER ONE: CD8⁺ T-CELL DEPLETION LEADS TO A DIFFERENT
PROFILE OF SIV VIRAL DECAY UNDER INTEGRASE INHIBITOR
MONOTHERAPY**

Benjamin Bruno Policicchio^{1,2}, Erwing Fabian Cardozo⁵, Cuiling Xu^{1,3}, Dongzhu Ma^{1,3}, Tianyu He^{1,3}, Kevin Raetz^{1,4}, Ranjit Sivanandham^{1,3}, Adam Kleinman^{1,4}, George Haret-Richter^{1,3}, Tammy Dunsmore^{1,3}, A. S. Perelson⁶, Cristian Apetrei^{1,2,4}, Ivona Pandrea^{1,2,3}, Ruy M. Ribeiro^{6,7}

¹Center for Vaccine Research, University of Pittsburgh, Pittsburgh, PA, 15261, USA;
²Infectious Diseases and Microbiology, Graduate School of Public Health, ³Pathology,
⁴Microbiology and Molecular Genetics, School of Medicine, University of Pittsburgh,
Pittsburgh, PA 15262; ⁵ Vaccine and Infectious Disease Division, Fred Hutchinson Cancer
Research Center, Seattle, WA, 98109, USA; ⁶Theoretical Biology and Biophysics Group, Los
Alamos National Laboratory, Los Alamos, NM, 87545, USA; ⁷Laboratorio de Biomatemática,
School of Medicine, University of Lisbon, Portugal

3.1 PREFACE

The research presented here was presented in part as a poster and oral presentation titled “CD8⁺ Cytotoxic T Lymphocytes Exert a Strong Cytolytic Effect on Virally-infected Cells Prior to Viral Integration in SIVmac251-infected RMs” presented at the 2016 International AIDS Society (IAS) conference in Durban, South Africa and as an oral presentation titled “CD8⁺ T-cell Depletion Leads to a Different Profile of SIV Viral Decay under Integrase Inhibitor Monotherapy” presented at the 2017 IAS conference in Paris, France.

The work presented in this chapter is for completion of Aim 1 in partial fulfillment of the requirements for the degree of Doctor of Philosophy. The data presented herein has been adapted from a submitted manuscript (Benjamin Bruno Policicchio, Erwing Fabian Cardozo, Cuiling Xu, Dongzhu Ma, Tianyu He, Kevin Raetz, Ranjit Sivanandham, Adam Kleinman, George Haret-Richter, Tammy Dunsmore, Alan S. Perelson, Cristian Apetrei, Ivona Pandrea, Ruy M. Ribeiro). Benjamin Policicchio processed blood, intestinal and LN samples, extracted viral RNA from plasma samples, performed qRT-PCR on viral RNA, analyzed and compiled flow cytometry data, wrote and edited the manuscript. Erwing Fabian Cardozo performed mathematical modeling on data sets. Cuiling Xu stained blood, intestine and LN samples and acquired stained samples on a flow cytometry machine. Dongzhu Ma helped design PCR conditions. Tianyu He, Kevin Raetz, Ranjit Sivanandham, Adam Kleinman processed blood, intestine and blood samples. George Haret-Richter and Tammy Dunsmore administered the drugs to the RMs, bled and sample intestine and LN biopsies from the RMs.

3.2 ABSTRACT

The mechanisms of CD8⁺ T lymphocyte control of HIV infection are not well understood. We hypothesized that the main effect of CD8⁺ T-cells occurs before viral integration. We developed a model of viral dynamics with pre- and postintegration stages to assess the effect of CD8⁺ cell depletion in SIV-infected RMs receiving integrase inhibitor RAL monotherapy. Twenty SIVmac251-infected RMs received just CD8-depleting antibody (M-T807R1), n=4, both RAL and CD8-depleting antibody, n=8, or just RAL, n=8. Plasma viral loads (pVLs) were measured by quantitative real-time polymerase chain reaction (qRT-PCR). T-cell counts and immune activation were monitored by flow-cytometry. We analyzed the pVL profiles using a viral dynamics model including infected cells pre- and postviral DNA integration and assuming different possible immune effector mechanisms. We fitted the model to the data using a nonlinear mixed effects approach to find what mechanisms best described the data. CD8⁺ T-cell depletion was profound and lasted throughout RAL therapy. Depletion of CD8⁺ T-cells led to pVL increases prior to RAL initiation. Macaques receiving just RAL treatment experienced much greater pVL decays than those treated with CD8⁺ cell depleting antibody and RAL. The latter group had small decays or rebounded early during RAL therapy. From the fits of the model, RAL efficacy in blocking integration was estimated at 97%. A model including CD8⁺ cell effects in killing infected cells pre-integration (cytolytic) and reducing viral production (non-cytolytic) was utilized to best explain the pVL profiles across all macaques. In the absence of CD8⁺ cells, the loss rate of infected cells pre-integration was reduced by 82% and viral production increased 2.5 times. Our results suggest that CD8⁺ T-cells have a cytolytic effect on infected cells before viral integration and a non-cytolytic effect reducing viral production.

3.3 INTRODUCTION

Understanding the host immune response against HIV/SIV infection is essential for developing effective therapeutic and preventive strategies. Unfortunately, HIV continually evades and subdues the host's immune responses, muddling our attempts at elucidating the nature of the immune mechanisms needed to control infection. Examples of HIV evasion strategies include: (i) undergoing rapid mutation of its proteins due to host immune pressures, effectively evading host adaptive responses (70, 132, 133, 291); (ii) inducing down regulation of MHC-I expression through the viral protein Nef, reducing host cytotoxic capabilities to target infected cells (292); (iii) taking advantage of virus-specific adaptive responses that generate activated CD4⁺ T cells, the preferential target of HIV, propagating the infection (293); (iv) chronic stimulation of the immune system resulting in production of nonfunctional "exhausted" CTLs (294, 295). As such, there is uncertainty regarding which immune response should be emphasized in current research endeavors.

Of the various immune responses against HIV, the cytotoxic response exerted by CD8⁺ CTLs has been shown to be critical for host's attempts to control HIV/SIV, as supported by the following observations: (i) a temporal association exists between the increase in virus-specific CD8⁺ T cell responses and the post-peak decline in plasma viremia (68, 70); (ii) CD8⁺ CTLs are able to suppress new infections *in vitro* (148, 149); (iii) virus escape mutations consistently arise in response to the host cytotoxic response during all stages of infection (131-135); (iv) a strong association can be described between specific host MHC-I alleles and HIV/SIV disease progression (130); (v) association of circulating escape mutants with the prevalence of specific human leukocyte antigens (HLAs) in the population (296, 297). Experimental *in vivo* CD8⁺ cell depletion studies in SIV-infected macaques have strengthened this argument and provided a

more direct evidence of the role of CD8⁺ cells in HIV infection (138, 140-143, 145, 146, 148, 298, 299). Thus, CD8⁺ cell depletion results in a rapid and sustained rebound of plasma viremia, which is controlled when CD8⁺ cells are restored. These results are consistent in every model of SIV infection: elite controllers (24, 298), nonpathogenic (137), rapid progressor (138, 139), antiretroviral treated (140-142) and untreated models (143-147). Accordingly, it is considered that understanding the mechanisms of action of CD8⁺ cells and identifying strategies to boost the CD8⁺-specific immune responses is a key priority of HIV research.

Though CD8⁺ cells hold strong potential for future cure efforts, their specific mechanism(s) of action is not well understood. CD8⁺ CTLs could exert a direct cytotoxic response against viral-infected cells *via* release of granzyme/perforin and/or stimulation of the Fas/FasL pathway (300, 301). Alternatively, CD8⁺ cells could act indirectly by interfering with *de novo* infections or the release of new virions through soluble antiviral factors, including the CCR5-binding proteins MIP-1 α , MIP-1 β , RANTES, CAF, α -defensins, and other factors (179, 190, 302). To help shed light on this question, two groups studied the lifespan of SIV-infected cells after reverse transcriptase inhibitor (RTI) treatment, either in the presence or absence of CD8⁺ cells. They showed that the average lifespan was not different with or without CD8⁺ cells, concluding that CD8⁺ CTLs do not exert a cytolytic effect on infected cells (141, 142). Another recent study, quantified the lifespan of infected cells after treatment in infected people with different HLA background, both favorable and unfavorable for HIV progression (303). They found no difference in the lifespan of infected cells and concluded that “protective CD8⁺ T-cells exert their effect on target-cells before onset of productive infection, or via noncytolytic mechanisms” (303). These data have both been corroborated and challenged (212, 213, 304), leaving the field to question what is the true mechanism(s) of CTLs against HIV. To help answer this question, we interrogated whether CD8⁺ cells exert a cytolytic response against infected cells prior to viral integration. To this end, we treated SIV-infected RMs with the integrase inhibitor RAL, in the presence or absence of CD8⁺ cells, and then fitted a viral dynamics model to the data

to study the possible effector mechanisms contributing to the observed viral load profiles. We found that the half-life of pre-integrated cells in the RAL-treated group is significantly shorter than in the RAL-treated and CD8⁺ depleted group, suggesting that CD8⁺ CTLs have a cytolytic role prior to viral integration. Further, the best model also indicated that the viral production rate increased in the absence of CD8⁺ cells, indicating that CD8⁺ CTLs also exert a non-cytolytic effect.

3.4 MATERIALS AND METHODS

3.4.1 Ethics statement

All RMs were housed and maintained at the University of Pittsburgh, Plum Borough animal facility, according to the standard of the Association for Assessment and Accreditation of Laboratory Animal Care (AAALAC) International, and experiments were approved by the University of Pittsburgh Institutional Animal Care and Use Committee (IACUC), protocol #16058287. The animals were cared for according to the *Guide for the Care and Use of Laboratory Animals* and the Animal Welfare Act (305). Efforts were made to minimize animal suffering: all RMs had 12/12 light/dark cycle, were fed twice daily with commercial primate diet, water was provided *ad libitum*, and were socially housed in pairs indoors in suspended stainless-steel cages. A variety of environmental enrichment strategies were employed: providing toys to manipulate and playing entertainment videos in the animal rooms. The animals were observed twice daily for any signs of disease or discomfort, any of which were reported to the veterinary staff for evaluation. For sample collection, animals were anesthetized with 10mg/kg ketamine HCL (Park-Davis, Morris Plains, NJ, USA). At the end of the study, the animals were sacrificed by intravenous administration of barbiturates.

3.4.2 Animals, infections, and treatments

Twenty Indian-origin RMs (*Macaca mulatta*) were included. They were IV-infected with 300 TCID₅₀ of SIVmac251 and were closely monitored during all stages of the study.

Fifty-six dpi at the beginning of early chronic infection, the CD8⁺ cell-depleting monoclonal antibody M-T807R1 (NIH Nonhuman Primate Reagent Resource, Boston, MA) was administered to 12 RMs at a dose of 50 mg/kg. The animals received an additional 50 mg/kg of M-T807R1 19 days later. Two days following the first CD8⁺ cell depletion, RAL monotherapy was initiated, at 20 mg/kg *bid* for 23 days, in 8 of these RMs; an additional 8 RMs without CD8⁺ cell depletion were also treated with RAL monotherapy under the same conditions.

3.4.3 Sample and sample processing

Blood was collected from all RMs -20, -15, -10 dpi, and then weekly after infection up to 56 dpi. This time point was selected for treatment start as it is early in infection, but after the virus reached a quasi-steady state, defined by three consecutive stable VLs. Starting at 58 dpi, with initiation of RAL, blood was sampled every 6 hours for 2 days, then every 2 days for 2 weeks and then every 3 days until 23 dpt.

Within one hour of blood collection, plasma was harvested and peripheral blood mononuclear cells (PBMCs) were separated from the blood using lymphocyte separation media (LSM, MPBio, Solon, OH).

3.4.4 Plasma viral load (pVL) quantification

We monitored levels of free, circulating virus at all times indicated above. Plasma from all animals was subject to a qRT-PCR, as described previously (306). The primer and probe sequences amplify a conserved region of Gag and are as follows: SIVmac251F: 5'-GTC TGC GTC ATC TGG TGC ATT C-3'; SIVmac251R: 5'-CAC TAG GTG TCT CTG CAC TAT CTG TTT TG-3'; SIVmac251Probe: 5'-CTT CCT CAG/ZEN/TGT GTT TCA CTT TCT CTT CTG CG/3IABkFQ/-3'. Real-time PCR was performed utilizing an ABI 7900 HT real-time machine (Applied Biosystems, Foster City, CA) with the following parameters: 95°C for 10 minutes, 45 cycles of 95°C for 15 seconds, 60°C for 1 minute.

3.4.5 Flow cytometry

Whole blood was stained at specific pre- and during treatment time points to monitor the impact of treatment on major immune cell populations. The two-step TruCount (BD Bioscience) technique was used to enumerate the absolute number of CD4⁺ and CD8⁺ T cells in blood, as previously described (298, 307). Blood was stained with fluorescently-labeled antibodies (all antibodies from BD Bioscience, San Jose, CA, USA, unless otherwise noted): CD4 (APC), CD8 (PE-CF594), CD3 (V450), CD45 (PerCP), NKG2A (PE). Ki-67 (PE) was stained by first fixing and permeabilizing cells prior to staining. Flow cytometry acquisitions were performed on an LSR II flow cytometer (BD Biosciences).

3.4.6 Mathematical modeling

To help interpret the virus load profiles during CD8⁺ cell depletion and RAL monotherapy, we used the slow and rapid integration virus dynamics model proposed by Cardozo et al (308),

which is a modification of the standard model of virus dynamics (309). In this model, equation (1), we follow two types of target cells, those that after infection will be short-lived (T_I) and those that will be long lived (T_M). The former, T_I , are created at a constant rate λ , die at rate d , and are infected by the virus (V) at rate β . These infected cells (I_1) are lost at rate δ_1 possibly influenced by effector $CD8^+$ cells, and undergo integration of the proviral DNA at rate k , to become productively infected cells (I_2). We assume that target cells T_M remain constant during the experiment and are infected by virus at rate β_1 . This infection event produces long-lived infected cells (M_1) that are lost at rate δ_{M_1} or undergo provirus integration at a slower rate k_1 to become productively infected cells (I_2). An integrase inhibitor, such as RAL, blocks proviral DNA integration with efficacy ω . Cells with integrated HIV DNA (I_2) are productively infected and are lost at rate δ_2 . Virions are produced by these cells at rate p per cell and are cleared from circulation at rate c per virion. The model equations are:

$$\begin{aligned}
\frac{dT_I}{dt} &= \lambda - dT_I - \beta T_I V \\
\frac{dI_1}{dt} &= \beta T_I V - k(1-\omega)I_1 - \delta_1 I_1 \\
\frac{dM_1}{dt} &= \beta_1 T_M V - k_1(1-\omega)M_1 - \delta_{M_1} M_1 \\
\frac{dI_2}{dt} &= k(1-\omega)I_1 + k_1(1-\omega)M_1 - \delta_2 I_2 \\
\frac{dV}{dt} &= pI_2 - cV
\end{aligned} \tag{1}$$

3.4.7 Data Fitting

To fit the model to the data, we used nonlinear mixed-effect modeling as previously described (308). In this approach, we assume that each parameter η_i has a common distribution in the animal population (or specific group) with a fixed part θ , which is the median value of the parameter in the population, and a random term φ_i , which is assumed to be normally distributed with zero mean. Unless otherwise specified, we assumed that parameters follow a lognormal

distribution. We fit the model to the data and estimate the median (by maximum likelihood) and variances of the distribution of each parameter using the software MONOLIX (www.lixoft.eu). For each model fit, we estimate the log-likelihood ($\log L$) and compute the Akaike Information Criteria (AIC) to perform model selection ($AIC=2m -2\log L$, where m is the number of parameters estimated (310)).

We performed the data fitting in two steps, as this allowed better convergence of the parameter estimates. We first fitted the model in equation (1) to the viral load data from the 8 animals under RAL monotherapy only. With this fit, we estimate parameter distributions for V_0 , δ_1 , δ_2 , δ_{M1} , ω , the pharmacological delay τ , and the fraction of virus produced by short-lived infected cells f_1 (see (308) for model details). We assumed the parameter ω follows a logit distribution to ensure values between 0 and 1. We fixed parameters $d=0.01 \text{ day}^{-1}$, $\beta=10^{-8} \text{ ml}/(\text{virus day})$, $p=10^4 \text{ virus}/(\text{cell day})$, $k=2.6 \text{ day}^{-1}$, $k_1=0.017 \text{ day}^{-1}$, and $c=23 \text{ day}^{-1}$ (308). In these fits, $t=0$ refers to initiation of RAL treatment. We assumed that the system in (1) is in steady state before $t=0$, allowing us to obtain the values of $I_1(0)$, $M_1(0)$, $I_2(0)$, $T_1(0)$, $\beta_1 T_M(0)$ and λ .

As a second step, we performed fits of the model in equation (1) to the viral load data from all 20 animals simultaneously, fixing the same parameters as before and fixing the distribution of the parameters δ_1 , δ_2 , and δ_{M1} as estimated in the RAL-only fits. We repeat each fit by assuming that CD8⁺ cell depletion has one or more different combinations of the following effects: (i) reduction of the death rate of short-lived infected cells before viral integration (δ_1), (ii) reduction of the death rate of productively infected cells (δ_2), or (iii) increasing the virus production rate of productively infected cells (p). This was done by changing these parameters in equation (1) to $(1-r_1)\delta_1$, $(1-r_2)\delta_2$, $(1+r_3)p$ and then estimating r_i , one at a time or in combination. We thus have eight different models, from all $r_i=0$ (our original model) to all $r_i \neq 0$ (indicating the CD8⁺ cells have an effect on the three parameters). Depending on the effect or combination of effects in each fit, we estimate the respective reduction or increase in each parameter. We also estimate parameters V_0 , f_1 , and ω (except for the group of animals not treated with RAL, where

$\omega=0$). In these fits, $t=0$ refers to the start of $CD8^+$ cell depletion, and we assume the viral load is in steady state before time 0, allowing us to obtain the values of $I_1(0)$, $M_1(0)$, $I_2(0)$, $T_1(0)$, $\beta_1 T_M(0)$ and λ .

3.5 RESULTS

3.5.1 M-T807R1 effectively depletes $CD8^+$ cells from blood and induces an increase in pVL

Depletion of various cell types have been useful in determining the correlates of a specific cell type to a known event, with depletion of $CD8^+$ cells affecting immunological control of HIV/SIV infection. To aid in our understanding of the effects of $CD8^+$ T-cells in controlling cells containing virus prior to integration, we depleted $CD8^+$ cells using the monoclonal antibody M-T807R1, as shown previously (138, 298), in four SIVmac251-infected RMs. Upon administration of the antibody, we saw a dramatic and sustained reduction in absolute number of circulating $CD8^+$ T cells (average >99% reduction) (Figure 2A). We consolidated the $CD8^+$ cell depletion with an additional depletion treatment to ensure a strong and sustained suppression of $CD8^+$ cells throughout the follow-up. Between the antibody infusions, the $CD8^+$ cells remained depleted, with only a small transient $CD8^+$ cell recovery (<200 cells/ μ L of blood) being observed at 19 dpt, at the time of the second administration of M-T807R1 (Figure 2A). Natural killer (NK) cell levels decreased immediately following M-T807R1 administration (average ~99% reduction) and remained suppressed throughout follow-up (Figure 3A).

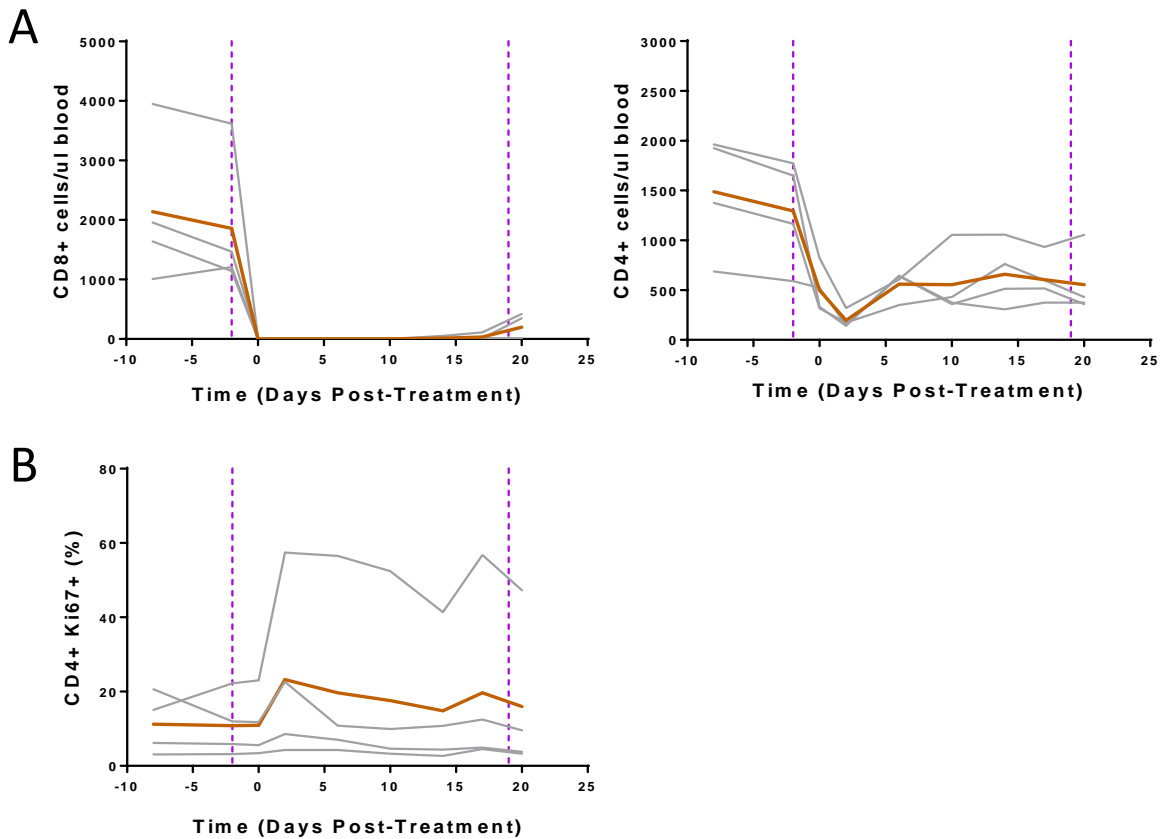


Figure 2. The effects of CD8⁺ cell depletion of CD4/CD8 dynamics and proliferation.

(A) The effects of CD8⁺ cell depletion treatment on the dynamics of (A) CD4⁺ and CD8⁺ cells in peripheral blood (absolute counts); (B) CD4⁺ Ki-67⁺ levels in peripheral blood (percentage). Gray lines represent individual animal values, bold orange line represents mean of data, dashed magenta lines represent CD8 depletion administrations.

Peripheral CD4⁺ T-cells decreased quickly upon the first round of M-T807R1 administration (average 85% reduction in CD4⁺ T-cells), after which CD4⁺ T cell levels recovered slowly throughout the follow-up (Figure 2A).

A large, but variable increase in CD4⁺ T-cell proliferation occurred after the first M-T807R1 administration, as illustrated by the increase of the CD4⁺ T-cell fraction expressing the proliferation marker Ki-67 (average increase from ~10% to ~20%). CD4⁺ T-cell proliferation then gradually declined, although one macaque showed important fluctuations in this marker (Figure 2B).

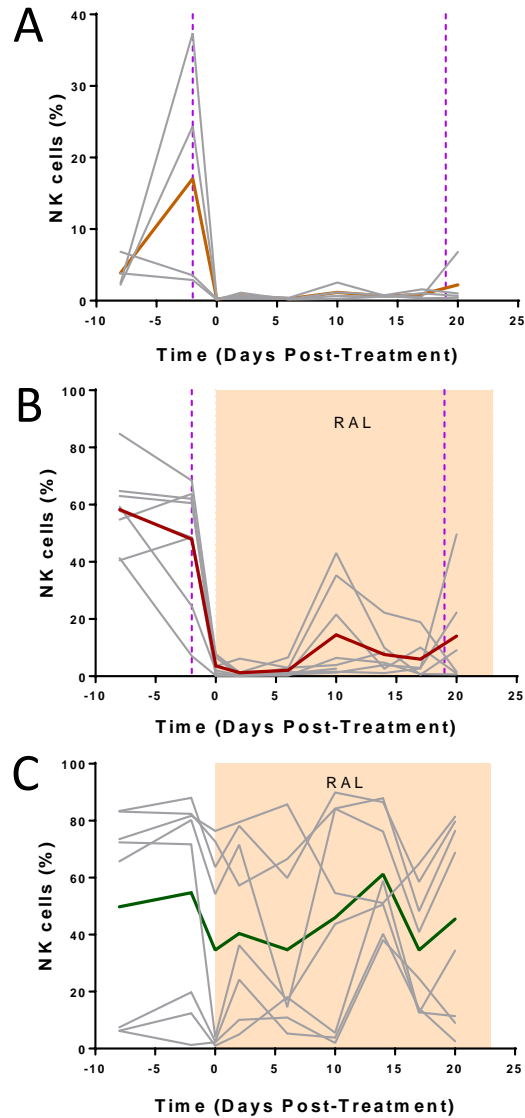


Figure 3. The effects of CD8⁺ cell depletion in the presence and absence of RAL on peripheral NK cells.

(A) CD8 depletion only [D]; (B) R treatment and CD8 depletion [RD]; (C) R monotherapy. Top graphs represent average pVL and bottom graphs represent individual animal values. pVL is presented as log₁₀. Dashed magenta lines represent CD8 depletion administrations, orange block represents RAL administration.

A rapid increase of the plasma viral load (pVL) levels occurred after CD8⁺ cell depletion, with an average increase of 0.88 log₁₀ (range: 0.41 – 1.44 log₁₀). pVLs then remained elevated throughout the follow-up (Figure 4A).

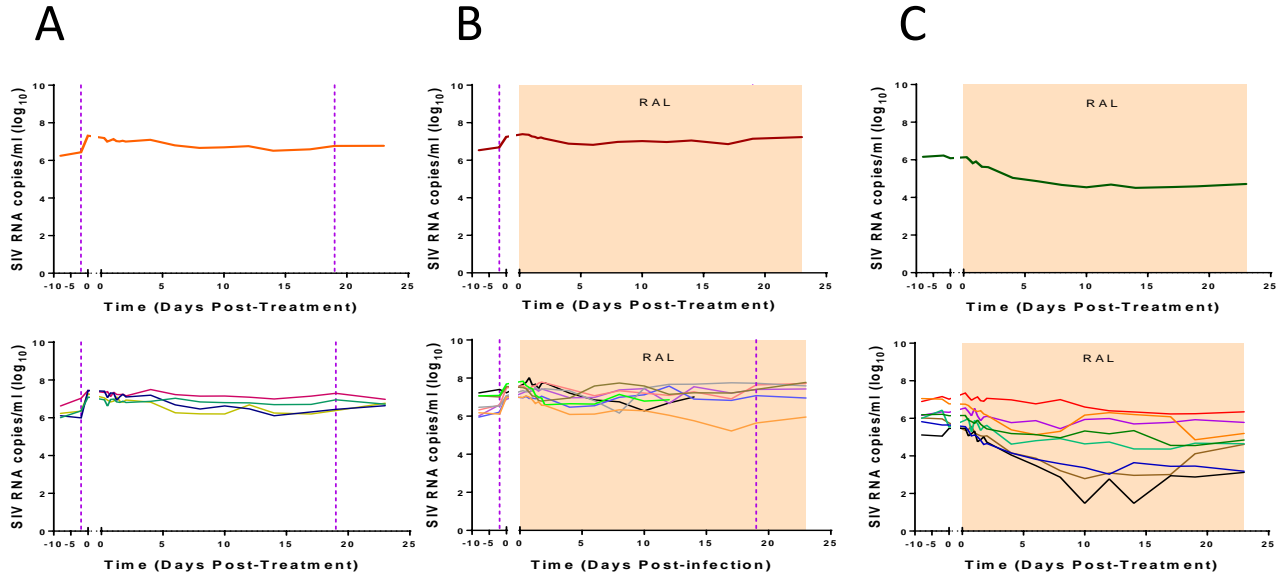


Figure 4. The effects of CD8 cell depletion in the presence and absence of RAL on pVL.

(A) CD8 depletion only; (B) RAL treatment and CD8 depletion; (C) RAL monotherapy. Top graphs represent average pVL and bottom graphs represent individual animal values. pVL is presented as \log_{10} . Dashed magenta lines represent CD8 depletion administrations, orange block represents RAL administration.

3.5.2 RAL monotherapy in CD8⁺ cell-depleted macaques results in a small decline in pVL

We next used an additional eight RMs that had been depleted of CD8⁺ cells (using M-T807R1) and treated them with RAL starting two days after CD8⁺ cell depletion. RAL was administered for 23 days, twice daily at a dose of 20 mg/kg. As with the first group, administration of M-T807R1 rapidly and effectively reduced the absolute count of circulating CD8⁺ cells (average >99% reduction) (Figure 5A). In one animal a limited, transient CD8⁺ cell recovery was observed at day 19 (RM194 with 302 CD8⁺ cells/ μ L blood), but CD8⁺ cell levels returned to near complete depletion upon the second dose of M-T807R1. The remaining RMs maintained CD8⁺ cell suppression throughout the follow-up (Figure 5A). NK cell levels decreased

immediately upon M-T807R1 administration (average 98% reduction), with a trend to recover during RAL therapy (Figure 3B).

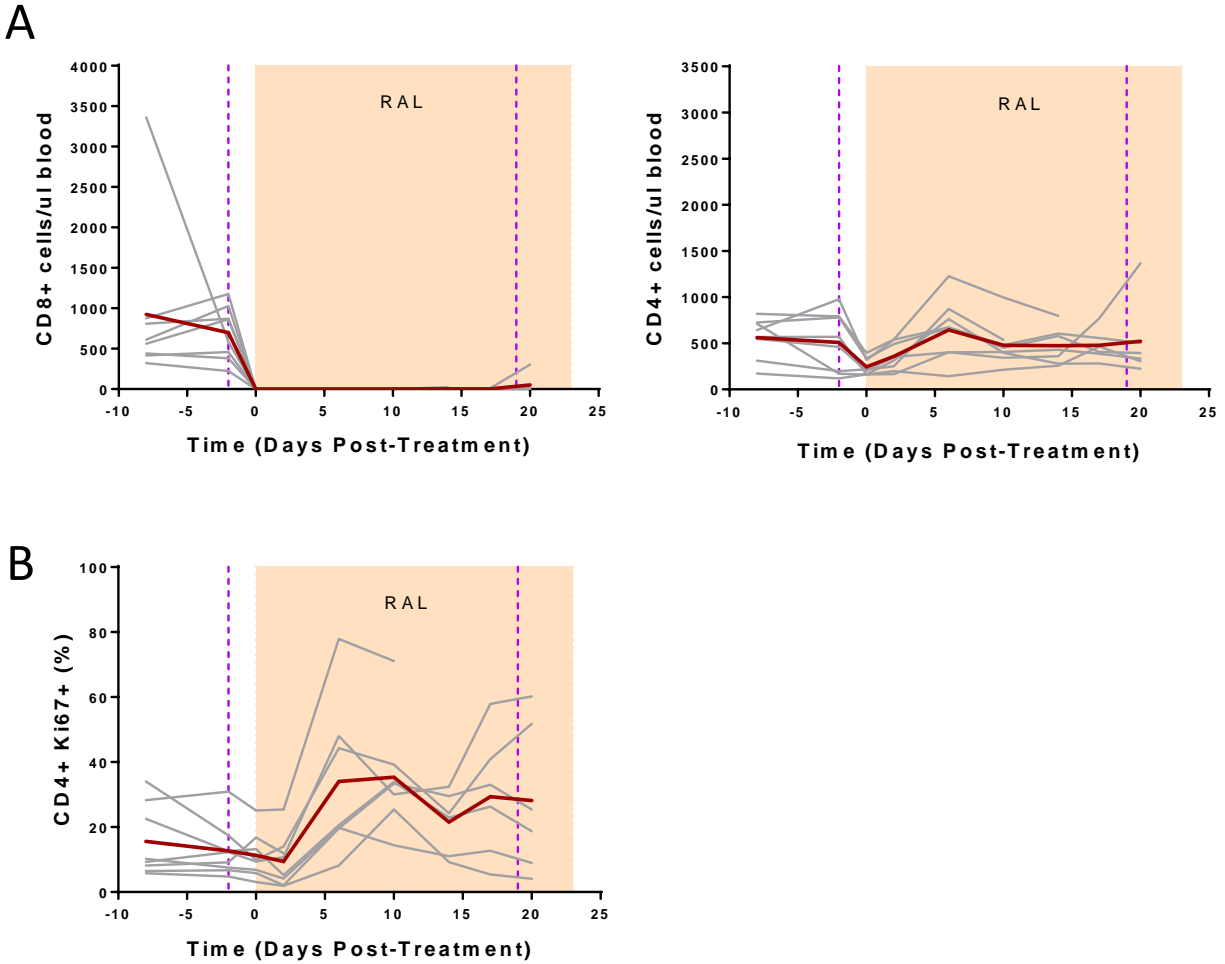


Figure 5. The effects of CD8⁺ cell depletion and RAL treatment on CD4/CD8 dynamics and proliferation.

The effects of CD8⁺ cell depletion treatment on the dynamics of (A) CD4⁺ and CD8⁺ cells in peripheral blood (absolute counts); (B) CD4⁺ Ki-67⁺ levels in peripheral blood (percentage). Gray lines represent individual animal values, bold red line represents mean of data. Dashed magenta lines represent CD8 depletion administrations, orange block represents RAL administration.

Peripheral CD4⁺ T-cells decreased following the first round of CD8⁺ cell depletion (average 51% reduction in CD4⁺ T-cells), but experienced a small recovery upon RAL initiation.

Thereafter, the CD4⁺ T cells remained stable throughout follow-up in 7 out of the 8 animals (Figure 5A). One RM (RM194) experienced a second more substantial bout of recovery of CD4⁺ T-cells during RAL treatment. Two RMs (RM124 and RM178) had to be euthanized at 70 and 72 dpi, respectively, during treatment due to AIDS-like manifestations (Figure 5A).

The proliferating fraction of CD4⁺ T cells did not immediately change following CD8⁺ cell depletion, but levels of Ki-67⁺ CD4⁺ T cells did increase noticeably following RAL initiation (increase from ~9% to ~35%). Similar to the depleted-only group, the levels of Ki-67⁺ CD4⁺ T-cells decreased starting from 17 dpt, with some variability (Figure 5B).

As with the depletion-only group, the first M-T807R1 administration induced an average 0.6 log₁₀ (range: -0.2 – 0.90 log₁₀) increase in pVL. Upon initiation of RAL, pVLs decreased an average of 0.86 log₁₀ (range: 0.22 – 1.78 log₁₀) (Figure 4B).

3.5.3 RAL monotherapy induces peripheral CD4⁺ T- cell recovery and a strong decline in pVL

Finally, a third group of eight RMs were administered RAL at the same times and dose as described above. Upon RAL initiation, the peripheral CD8⁺ T-cell counts decreased by an average of 576 CD8⁺ T-cells/ μ L blood (range: 155 – 1315 CD8⁺ T-cells/ μ L blood); followed by small fluctuations during the follow-up (Figure 6A). NK cell levels decreased upon RAL initiation an average 20% followed by fluctuations to the end of follow-up, starting at 14 dpt (Figure 3C).

At RAL initiation, the peripheral CD4⁺ T-cells increased, and then remained stable or decreased somewhat throughout the RAL treatment (Figure 6A). CD4⁺ T-cell proliferation experienced an immediate, small decline (average 2.4% decrease by 2 dpt [range: -2.1 – 9%])

followed by an average 7.2% increase by 10 dpt [range: -1.3 – 18.9%]. This is followed by the Ki-67 levels returning to pretreatment levels for the remainder of the RAL treatment (Figure 6B).

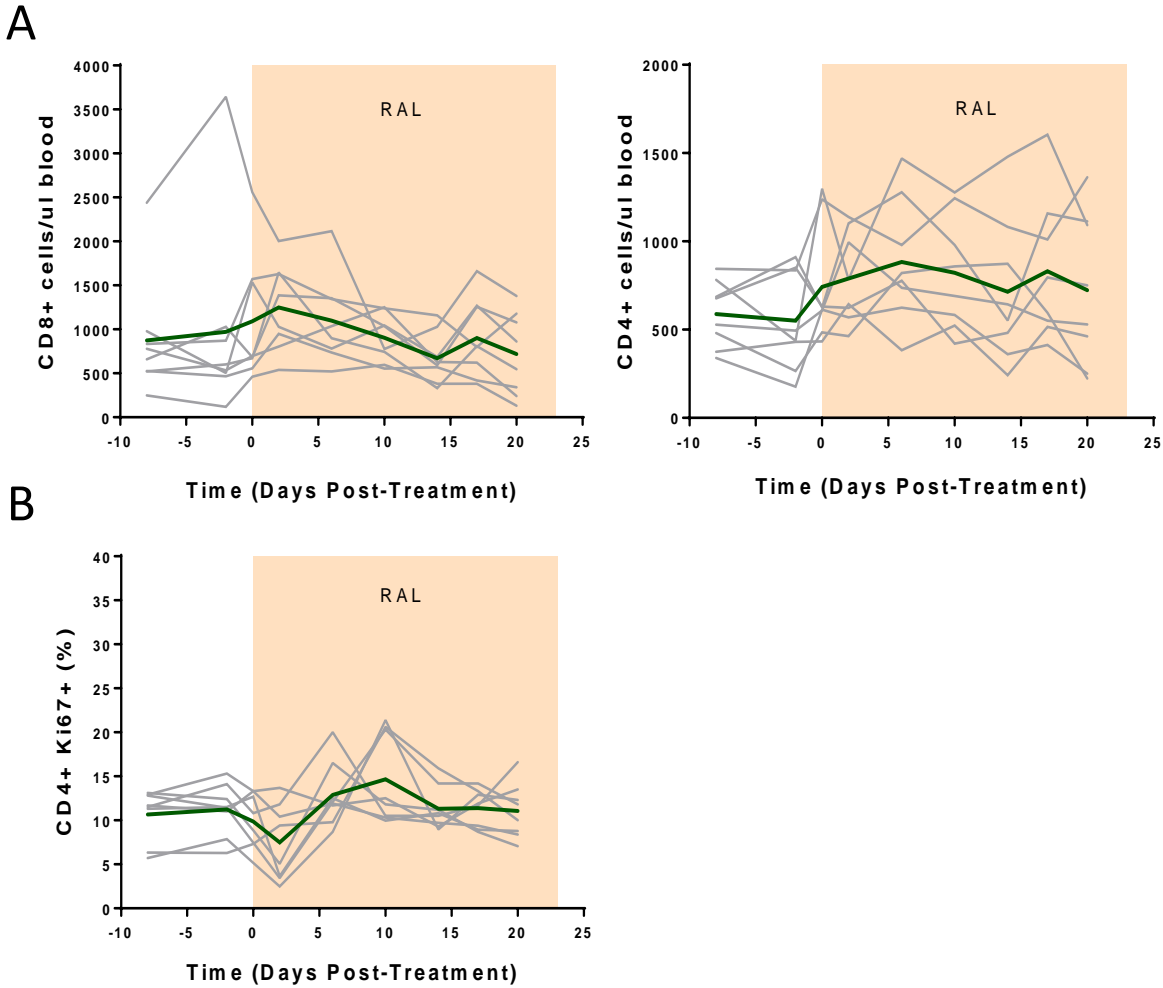


Figure 6. The effects of RAL monotherapy on CD4/CD8 dynamics and proliferation.

The effects of CD8⁺ cell depletion treatment on the dynamics of (A) CD4⁺ and CD8⁺ cells in peripheral blood (absolute counts); (B) CD4⁺ Ki-67⁺ levels in peripheral blood (percentage). Gray lines represent individual animal values, bold green line represents mean of data. Orange block represents RAL administration.

pVL experienced a robust multiphasic decline following RAL initiation, with an average decrease of 1.99 log₁₀ observed during treatment (range: 0.79 – 3.99 log₁₀) (Figure 4C).

3.5.4 Modeling indicates that CD8⁺ cells exert an effect in removing cells before integration and in reducing viral production from infected cells

We used the model in equation (1) to help interpret the differences observed in the virus dynamics for each treatment group (see Methods for a description of the model). We analyzed different combinations of three possible assumptions previously suggested for the effects of CD8⁺ cells (141, 142, 146, 148, 303, 311-313), *i.e.*, CD8⁺ cells could (i) kill infected cells before integration; (ii) kill productively infected cells; or (iii) reduce viral production through non-cytolytic mechanisms.

We first fitted the model to the data from the group of animals receiving RAL monotherapy only, which has also been done for HIV (314). Virus kinetics analyses have shown that the different phases of viral decline after initiation of treatment can reveal the kinetics of infected cells (308, 314). Therefore, from these fits we aim to estimate the death rate of infected cells before (δ_1) and after integration (δ_2). These estimates will be used as reference when analyzing the effects of CD8⁺ cell depletion. From the best fits, our model predicts that productively infected cells have a median half-life of ~15 hrs ($\delta_2 \sim 1.1 \text{ day}^{-1}$), short-lived infected cells before integration have a median half-life of ~2.2 days ($\delta_1 \sim 0.31 \text{ day}^{-1}$), and long-lived infected cells prior integration have a median half-life of ~34 days ($\delta_{M1} \sim 0.02 \text{ day}^{-1}$), characterizing phases 1a, 1b and 2 of the viral decline during RAL monotherapy (308). Our model also predicts that the median efficacy of RAL is 97%, except for animals RM238 and RM239 where this efficacy is only to 64% ($p=0.0003$ log-likelihood ratio test, comparing to a fit assuming animals RM238 and RM239 have the same RAL efficacy as the others). Although we do not know why RAL showed less efficacy in these macaques, it is clear that their viral load decays less upon treatment than in the other macaques. Indeed, the maximum viral load decline in these macaques was $0.76 \log_{10}$ (RM238) and $0.89 \log_{10}$ (RM239).

We then fitted the model to the three treatment groups together to see what effect of CD8⁺ cell depletion best explained all the data. In this analysis, we fixed the distributions of the death rate of short-lived and long-lived infected cells before (δ_1 , δ_{M1}) and after (δ_2) integration to those estimated above with the RAL-only fits (see Methods for details). Figures 7A-C show the model predictions using the median estimates of best fits to each group of animals (see individual predictions in Figures 8-10, using the estimates in Table 1). From the best fit, our model predicts that CD8⁺ cell depletion affects both the loss rate of infected cells before integration (effect in δ_1) and the rate of virus production (effect in p) ($\Delta\text{AIC}>4$ comparing to all other combinations of CD8 effects; $p=7\times 10^{-5}$ and $p=1\times 10^{-40}$, using log-likelihood ratio tests comparing to model fits assuming that CD8⁺ depletion has effects only in p or only in δ_1 , respectively).

3.6 DISCUSSION

CD8⁺ T-cells are strongly associated with the control of HIV/SIV in various models of SIV infection and multiple progression scenarios of HIV and SIV infection (24, 68, 70, 137, 138, 143, 145, 146, 148, 298, 299, 315, 316). They have been shown to contribute to suppressing pVL in SIV-infected RMs on long-term ART (140). This control is exerted through either a direct, cytotoxic killing of the cell and/or through an indirect, noncytotoxic manner whereby the release of chemokines and cytokines inhibits viral replication (148, 179, 190, 302, 311, 317, 318). At least three papers, using two completely different approaches, independently concluded that CD8⁺ cells exert a noncytolytic response against SIV-infected cells by measuring the lifespans of infected cells during combination treatment including nucleotide-reverse transcriptase inhibitors (141, 142). However, these conclusions are not completely accepted (212, 312, 319).

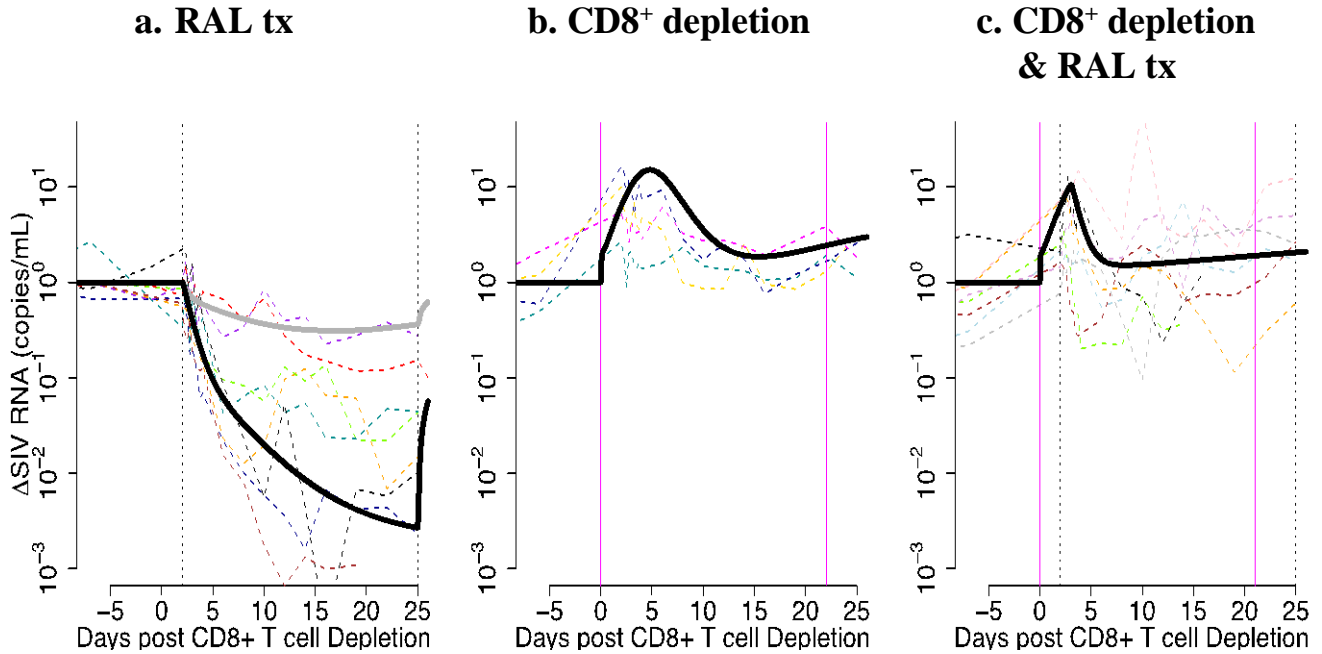


Figure 7. Virus dynamics when CD8⁺ cells affect death rate of infected cells prior to integration and virus production rate.

A model of viral dynamics was developed to analyze the observed data for animals during (a) RAL monotherapy only; (b) CD8⁺ cell depletion only; and (c) CD8⁺ depletion and RAL monotherapy. Vertical black-dashed line represents the start time of RAL monotherapy and magenta-solid line the start of CD8⁺ depletion. Other colored-dashed lines represent normalized SIV RNA copies/ml data (to the pre-intervention levels) for each RM; solid, bold line represents model predictions using the median of the population estimates. Fixed parameters of the model were: $\beta=10^{-8}$ (copies/ml day)⁻¹; $p=10^4$ virion/(cell day); $c=23$ /day; $d=0.01$ /day; $k=2.6$ /day; $k_1=0.017$ /day. Population estimated parameters were: $f_i=0.91$, $V_0=10^{6.4}$ copies/ml, $\delta_1=0.31$ /day; $\delta_2=1.1$ /day; $\omega=0.97$ and $\tau=0.04$ and 0.54 days for animals on RAL monotherapy only or RAL + CD8⁺ depletion, respectively. Gray solid line in the left panel represents the population predictions for animals RM238 and RM239 with $\omega=0.64$. We assumed steady state before any intervention, which allows one to estimate λ and initial states. The estimated effects of CD8⁺ cell depletion where a 82-fold reduction in δ_1 and a 2.5-fold increase in p .

Our goal was to clarify the possible mode of action of CD8⁺ cells, namely their effect in SIV-infected cells after reverse transcription but before integration. By utilizing RAL, we are able to specifically analyze the effects of CD8⁺ cells on infected cells prior to viral integration, a phase of the SIV infection cycle not studied previously. We discovered that the decline of viral load during RAL monotherapy was indeed different in the presence and absence of CD8⁺ cells, which had not been seen before in other models testing the effect of CD8⁺ cells (141, 142, 303).

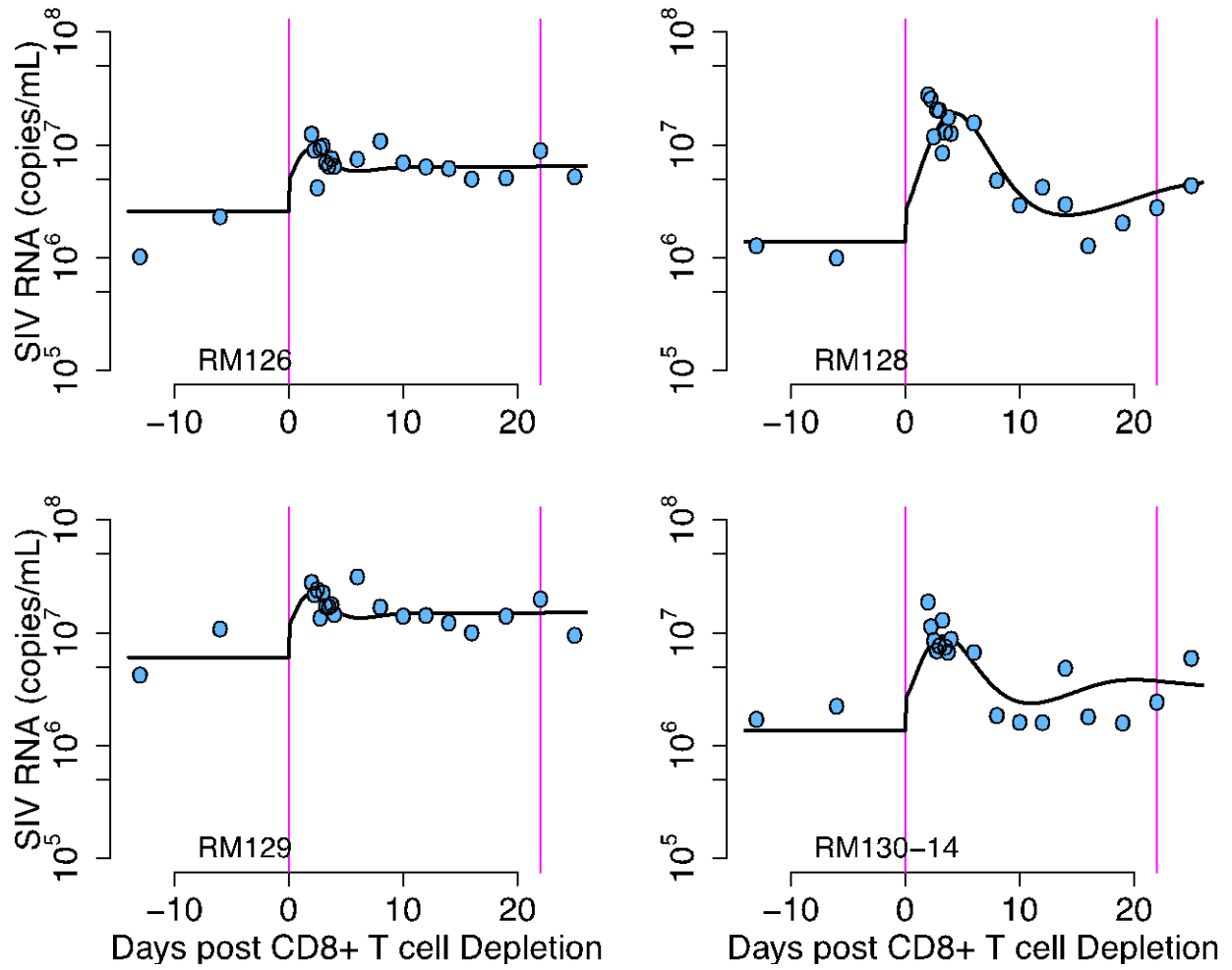


Figure 8. Model fit of individual macaque pVL data in the CD8⁺ cell depletion group.
 Symbols represent the pVL and the solid lines are the best fit solution of the model to the data.

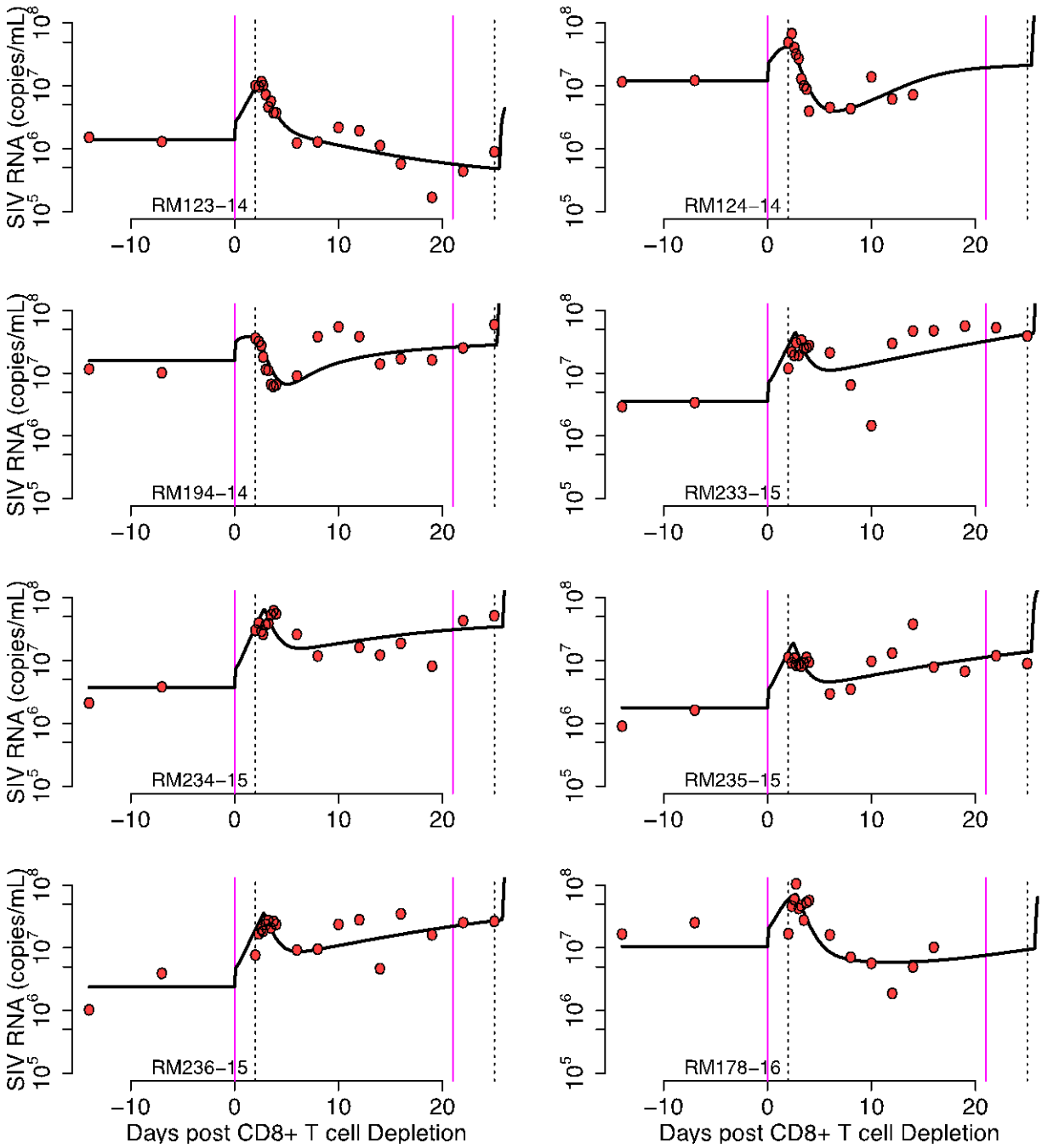


Figure 9. Model fit of individual macaque pVL data in the CD8⁺ cell depletion and RAL treatment group.

Symbols represent the pVL and the solid lines are the best fit solution of the model to the data.

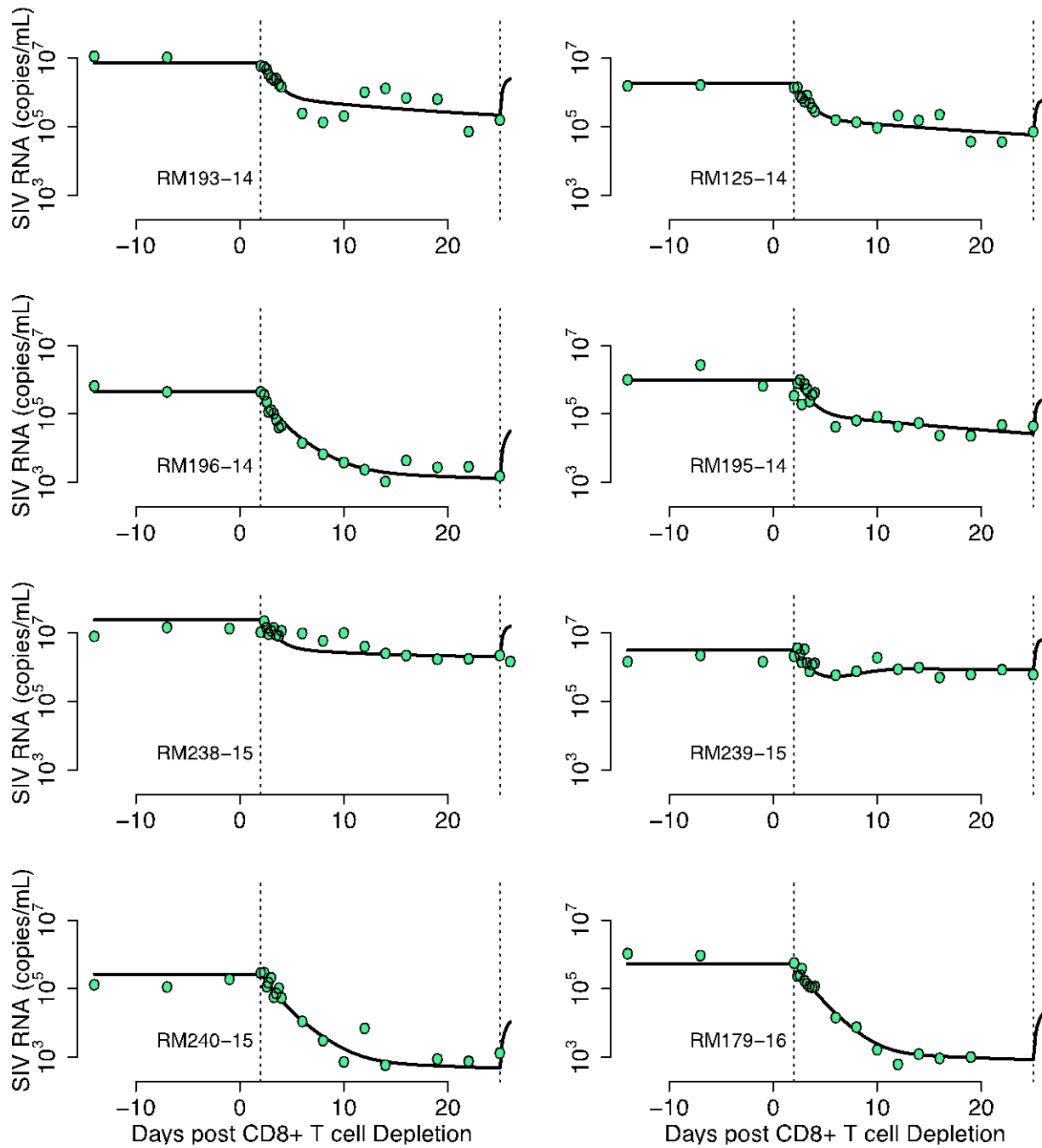


Figure 10. Model fit of individual macaque pVL data in the RAL monotherapy group.
 Symbols represent the pVL and the solid lines are the best fit solution of the model to the data.

Table 1. Model estimates obtained from fitting the viral dynamics model to the data.

	ID	f_I	$\log_{10}(V_0)$	δ_1	δ_2	δ_{M1}	p	$\log_{10}(\beta)$	ω	τ	δ_1/x	$\chi \times p$
RAL Tx	RM193	0.91	6.9	0.08	0.09	0.02	9870.3	-8.4	0.97	0.04	-	-
	RM125	0.91	6.3	0.07	1.08	0.02	9642.6	-8.1	0.97	0.04	-	-
	RM196	0.87	5.7	0.55	1.17	0.02	9423.0	-7.8	0.97	0.04	-	-
	RM195	0.91	6.0	0.07	1.05	0.02	9951.5	-8.0	0.97	0.04	-	-
	RM238	0.91	7.4	0.05	1.00	0.02	10245.0	-8.9	0.64	0.04	-	-
	RM239	0.91	6.5	0.32	1.05	0.02	10134.0	-5.9	0.64	0.04	-	-
	RM240	0.92	5.4	0.66	1.07	0.02	10244.0	-8.0	0.97	0.04	-	-
RM179	0.93	5.7	0.80	1.11	0.02	9896.4	-8.1	0.97	0.04	-	-	
CD8 ⁺ depletion	RM126	0.91	6.4	0.35	1.08	0.02	10000.0	-6.8	-	-	75.8	2.1
	RM128	0.92	6.1	0.37	1.10	0.02	10000.0	-7.6	-	-	74.9	2.1
	RM129	0.91	6.8	0.32	1.08	0.02	9930.1	-7.2	-	-	75.4	2.1
	RM130	0.92	6.1	0.21	1.10	0.02	10001.0	-7.2	-	-	74.5	2.1
CD8 ⁺ depletion & RAL Tx	RM123	0.91	6.1	0.55	1.07	0.02	8979.9	-7.7	0.97	0.49	3.9	2.0
	RM124	0.91	7.1	0.27	1.11	0.02	9321.8	-7.4	0.97	0.41	74.2	2.0
	RM194	0.92	7.2	0.40	1.13	0.02	10217.0	-6.6	0.97	0.27	117.8	2.1
	RM233	0.92	6.6	0.56	1.04	0.02	9499.8	-9.4	0.97	0.64	176.4	2.1
	RM234	0.92	6.6	0.74	1.06	0.02	9848.8	-8.9	0.97	0.81	76.2	2.1
	RM235	0.92	6.2	0.56	1.05	0.02	9514.0	-8.6	0.97	0.43	117.9	2.1
	RM236	0.91	6.4	0.61	1.05	0.02	9419.4	-9.0	0.97	0.78	117.0	2.1
RM178	0.91	7.0	0.46	1.05	0.02	11022.0	-8.1	0.97	0.73	7.9	2.1	

Having found this major difference, we next fitted a mechanistic model of viral dynamics to the data and tested multiple mechanisms of CD8⁺ cells' action to reduce viral replication: (i) killing infected cells prior to viral integration; (ii) killing infected cells following viral integration (i.e., productively infected cells); (iii) noncytolytically reducing viremia through indirect mechanisms. We used a mixed-effects fitting approach, which allowed us to use all the data simultaneously to achieve more robust results.

The observed decay characteristics between the two RAL-treated groups reflect the inherent ability of infected cells to present infecting viral peptides to cognate CD8⁺ cells for clearance. It is known that infected cells are able to present Gag-derived epitopes as early as 2 hours postinfection (320) and that the first wave of antigen presentation occurs between 3 and 6 hours postinfection of a cell (321), corresponding to a timeframe following the initial reverse transcription (47). The presence of RAL allows us to analyze the effects of direct CD8⁺ cell

killing on the period of time when antigen presentation from the infecting virus is optimal while minimizing virus-induced cell death.

Our results support two different effects of CD8⁺ cells. They exert a cytolytic effect against infected cells prior to viral integration and a noncytolytic effect against viral production by infected cells. This is in partial contrast to previous results indicating a non-cytolytic effect (141, 142, 303), because we show that CD8⁺ cells in addition to a noncytolytic effect also act cytolytically during a small window of infection, before pro-viral integration. The observed results from Klatt *et al.* (142) and Wong *et al.* (141) may be attributed to the fact that NRTI therapy (and protease inhibitor therapy) only allows the measurement of the decay of productively infected cells. It is known that following integration, viral-induced cytopathicity occurs, obscuring and preventing one from differentiating the effects of CD8⁺ cells on infected cells (319, 322).

The multiple rounds of M-T807R1 administration permitted us to maintain complete suppression of CD8⁺ cells throughout the treatment. The small, transient rebounds in CD8⁺ cells observed during treatment did not affect the subsequent analysis, as these cells are most likely nonfunctional (143). The observed increase in pVL following CD8⁺ cell depletion supports the role that CD8⁺ cells play in controlling viremia, as evidenced by all animals that received M-T807R1. In this context, fitting the data of the CD8⁺ cell depleted group without RAL therapy helped us to identify the effect of these cells in viral production *p*. We note that one of the first papers on CD8⁺ cell depletion had mentioned this possibility, but they did not have enough data (e.g., the frequent sampling) for definitive conclusions (146).

The depleting antibody M-T807R1 binds to the CD8 α receptor on cells and efficiently depletes CD8⁺ T-cells, as seen in Figures 1 and 3. This antibody also depletes NK cells and natural killer T (NKT) cells, both of which express the CD8 molecule on their surface. This represents a potential issue in our study, as both NK and NKT cells exert antiviral effects during HIV infection (323, 324). Indeed, we see a partial depletion of NK cells in the blood following

CD8⁺ cell depletion. Thus, we cannot be certain that the effects we see in viral load and that our model estimates are not due to NK or NKT cells in addition to CD8⁺ T cells. However, it has been shown that NK cells upregulate inhibitory receptors during viremic HIV infection, affecting the killing ability of NK cells (325, 326). If that is the case, any effect of NK cells on affecting viral replication would be minimal, regardless of CD8 depletion.

A potential factor that could bias our analysis would be an increase in CD4⁺ T-cell activation following CD8⁺ cell depletion, which would increase the availability of target cells leading to more infections and more viral production. Indeed, this could be a contributing factor for the observed increase in p . Further, a fraction of CD4⁺ cells are able to act as CTLs and exert a cytolytic control against virally-infected cells (327-329), and their proliferation could skew our results. Though we did see an increase in the fraction of CD4⁺ T-cells expressing Ki-67⁺ in both depletion groups following the first depletion event (10% increase in depletion-only group; and 26% increase in the depletion + RAL group) (Figures 2, 5), the increase occurred between 4 and 6 days following the initial depletion event for each respective group. This is combined with the fact that the cytotoxic ability of cytotoxic CD4⁺ cells in killing HIV-infected cells *in vivo* is under debate and may be limited to macrophages (328, 330, 331). Further studies will be required to investigate and model the specific cytotoxic effects of CD4⁺ cells and to compare them to the observed effects presented here.

In conclusion, this study demonstrates that CD8⁺ cells do exert a direct cytolytic effect against infected cells (prior to viral integration). The data further suggests that, as previously reported, CD8⁺ cells exert a noncytolytic response to reduce viral production after viral integration occurs. Our results expand on previously published data and greatly contribute to our understanding of the functions CD8⁺ cells exert during HIV/SIV infection, by pinpointing involved mechanisms of action. Our data will help inform future studies focused on both developing a vaccine to prevent new HIV infections and new cure strategies for those already infected.

4.0 CHAPTER TWO: THE DYNAMICS OF SIV 2-LTR CIRCLES IN SIV- INFECTED RHESUS MACAQUES

Benjamin B. Policicchio^{1,2}, Erwing Fabian Cardozo⁵, Paola Sette^{1,3}, Cuiling Xu^{1,3}, George Haret-Richter^{1,3}, Tammy Dunsmore^{1,3}, Cristian Apetrei^{1,2,4}, Ivona Pandrea^{1,2,3}, Ruy M. Ribeiro^{5,6}

¹Center for Vaccine Research, University of Pittsburgh, Pittsburgh, PA, 15261, USA;
²Infectious Diseases and Microbiology, Graduate School of Public Health, ³Pathology,
⁴Microbiology and Molecular Genetics, School of Medicine, University of Pittsburgh,
Pittsburgh, PA 15262; ⁵Theoretical Biology and Biophysics Group, Los Alamos National
Laboratory, Los Alamos, NM, 87545, USA; ⁶Laboratorio de Biomatemática, School of
Medicine, University of Lisbon, Portugal

4.1 PREFACE

The research presented here was presented in part as a poster presentation titled “2LTR Circle Dynamics During Integrase Inhibitor Monotherapy in the Presence and Absence of CD8⁺ Cells” at the 2017 International AIDS Society (IAS) conference in Paris, France.

The work presented in this chapter is for completion of Aim 2 in partial fulfillment of the requirements for the degree of Doctor of Philosophy. The data presented herein has been adapted from a submitted manuscript (Benjamin Bruno Policicchio, Erwing Fabian Cardozo, Paola Sette, Taruna Joshi, Cuiling Xu, George Haret-Richter, Tammy Dunsmore, Cristian Apetrei, Ivona Pandrea, Ruy M. Ribeiro). Benjamin Policicchio processed blood samples, extracted viral RNA from plasma samples, extracted viral DNA from PBMCs and LN lymphocytes, performed qRT-PCR on viral RNA and viral DNA, analyzed and compiled flow cytometry data, wrote and edited manuscript. Erwing Fabian Cardozo performed mathematical modeling on data sets. Paola Sette and Taruna Joshi extracted viral DNA from PBMCs and performed qRT-PCR on viral DNA. Cuiling Xu acquired flow samples of a flow cytometry machine. George Haret-Richter and Tammy Dunsmore administered the drugs, bled and sampled LN biopsies from the RMs.

4.2 ABSTRACT

CD8⁺ cells are known to play a key role in HIV/SIV infection, but their specific mechanism(s) of action in controlling the virus are unclear. 2-LTR circles are extrachromosomal products generated upon failed integration of HIV/SIV into the host genome. To understand the specific effects of CD8⁺ cells on infected cells, we monitored and modeled the dynamics of 2-LTR circles in the presence or absence of CD8⁺ cells with and without INT monotherapy in SIV-infected rhesus macaques (RMs). Twenty RMs were intravenously-infected with SIVmac251 and underwent CD8⁺ cell depletion, received RAL monotherapy, or a combination of both. Blood, LNs and gut biopsies were routinely sampled. pVLs and 2-LTR circles from PBMCs and LN lymphocytes were measured with qRT-PCR. In the CD8⁺ cell depletion group, an ~1 log increase in pVLs and a slow increase in PBMC 2-LTRs occurred following depletion. In the INT group, a strong decline in pVLs upon RAL initiation, and no change in 2-LTR levels were observed. In the RAL and CD8⁺ cell depletion group, a similar increase in pVLs following CD8⁺ cell depletion was observed, with a modest decline following initiation of RAL. 2-LTR circles significantly increased in both PBMCs and LNs following RAL initiation. Analyzing the data with a mathematical model indicated that an effect of CD8⁺ cells in killing infected cells prior to viral integration is the best assumption for the observed dynamics of 2-LTR across all treatment groups. We have shown for the first time that INT does not significantly increase the levels of 2-LTR circles in blood or lymphoid tissues, likely due to the rapid decrease in pVLs following treatment initiation. However, CD8⁺ cell depletion increases the 2-LTR levels, which are enhanced in the presence of an integrase inhibitor.

4.3 INTRODUCTION

Multiple lines of evidence demonstrate that CD8⁺ cells are important in controlling HIV/SIV infection: (i) a strong association exists between specific host MHC-I alleles and HIV/SIV disease progression (130); (ii) a temporal association can be established between the postpeak decline in plasma viremia and the increase in virus-specific CD8⁺ CTL responses (68, 70); (iii) virus escape mutations consistently arise in the face of host cytotoxic responses during all stages of infection starting from the time when cellular immune responses are generated (131-134); (iv) CD8⁺ cell depletion *in vivo* results in a rapid and sustained increase in plasma viremia, which then returns to predepletion levels following the rebound of CD8⁺ cells (24, 136-147). Furthermore, CD8⁺ T cells suppress HIV infection *in vitro* (148, 149). However, the specific mechanism(s) of action these cells take to control viral replication are poorly understood. To gain some insight, we assessed the role of CD8⁺ cells in controlling 2-LTR⁺ cells, which we used as a surrogate for HIV-infected cells pre-integration. A recent study showed that cells containing virus prior to integration can represent a sizeable fraction of the total population of infected cells (308).

Long-term administration of ART to HIV-infected individuals results in virus suppression for the duration of treatment (91). ART interruption is followed by a rapid virus rebound to virtually pretreatment levels, confirming the persistence of a latent reservoir that cannot be eradicated by ART alone (332-334). The mechanism of reservoir formation involves integration of the linear reverse-transcribed proviral DNA genome into the host genome. However, due to poor efficiency of this process, the viral genome is not always able to integrate, leading to the production of extrachromosomal elements (335, 336). An increase of these extrachromosomal products also occurs when HIV-infected subjects receive ARV regimens containing integrase inhibitors INT. The viral isoforms represent viral genomes circularized by host DNA repair enzymes or by undergoing recombination with itself, and are represented by 2-

LTR and 1-LTR circles, respectively. These episomes, particularly the 2-LTR circles, have been reported to be useful surrogate markers of viral replication (337). However, this aspect is still under debate, as some suggested that 2-LTR circles have a short half-life while other studies have shown that 2-LTR circles can still be detected by qPCR when pVLs are undetectable (109-111). Further, 2-LTR circles have been shown to act as substrates for integration by cleavage of the palindromic site at the LTR-LTR junction by the viral integrase protein, resulting in a linear viral cDNA genome that can be effectively integrated and produce infectious virions (112, 113).

Upon the introduction of INT, such as RAL, 2-LTR circles became more relevant to investigate, particularly since intensification of ongoing ART regimens with an INT induces an increase in 2-LTR circles. These levels of 2-LTRs were reported to increase immediately after RAL intensification, but these increases were transient and eventually followed by the return to pretreatment levels (114-116). The transient increases of 2-LTRs have been attributed to RAL preventing new integration events, thus inducing 2-LTR formation (117).

Here, we investigated the effect of CD8 depletion with or without RAL monotherapy on 2-LTR levels in SIV-infected RMs. Monotherapy was used to allow maximal production of 2-LTR circles, since cells are still *de novo* infected during therapy, thus allowing better detection of the effects of CD8⁺ cells. We then compared our data to an extended model of viral dynamics to explore the effect of CD8⁺ cells on 2-LTR circle dynamics. We report that the levels of 2-LTR circles modestly increase following CD8⁺ cell depletion, are unchanged after RAL monotherapy, and dramatically increase following the combined CD8 depletion and RAL monotherapy. Using the model of viral dynamics including 2-LTR circles, we found that model predictions are most similar to the observed data when CD8⁺ cell killing of infected cells occurs prior to viral integration.

4.4 MATERIALS AND METHODS

4.4.1 Ethics statement

All RMs were housed and maintained at the University of Pittsburgh, Plum Borough Research Facility, according to the standards of the AAALAC, and experiments were approved by the University of Pittsburgh IACUC. The animals were cared for according to the *Guide for the Care and Use of Laboratory Animals* and the Animal Welfare Act (16). These studies were approved by the IACUC (protocol # 16058287). Efforts were made to minimize animal suffering; all RMs in this study were socially housed in pairs indoors in suspended stainless-steel cages, had 12/12 light cycle, were fed twice daily with commercial primate diet, and water was provided freely at all times. A variety of environmental enrichment strategies were employed, including providing toys to manipulate and playing entertainment videos in the animal rooms. The animals were observed twice daily for any signs of disease or discomfort, of which were reported to the veterinary staff for evaluation. For sample collection, animals were anesthetized with 10mg/kg ketamine HCl (Park-Davis, Morris Plains, NJ, USA). At the end of the study, the animals were sacrificed by intravenous administration of barbiturates.

4.4.2 Animals, infections and treatments

Twenty Indian-origin RMs (*Macaca mulatta*) were included. They were intravenously infected with 300 tissue culture infectious doses (TCID-50) of SIVmac251 and were closely clinically monitored throughout the follow-up.

Fifty-six dpi (during the early chronic infection), 12 RMs received the CD8⁺ cell-depleting monoclonal antibody M-T807R1 (NIH Nonhuman Primate Reagent Resource, Boston, MA) at a dose of 50 mg/kg. An additional 50 mg/kg dose of M-T807R1 was administered 19

days later. Two days following the first CD8 depleting antibody infusion, RAL monotherapy was initiated for 23 days in 8 of these RMs at a dose of 20 mg/kg *bid*. In addition, 8 RMs without CD8 depletion were treated with RAL monotherapy in identical conditions.

4.4.3 Sampling and sample processing

Blood was collected from all RMs prior to (-8, -2 and 0 dpt) and during RAL treatment (every 6 hours for the first two days; every 2 days for two weeks; every three days until 23 dpt was reached). Within one hour of blood collection, plasma was harvested and PBMCs were separated from the blood using lymphocyte separation media (LSM, MPBio, Solon, OH).

Superficial LN biopsies were taken from all RMs at the time of RAL treatment initiation, and at 14 days post-treatment. Lymphocytes were separated from LNs by pressing the tissue through a nylon mesh screen, were filtered through nylon bags and washed with RPMI medium (Cellgro, Manassas, VA) containing 5% heat-inactivated newborn calf serum, 0.01% penicillin-streptomycin, 0.01% L-glutamine and 0.01% HEPES buffer, as previously described (17,18).

Jejunal biopsies were taken at -7, 0 and 14 dpt, rinsed and digested with EDTA and collagenase, respectively, followed by layering over top a 60%-35% percoll layer to separate lymphocytes.

4.4.4 Plasma viral load quantification

The levels of viral replication were monitored by measuring the plasma viral loads at all time points, as previously described (298). The primer and probe sequences amplify a conserved region of Gag and are as follows: SIVmac251F: 5'-GTC TGC GTC ATC TGG TGC ATT C-3';

SIV_{mac251R}: 5'-CAC TAG GTG TCT CTG CAC TAT CTG TTT TG-3'; SIV_{mac251Probe}: 5'-CTT CCT CAG/ZEN/TGT GTT TCA CTT TCT CTT CTG CG/3IABkFQ/-3'.

4.4.5 Flow cytometry

Whole blood taken at specific times during treatment were stained using a two-step TruCount technique to enumerate PBMCs (described as lymphocytes plus monocytes/macrophages) in the blood, as previously described (20). The number of PBMCs was quantified using 50 μ L of whole blood stained with antibodies in TruCount tubes (BD Biosciences) that contained a defined number of fluorescent beads to provide internal calibration.

4.4.6 2-LTR circle extraction and quantification

$1-2 \times 10^6$ PBMCs and lymphocytes from LNs were pelleted, supernatant removed, and flash frozen at -80°C . 2-LTR circles in PBMC were determined at days -8, 1, 12, and 17 post-treatment. Total DNA was extracted from each sample using a TRIzol-based extraction, as follows: 400 μ L Tri-reagent (Molecular Research Center, Inc, Cincinnati, OH) was added to each tube and samples vortexed until pellets are dissolved. 100 μ L 1-bromo-3-chloropropane (BCP) (Molecular Research Center, Inc, Cincinnati, OH) was added to each tube, vortexed for 15 seconds and centrifuged at 14,000 x g for 15 minutes at 4°C . The upper aqueous phase was removed, followed by the addition of 500 μ L DNA back extraction (GuSCN, Trizma base, sodium citrate), vortexing (15 sec) and centrifugation at 14,000 x g for 15 min at 4°C . The upper aqueous DNA phase was removed and 12 μ L 20 mg/ml glycogen was added and mixed by pipetting, followed by addition of 400 μ L isopropanol, mixing and centrifugation at 21,000 x g for 10 minutes at room temperature. Isopropanol was removed, and DNA pellets washed with 70% ethanol for two days at 4°C to ensure complete leaching of salts from the pellets. After two

days, the ethanol was removed, and pellets were resuspended in 5 mM Tris, followed by denaturing at 100°C for 10 minutes and a quick chill on ice, to ensure uniform distribution of samples for accurate quantitative PCR (qPCR) results.

Extracted DNA samples were tested in duplicate and quantified in a 2-LTR qPCR using specific primers and probes: forward primer SIVmac251 2-LTR F: 5'-CGC CTG GTC AAC TCG GTA CTC-3' based in the 5' U5; reverse primer SIVmac251 2-LTR R: 5'-GGT ATG ATG CCT TCT TCC TTT TCT AAG-3' based in the 3' U3; and probe SIVmac251 2-LTR Probe: 5'-/56-FAM/CCC TGG TCT/ZEN/GTT AGG ACC CTT TCT GCT TTG /3IABkFQ/-3' overlapping the junction between the two primers. The number of tested cells was assessed by quantifying RM-CCR5 expression in each sample using the forward primer RM-CCR5 F: 5'-CCA GAA GAG CTG CGA CAT CC-3'; the reverse primer RM-CCR5 R: 5'-GTT AAG GCT TTT ACT CAT CTC AGA AGC TAA C-3'; and the probe 5'-/56-FAM/TTC CCC TAC/ZEN/AAG AAA CTC TCC CCG GTA AGT A/3IABkFQ-3'. Real-time PCRs and data analyses were performed utilizing an ABI 7900 HT real-time machine (Applied Biosystems, Foster City, CA). All primers and probes were produced by Integrated DNA Technologies (IDT), Coralville, IA.

Using the absolute count of PBMCs determined from the TruCounts, we transformed the data from 2-LTR circles/million PBMCs to 2-LTR circles/mL blood.

Due to low cell counts in the jejunal biopsies, we were unable to quantify levels of 2-LTR circles in these samples.

4.4.7 Statistics

Linear mixed effects models were performed on 2-LTR circles in blood and paired t-test was performed on 2-LTR circles in LNs. Linear mixed effects models were performed in R (The Comprehensive R Archive Network [CRAN], Vienna, Austria); t-tests were performed in GraphPad Prism (GraphPad software, La Jolla, CA).

4.4.8 Modeling 2-LTR dynamics

To help interpret the observed dynamics of 2-LTR, we extended a model of viral dynamics under integrase inhibitor therapy (314, 338, 339), by including an equation for 2-LTR⁺ cells. We assumed that a fraction of reverse transcribed HIV DNA in infected cells originate 2-LTR circles. In this model, target cells (T) are created at a constant rate λ , die at rate d , and are infected by the virus (V) at rate β . Infected cells (I_1 cells) are generated by infection and reverse transcription of HIV RNA. These cells are lost by death (δ_1), possibly due to effector CD8⁺ cells, by integration of the proviral DNA at rate k , and circularization of the HIV DNA at rate ρ . Cells containing 2-LTR circles are also lost by death at rate δ_1 . We assume RAL reduces the integration step with efficacy ω . Cells with integrated HIV DNA (I_2) are productively infected, producing virus at rate p per cell and are lost at rate δ_2 , again possibly dependent on CD8⁺ cells. The model equations are:

$$\begin{aligned}\frac{dT}{dt} &= \lambda - dT - \beta VT \\ \frac{dI_1}{dt} &= \beta VT - (\delta_1 + \rho)I_1 - k(1-\omega)I_1 \\ \frac{dR}{dt} &= \rho I_1 - \delta_1 R \\ \frac{dI_2}{dt} &= k(1-\omega)I_1 - \delta_2 I_2 \\ \frac{dV}{dt} &= pI_2 - cV\end{aligned}$$

We assumed steady state before CD8⁺ cell depletion, with $V_0=10^6$. We then parameterized the model with values from previous publications (308, 314), and performed simple fits of the model to the changes in 2-LTR/ml to estimate ρ and the effect of CD8⁺ cell depletion. In these fits, we searched for one best set of parameters for all the data together, *i.e.*, the 20 RMs, normalized at the initial time and assuming three different effects of CD8⁺ cell depletion: (i) on the death of infected cells before integration, by reducing δ_1 in the model; (ii) on the death of productively infected cells by reducing δ_2 ; or (iii) on the viral production, by increasing p . However, our interest is not in the specific values of the parameters, but rather in the general behavior of the model and how it compares with our observed 2-LTR dynamics under different treatment conditions. The model was simulated using R and for the fits, we used the “DEoptim” package of R. We compared models and selected the best one based on the corrected AIC (310).

4.5 RESULTS

4.5.1 CD8⁺ cell depletion increases the levels of pVL and of the 2-LTR circles in the periphery but it has minimal impact on 2-LTR levels in the LNs

CD8⁺ cells were depleted by administering 50 mg/kg of the monoclonal antibody M-T807R1 to 4 SIVmac251-infected RMs at 56 dpi and then again after 22 days. M-T807R1 administration resulted in a rapid depletion of the CD8⁺ cells from the periphery for the duration of the follow-up (Figure 11A). In the intestine, >99% of the CD8⁺ cells were also depleted (Figure 11B). However, the impact of the depleting antibody was minimal on the CD8⁺ cells in the LNs (Figure 11C).

Peripheral CD4⁺ cells experienced a rapid, but transient decrease at time of the first CD8 depletion, with a slight recovery occurring between the two depletion points (Figure 11A). In both the gut biopsies and LNs, CD4⁺ T cells were not impacted by the CD8⁺ cell depletion (Figure 11B-11C).

As a result of the CD8⁺ cell depletion, a median increase in pVL of 0.8 log₁₀ (range: 0.4 – 1.4 log₁₀) occurred, which persisted throughout follow-up (Figure 11D). We then quantified the levels of 2-LTR circles in mononuclear cells isolated from both circulation and superficial LNs collected at specific points posttreatment. After quantifying 2-LTR circles/million PBMCs, we transformed the data to 2-LTR circles/mL of blood utilizing the absolute count of PBMCs obtained from TruCount staining of whole blood. The levels of 2-LTR circles increased in the whole blood after the first M-T807R1 administration (p=0.022) (Figure 12A). Conversely, 2-LTR circle levels did not change in the LNs of the RMs (p=0.3734) (Figure 12A) and we did not quantify the 2-LTR circles in the gut, as we did not recover enough cells from the gut biopsies.

4.5.2 RAL monotherapy decreases pVL but does not impact the 2-LTR circles

To better understand the impact of the CD8⁺ cell depletion on the fate of the virus in RMs, we performed an additional study in which 8 RMs were administered RAL monotherapy for 23 days. Peripheral and LN CD4⁺ cells slightly recovered during RAL treatment (with a recovery of <200 CD4⁺ T cells/ μ L in blood, and average of 5% of CD4⁺ T cells recovered in the LNs). Conversely, the levels of CD4⁺ T cells remained unchanged in the gut. Peripheral CD8⁺ T cells were slightly boosted immediately after RAL initiation (average 200 CD8⁺ T cells/ μ L blood), while the treatment had no impact on the CD8⁺ T cells from the gut and LNs (Figures 13A-C).

Upon RAL initiation, a median reduction in pVL of 1.75 log₁₀ (range: 1.1 – 4 log₁₀) was observed (Figure 13D).

Interestingly, the 2-LTR circles did not statistically increase during RAL (p=0.51) treatment in neither the blood (p=0.51) nor the LNs (p=0.1467) (Figure 12B).

4.5.3 Combined RAL monotherapy and CD8⁺ cell depletion results in a slight decline of plasma VLs associated with a sustained increase in 2-LTR circles

Finally, to assess the role of the CD8⁺ cells in controlling 2-LTR circles, we performed an experiment in which RMs were administered both M-T807R1 and RAL monotherapy. CD8⁺ cell depletion and RAL were administered as in the first two groups, with the initiation of the RAL monotherapy following two days after the first CD8⁺ cell depletion.

Peripheral and jejunal CD8⁺ cells were rapidly and completely depleted after the first administration of M-T807R1, and remained depleted throughout the follow-up (Figure 14A,B). CD8⁺ cell depletion after administration of M-T807R1 was slower and less prominent in the LNs (Figure 14C).

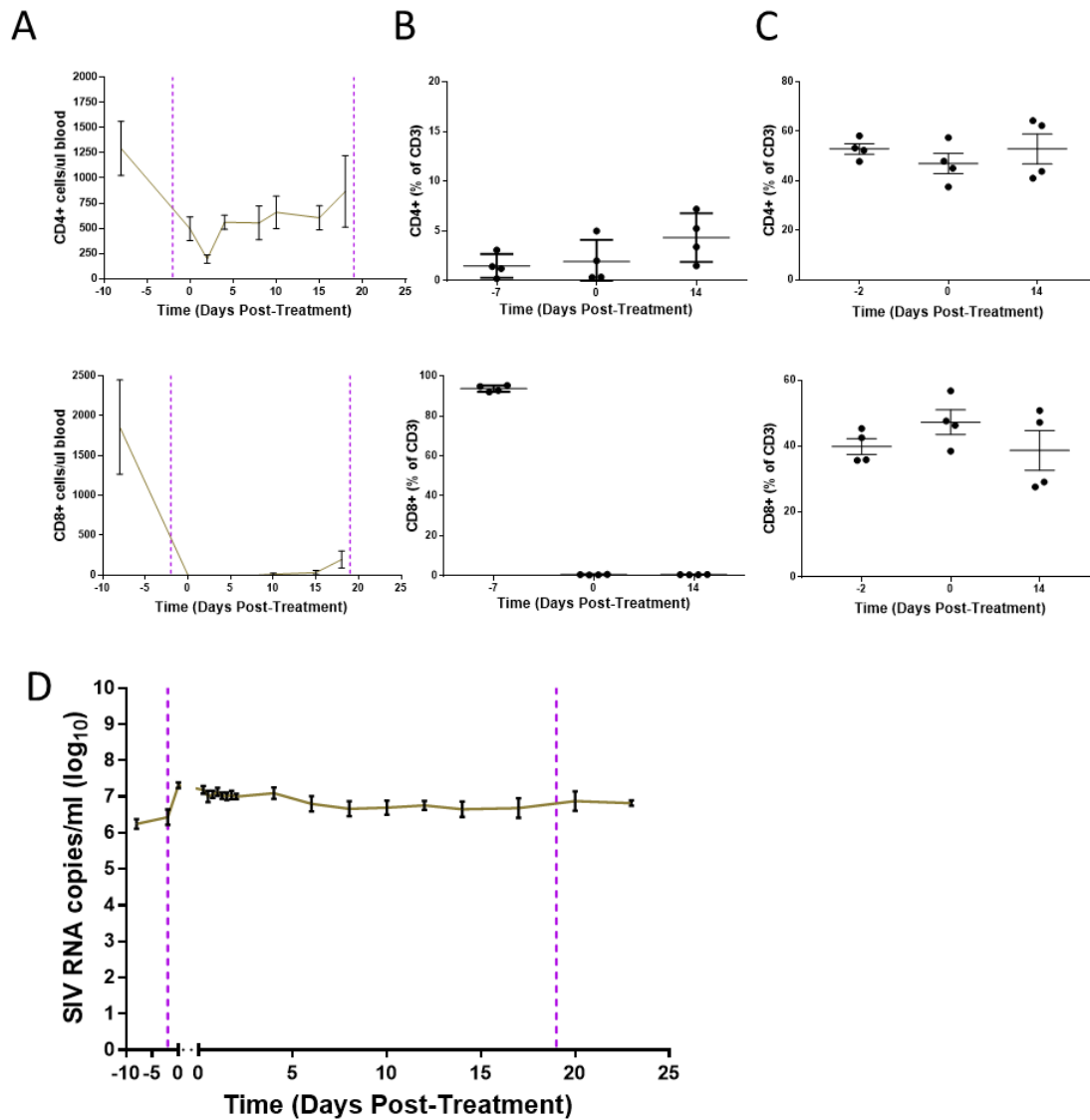


Figure 11. Effects of CD8⁺ cell depletion alone.

The effects of CD8⁺ cell depletion on CD4⁺ and CD8⁺ cells in (A) peripheral blood (absolute values), (B) jejunal biopsies (percentage of CD3⁺ cells), (C) superficial LNs (percentage of CD3⁺ cells), and on (D) plasma viral load (pVL). Error bars represent SEM. LN data includes historical reference values before CD8⁺ cell depletion (day -2).

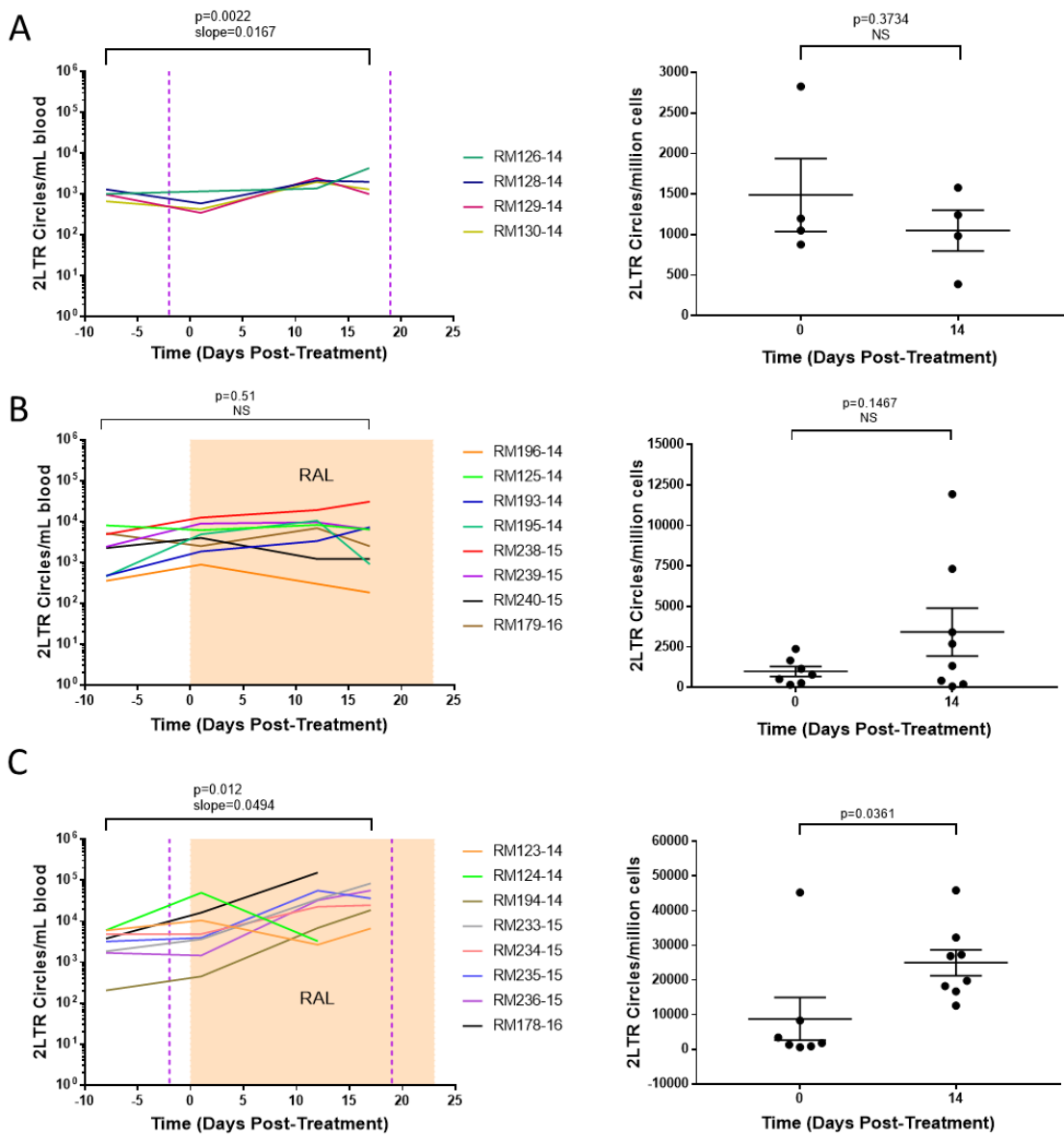


Figure 12 Effects of CD8 depletion with or without RAL monotherapy on 2-LTR circles in blood and LNs.

(A) 2-LTR circles in blood are represented as number of circles per mL of blood, (B) 2-LTR circles in LNs are represented as number of circles per million cells. A linear mixed effects model was used to analyze the dynamics in blood and a paired t-test was performed for LN.

Peripheral CD4⁺ T cells experienced a sharp drop (260 CD4⁺ cells/ μ L blood) after the first round of M-T807R1 administration (Figure 14A), followed by a recovery during RAL therapy (Figure 14A). Gut and LN CD4⁺ T cells recovered during RAL treatment (average recovery of 4.2% and 13.7%, respectively) (Figure 14B,C).

Similar to the CD8⁺ cell depletion only group, we observed an immediate median increase in pVL of 0.6 log₁₀ (range: -0.2 – 0.9 log₁₀) following the first round of the M-T807R1 administration. In these macaques, initiation of RAL therapy, two days after the CD8⁺ cell depletion, led to only a small decrease in pVL (median: 0.975 log₁₀; range: 0.5 – 1.78 log₁₀) (Figure 14D).

Unlike the CD8⁺ cell depletion only or the RAL monotherapy only groups, the RMs subjected to both CD8⁺ cell-depletion and RAL monotherapy experienced a fast and significant increase in both peripheral (p=0.012) and LN (p=0.0361) 2-LTR circles (Figure 12C).

4.5.4 What effector mechanism of CD8⁺ cells is responsible for the observed 2-LTR dynamics?

We used a model of viral and 2-LTR dynamics to help interpret the results described above (see Methods for a description of the model). We analyzed three possible assumptions previously suggested for the effects of CD8⁺ cells (141, 142, 146, 148, 303, 311-313), *i.e.*, CD8⁺ cells could (i) kill infected cells before integration; (ii) kill productively infected cells; or (iii) reduce viral production through non-cytolytic mechanisms. We fitted the model to the three treatment groups together to see what effect of CD8⁺ cell depletion best explained all the data.

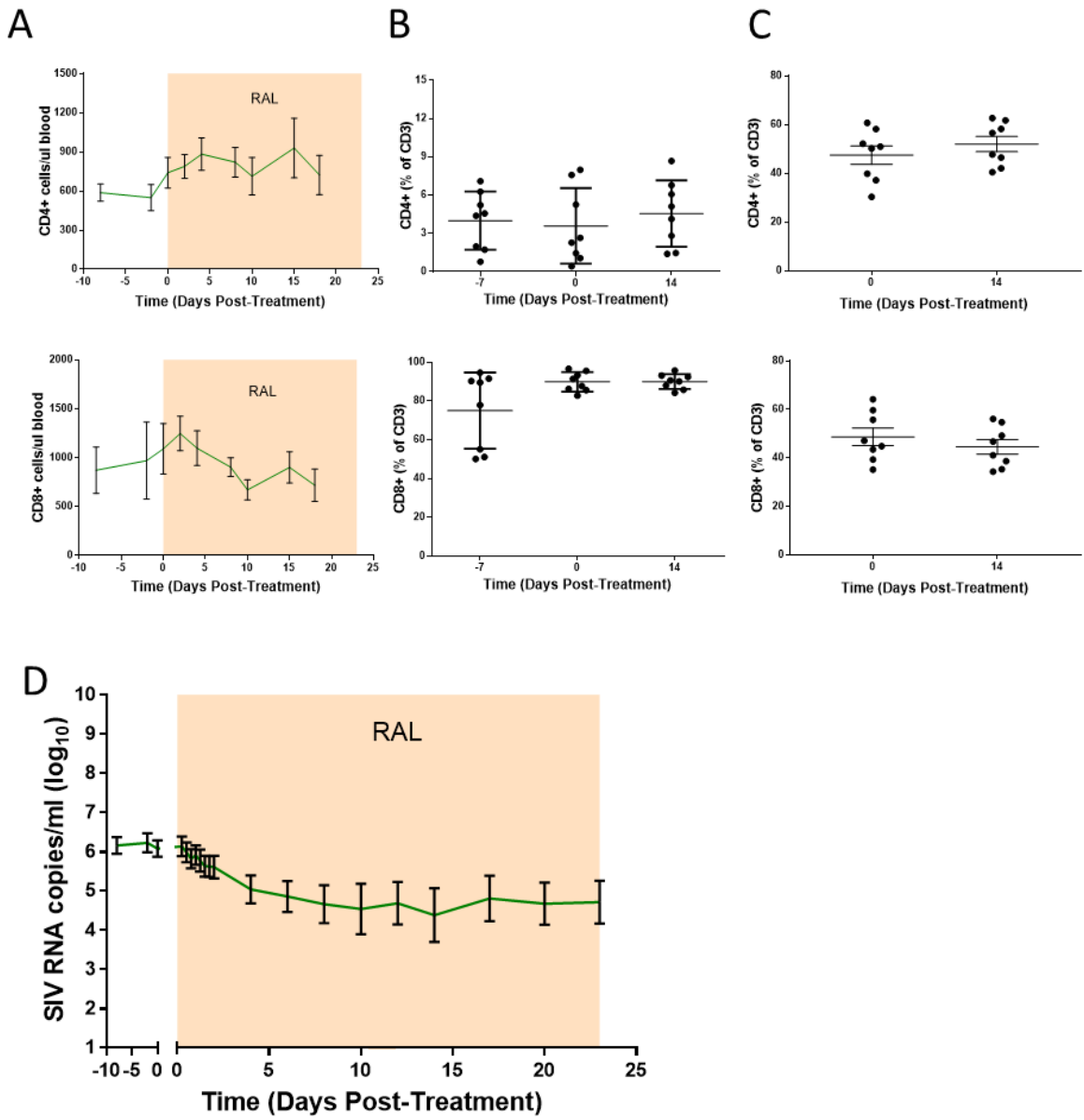


Figure 13. Effects of RAL monotherapy alone.

The effects of RAL monotherapy on CD4⁺ and CD8⁺ cells in (A) peripheral blood (absolute values), (B) jejunal biopsies (percentage of CD3⁺ cells), (C) superficial LNs (percentage of CD3⁺ cells), and on (D) pVL. Error bars represent SEM.

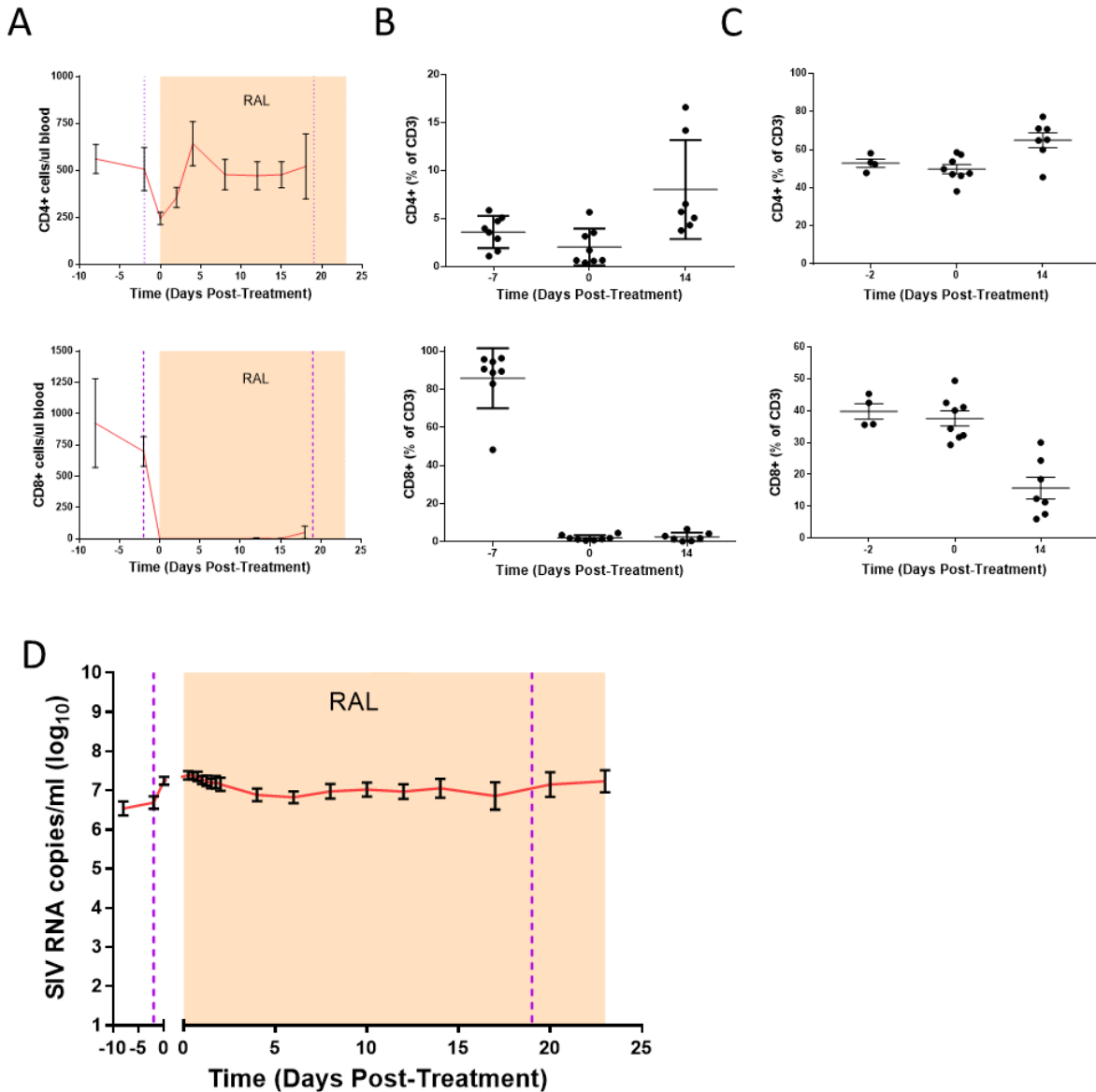


Figure 14. Effects of CD8⁺ cell depletion and RAL monotherapy.

The effects of CD8⁺ cell depletion and RAL monotherapy on CD4⁺ and CD8⁺ cells in (A) peripheral blood (absolute values), (B) jejunal biopsies (percentage of CD3⁺ cells), (C) superficial LNs (percentage of CD3⁺ cells), and on (D) pVL. Error bars represent SEM. LN data includes historical reference values before CD8⁺ cell depletion (day -2).

In Figure 15, we show the best fits of the model to the data in each CD8⁺ cell depletion scenario. We found that the best fit was when the assumed effect was in that killing infected cells

occurred before integration, δ_1 (AIC = -114.13), although an effect on viral production, p , also resulted in a good fit to the data (AIC = -112.44). Both the effects on killing productively infected cells and on reducing viral production predict too fast initial increase in 2-LTR⁺ cells under CD8⁺ cell depletion (with or without RAL) (Figure 6, bottom two rows). We also tested whether or not the possible CD8⁺ cell effect is a combination of two of these mechanisms simultaneously, but that did not improve the results.

4.6 DISCUSSION

Experimental *in vivo* CD8⁺ cell depletion in nonhuman primates has been strategically used to analyze the role of the CTLs, as well as other CD8⁺ cells (particularly natural killer cells) on controlling viral replication in both pathogenic and nonpathogenic SIV infections (24, 140-143, 145, 146, 299). More recently, CD8⁺ cell depletion was utilized to support the role of the SIV-specific CD8⁺ cells in controlling the viral rebound after viral reactivation with latency reversing agents (LRAs) in posttreatment controller RMs (298). In addition, CD8⁺ cells, in particular CD8⁺ T lymphocytes, critically contribute to suppressing viremia in SIV-infected RMs on ART (140). However, the specific mechanisms by which CD8⁺ cells suppress viremia are poorly understood.

In this study, our goal was to measure the changes in 2-LTR circles, as a surrogate of cells containing unintegrated virus, in SIV-infected RMs depleted of CD8⁺ cells in the presence or absence of RAL. We compared the data to the predictions of a mathematical model of viral and 2-LTR dynamics. Our results suggest that CD8⁺ cells are able to cytolytically eliminate infected cells containing 2-LTR circles prior to integration. Indeed, the overall behavior of 2-LTR⁺ cells across the three animal groups is best captured by an effect of CD8⁺ cells on δ_I .

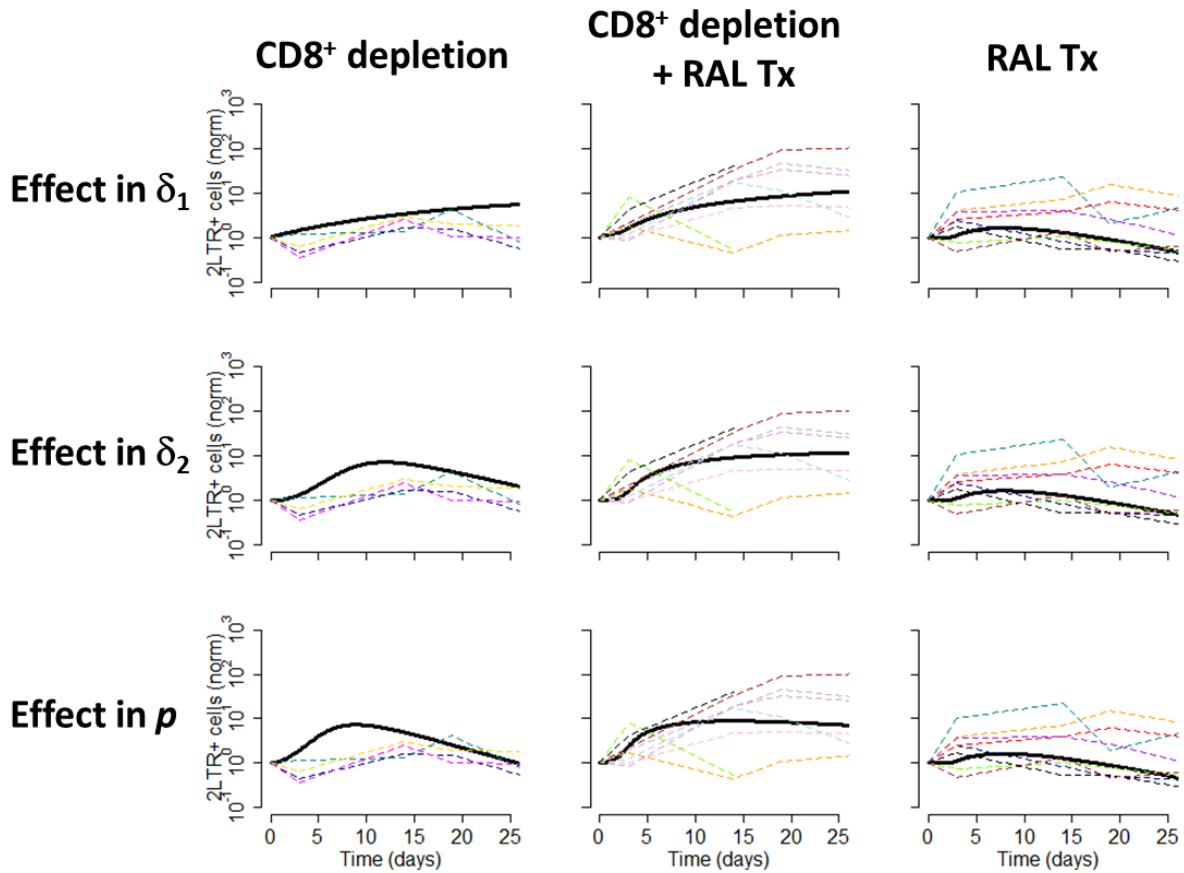


Figure 15. CD8⁺ cells affect death rate of infected cells prior to integration.

A model of viral and 2-LTR dynamics was developed to analyze the observed data and potential effects of CD8⁺ cell: (i) killing of infected cells prior to integration (effect in δ_1); (ii) killing of productively infected cells (effect in δ_2), or (iii) non-cytolytically reducing viral production (effect in p) between the three treatment groups. Dashed lines represent normalized 2-LTR⁺ cells/ml data (to the pre-intervention levels) for each RM; solid, bold line represents model projection for best fit. Parameters of the model were: $V_0=10^6$ copies/ml, $\beta=10^{-8}/(\text{copies/ml day})$, $p=10^3$ virion/(cell day); $c=23/\text{day}$, $d=0.01/\text{day}$; $k=2.6/\text{day}$; $\delta_1=0.15/\text{day}$; $\delta_2=1.0/\text{day}$; $\omega=0.95$; and $p=0.02/\text{day}$ (estimated). We assumed steady state before any intervention, which allows one to estimate λ . The estimated effects of CD8⁺ cell depletion where a 14-fold reduction in δ_1 (top row), a 2.4-fold reduction in δ_2 (middle row) and a 2-fold increase in p (bottom row).

With hindsight, the observed effects of the three treatment strategies are clear indications of the mechanisms operating and their relative strengths. In the CD8⁺ cell depletion group, the absence of effective anti-SIV specific cells leads to an increase in infection events with concomitant probability of formation of 2-LTR circles, and thus originates the observed increase in the number of these cells. In the combination CD8⁺ cell depletion and RAL therapy group, this

increase is exacerbated. Although productive infections are blocked by therapy, reverse transcription events still occur and, as such, there is an enhanced opportunity to form 2-LTR circles, since RAL treatment leads to 2-LTR circle formation preference over integration. In the RAL monotherapy group, the minor changes in 2-LTR circles reveal the balance between a higher probability of forming these circles induced by therapy, with the rapid control of pVL.

Overall, the data presented here emphasizes the controlling effects of CD8⁺ cells on cells containing 2-LTR circles *in vivo*, further documenting the contribution of the CD8⁺ cells to the success of ART (140). The multiple conditions tested here (presence or absence of RAL monotherapy, with and without CD8⁺ cells) point to how sensitive the development and persistence of 2-LTR circles are to the environment and document the validity of monitoring of the 2-LTR circles as a surrogate of HIV persistence. Further, modeling results indicate that CD8⁺ cells exert an effect on infected cells prior to integration. Due to the potential role 2-LTR circles have in maintaining the viral reservoir, it is important to continue exploring these viral isoforms in future research endeavors targeting cure.

5.0 CHAPTER THREE: EMERGENCE OF RESISTANCE MUTATIONS IN SIMIAN IMMUNODEFICIENCY VIRUS (SIV)-INFECTED RHESUS MACAQUES RECEIVING NON-SUPPRESSIVE ANTIRETROVIRAL THERAPY (ART)

Benjamin Bruno Policicchio ^{1,2*}, Paola Sette ^{1,3*}, Cuiling Xu ^{1,3}, George Haret-Richter ^{1,3}, Tammy Dunsmore ^{1,3}, Ivona Pandrea ^{1,2,3}, Ruy M. Ribeiro ^{5,6}, and Cristian Apetrei ^{1,2,4}

¹Center for Vaccine Research, University of Pittsburgh, Pittsburgh, PA, 15261, USA; ²Infectious Diseases and Microbiology, Graduate School of Public Health, ³Pathology, ⁴Microbiology and Molecular Genetics, School of Medicine, University of Pittsburgh, Pittsburgh, PA 15262; ⁵Theoretical Biology and Biophysics Group, Los Alamos National Laboratory, Los Alamos, NM, 87545, USA; ⁶Laboratorio de Biomatemática, School of Medicine, University of Lisbon, Portugal

*These authors contributed equally to this work.

5.1 PREFACE

The data presented herein has been adapted from a submitted manuscript: Benjamin Bruno Policicchio, Paola Sette, Cuiling Xu, George Haret-Richter, Tammy Dunsmore, Ivona Pandrea, Ruy M. Ribeiro, and Cristian Apetrei. Emergence of resistance mutations in simian immunodeficiency virus (SIV)-infected rhesus macaques receiving non-suppressive antiretroviral therapy (ART).

The work presented in this chapter is for completion of Aim 3 in partial fulfillment of the requirements for the degree of Doctor of Philosophy. Benjamin Policicchio processed blood samples, extracted viral RNA from plasma samples and performed quantitative reverse transcriptase PCR (qRT-PCR) on plasma samples, analyzed and compiled flow cytometry data, produced figures, wrote and edited the manuscript. Paola Sette performed PCR on plasma samples, sequenced resulting PCR samples and analyzed for existence of resistance mutations. Cuiling Xu stained blood and acquired stained samples on a flow cytometer. George Haret-Richter and Tammy Dunsmore administered the drugs to the RMs and bled the RMs.

5.2 ABSTRACT

Two SIVmac251-infected rhesus macaques received tenofovir/emtricitabine with raltegravir intensification. Viral rebound occurred during treatment and sequencing of reverse transcriptase and integrase genes identified multiple resistance mutations. Similar to HIV infection, antiretroviral-resistance mutations may occur in SIV-infected nonhuman primates receiving nonsuppressive ART. As ART administration to nonhuman primates is currently dramatically expanding, fueled by both cure research and the study of HIV-related comorbidities, viral resistance should be considered for study design and data interpretation.

5.3 INTRODUCTION

Due to the RT infidelity (340), HIV replication associates rapid and frequent development of viral mutations, often leading to the emergence of either noninfectious or less fit strains. ARV drug administration selects for specific mutations allowing the virus to evade the drug(s) (341, 342). Resistance mutations occur more frequently in ARV-treated HIV-infected subjects with incomplete viral suppression. These aspects are largely ignored for SIV-infected NHPs on ART, even though, until recently, ARV regimens were only partially effective in SIV-infected macaques (343, 344).

SIV variants engineered to harbor known HIV mutations to NRTIs and INTIs become resistant to these drugs; HIV and SIV share resistance profiles (345, 346). Furthermore, SIV may develop *in vitro* mutations against INTI (347), and monotherapy with NRTIs and INTIs may result in emergence of drug-resistant SIV strains *in vivo* (348-350).

Here, we report the development of resistance mutations in SIV-infected RMs receiving suboptimal ART. These results are relevant, as ARV administration to SIV-infected NHPs is currently dramatically expanding, fueled by both cure research and research targeting HIV-related comorbidities.

5.4 MATERIALS AND METHODS

5.4.1 Ethics Statement

RMs were housed and maintained at the University of Pittsburgh, according to the standards of the AAALAC, and experiments were approved by the University of Pittsburgh IACUC (protocol

16058287). The animals were cared for according to the Guide for the Care and Use of Laboratory Animals and the Animal Welfare Act (351). Efforts were made to minimize animal suffering: RMs were socially housed together indoors in suspended stainless steel cages, received 12/12 light/dark cycle, were fed twice daily with commercial primate diet, and water was provided *ad libitum*. A variety of environmental enrichment strategies were employed, including providing toys to manipulate and playing entertainment videos in the animal rooms. The animals were observed twice daily for signs of disease or discomfort, any of which were reported to the veterinary staff for evaluation. For sample collection, animals were euthanized with 10 mg/kg ketamine HCl (Park-Davis, Morris Plains, NJ, USA).

5.4.2 Animals, infections and treatments

Two Indian-origin RMs (*Macaca mulatta*) were included in this study. They were intravenously infected with 300 TCID-50 of SIVmac251 and were closely clinically monitored throughout infection and treatment.

During chronic infection (250 days postinfection), both RMs received TFV and FTC subcutaneously at 20mg/kg and 40mg/kg once daily, respectively, for 4 weeks, followed by intensification with orally-administered RAL (20mg/kg *bid*). RAL was then interrupted after 12 weeks.

5.4.3 Sample and sample processing

Blood was collected from all RMs biweekly, with daily blood sampled upon initiation and interruption of RAL for one week. Within one hour of blood collection, plasma was harvested and PBMCs were separated from the blood using lymphocyte separation media (LSM, MPBio, Solon, OH).

5.4.4 Plasma viral load quantification

We monitored the degree of viral suppression by measuring pVLs on all samples collected. pVLs were tested by using qRT-PCR, using the following primers and probe: SIVmac251F: (5'-GTC TGC GTC ATC TGG TGC ATT C-3'); SIVmac251R: (5'-CAC TAG GTG TCT CTG CAC TAT CTG TTT TG-3'); SIVmac251Probe: (5'-CTT CCT CAG/ZEN/TGT GTT TCA CTT TCT CTT CTG CG/3IABkFQ/-3') and the conditions described in (343).

5.4.5 Flow cytometry

Whole blood was stained using a two-step TruCount technique to enumerate the absolute levels of CD4⁺ T cells in the blood, as previously described (352). The following fluorescently-labeled antibodies were used for staining blood (all antibodies from BD Biosciences, San Jose, CA, USA): CD4 (APC), CD8 (PE-CF594), CD3 (V450), CD45 (PerCP), Ki-67 (PE). Ki-67 was stained by first fixing and permeabilizing cells prior to staining. Flow cytometry acquisitions were performed on an LSR-II flow cytometer (BS Biosciences).

5.4.6 Assessment of the occurrence of resistance mutations

The RT and INT genes of the SIVmac variants circulating in plasma samples at collected prior to initiation of ART [0 weeks posttreatment (wpt)], as well as 2, 8, 12 wpt and finally, after cessation of RAL (20 wpt) were sequenced to determine the presence of resistance mutations. The following primers were used for PCR and sequencing: RT outer primers RT3 (5'-GTT GCA TTA AGA GAA ATC TGT GAA AAG ATG G-3') and RT5 (5'-CCA GGT CTC TCT TTG TGG CAA CTC-3') and inner primers RT6 (5'-CCA ATC CAT ACA ACA CCC CCA C-3') and RT7 (5'-CAA CTT CCA TTT TGT CGG CCA C-3'); INT outer primers INTF1 (5'-CAT

GGG CAG GTA AAT TCA GAT C-3') and INTR1 (5'-TAT CCC CTA TTC CTC CCC TTC-3'), and nested primers INTF2 (5'-TAG GGA CTT GGC AAA TGG AYT G-3') and INTR2 (5'-CTG AAT TTG CTT GTT CCC TGA TTC-3'). These partial gene sequences correspond to specific regions within the RT (566 bp fragment, between N54 and L241) and INT (342 bp fragment, between G59 and S171) known to encompass common resistance mutations. PCR conditions were as follows: RT outer: initial denaturation of 5 minutes at 95°C; 30 cycles of 1 min at 95°C, 30 sec at 54°C, 45 sec at 68°C; and a final elongation of 5 min at 68°C. RT inner: initial denaturation of 5 min at 95°C; 40 cycles of 1 min at 95°C, 30 sec at 51°C, 45 sec at 68°C; and a final elongation of 5 min at 68°C. INT outer: initial denaturation of 5 min at 95°C; 30 cycles of 1 min at 95°C, 30 sec at 50°C, 30 sec at 68°C, 30 sec; and a final elongation of 5 min at 68°C. INT inner: initial denaturation of 5 min at 95°C; 40 cycles of 1 min at 95°C, 30 sec at 51°C, 30 sec at 68°C; and a final elongation of 5 min at 68°C. PCR products were gel-purified and submitted to conventional sequencing using the nested primers.

The obtained RT and INT sequences were aligned to the SIVmac251 isolate Mm251 (GenBank: M19499.1) using Sequencher software and the emergence of resistance mutations was assessed based on the Stanford HIV Drug Resistance Database (<https://hivdb.stanford.edu>).

5.5 RESULTS AND DISCUSSION

Upon initiation of the TFV/FTC treatment, a ~1.5 log decrease was achieved within the first two weeks in RM130, followed by a 0.7 log rebound in pVL. In RM127, a ~2.5 log decrease in pVL occurred, which was maintained through week 4. Following RAL intensification, a ~0.5 log decrease in pVLs occurred in RM130, which was maintained for 2 weeks, but was rapidly followed by a robust pVL rebound throughout the follow-up. Conversely, in RM127, RAL intensification further suppressed the virus, with pVLs below the limit of detection for at least

four weeks. However, at week 8, pVLs rebounded by ~3 log and remained high throughout RAL treatment. Robust pVL rebounds were observed in both animals (~2 log in RM130 and ~1.5 log in RM127) after RAL discontinuation (Figure 16a).

In both animals, CD4⁺ T cells recovered slightly after initiation of NRTIs, with a further recovery following RAL intensification, which was reversed after RAL cessation (Figure 7b). The frequency of CD4⁺ and CD8⁺ T cells expressing Ki-67 remained stable during RAL intensification, and increased after RAL cessation (Figure 16c).

Such patterns of viral replication under ART being suggestive of resistance mutations, we investigated whether this partially suppressive treatment resulted in the emergence of drug-resistant strains. Serial sequence analyses demonstrated that major and minor mutations emerged in both genes in both animals (Figure 16a). Thus, sequence analyses showed that, in RM130, major drug resistance mutations occurred at the same time point (12 wpt) in both INT (Q148R) and RT (K65R). Conversely, in RM127, only one major mutation was observed to occur only in the RT at one timepoint (K65R, 12 wpt). In humans, occurrence of these mutations was reported to be associated with treatment failure: K65R results in a 3.3-3.6-fold increase in resistance to TFV and Q148R results in a 44-46-fold increase in resistance to RAL (353).

Multiple minor mutations were observed at multiple time points (2, 8, and 20 wpt) in RM130 RT, with no minor mutations occurring in RM127 (Figure 16). Interestingly, in spite of cessation of RLT treatment, VLs decreased in RM127 at 20 wpt. This may be due to a boost of cell-mediated immune responses against the rebounding resistant virus, as previously reported (350).

As such, our analysis documents accumulation of ART resistance mutations as the cause of treatment failure in these RMs. To our knowledge, this is the first documentation of SIV resistance to ARVs *in vivo* in RMs on nonsuppressive tritherapy. Previous studies reporting that SIV may share similar resistance profiles to HIV and can develop resistance mutations against NRTI or INTI were performed in monotherapy (345-350).

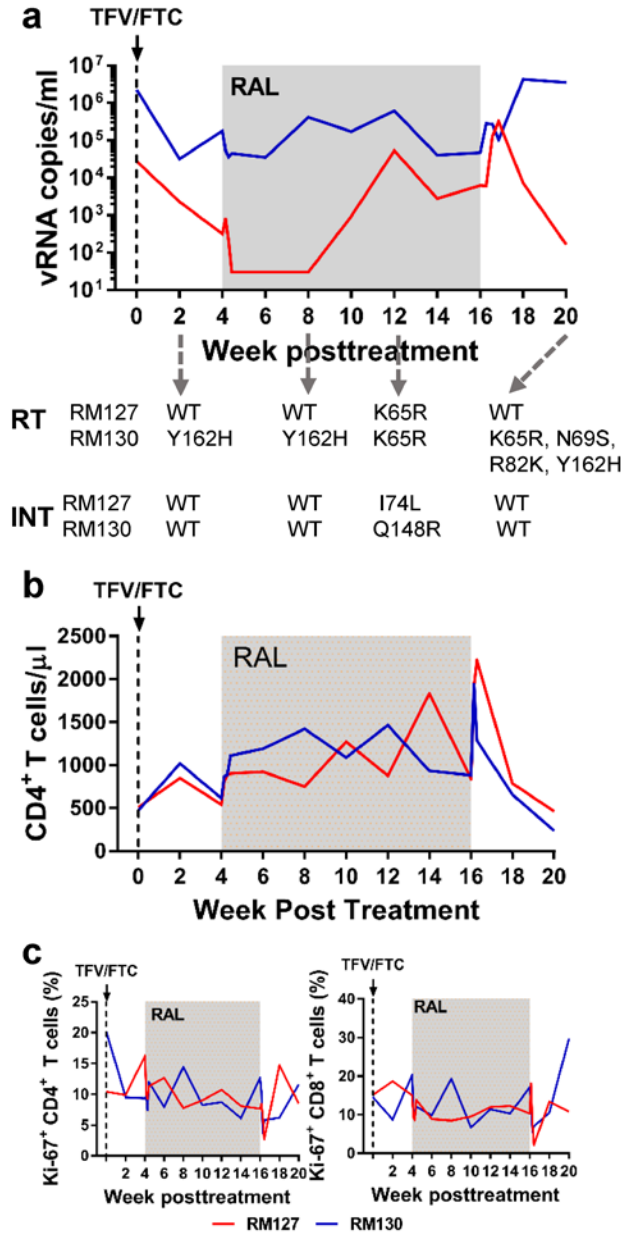


Figure 16. Administration of nonsuppressive ART to two SIVmac251-infected rhesus macaques resulted in development of resistance mutations and treatment failure.

(a) Plasma viral load levels following treatment with TFV/FTC followed by intensification with RAL four weeks later. Reverse transcriptase (RT) and integrase (INT) regions of virus amplified from plasma at select points posttreatment listed in the figure were sequenced to determine the presence or absence of ART-resistance mutations. In the absence of detected resistance mutations at the selected timepoints, those strains are considered wild type. (b) The ratio of circulating CD4⁺-CD8⁺ T cell counts during the follow-up; (c) Changes in the levels of circulating CD4⁺ and CD8⁺ T cell activation during the follow-up, as documented by the frequency of Ki-67 expression.

Clinical trials conducted during the last two decades were plagued by aspects related to HIV resistance to ART (354), but these aspects tend to be ignored when designing and performing NHP studies involving ART. The emerging fields of HIV cure and comorbidities combined with new highly-effective suppressive ART regimens for macaques have increased the use of the ART-treated macaque model (355). As such, it is to be expected that viral resistance to ART will emerge as a significant problem for animal studies too. Our results emphasize the need to consider drug resistance as a potentially critical limitation factor in the rapidly emerging field of modeling ART in NHPs, particularly when nonsuppressive ART regimens are used.

6.0 OVERALL DISCUSSION

The goal of this study was to understand the effector mechanism(s) of CD8⁺ T cells against SIV-infected cells. CD8⁺ T cells are known to play an important role in suppressing viral replication in HIV/SIV infections, most clearly seen when CD8⁺ cells are depleted in SIV-infected nonhuman primates (24, 68, 70, 137, 138, 140, 143, 145, 146, 148, 298, 299, 315, 316). However, the exact mechanism(s) employed by CD8⁺ T cells to suppress viral replication are not well understood. It has been shown that they may exert a direct, cytolytic response against infected cells through either the stimulation of the Fas/FasL pathway and/or release of granzyme/perforin (300, 301). Furthermore, CD8⁺ T cells indirectly interfere with *de novo* infections and the release of new virions by releasing several antiviral factors, including: CAF, RANTES, MIP-1 α , MIP-1 β , and α -defensins (179, 190, 302). However, up until 2010, no one was able to directly probe which mechanism (or both) is utilized by CD8⁺ cells *in vivo*. Three independent research groups published data concluding that CD8⁺ cells most likely exert a non-cytolytic role during HIV/SIV infection. Two groups reached these conclusions by comparing the lifespans of infected cells in SIV-infected RMs treated with NRTIs in the presence or absence of CD8⁺ cells and observing that the infected cell lifespans between these groups are not different (141, 142). However groundbreaking these papers are, their conclusions are not universally accepted by the field of HIV research due to multiple criticisms in their study designs and the resulting mathematical modeling in each publication (212, 311, 312, 319).

Our overall hypothesis was that CD8⁺ T cells exert a cytotoxic response against infected cells prior to viral integration. Though this goes against the aforementioned papers' conclusions,

our use of RAL in place of NRTI allows us to more directly dissect a potential role of the cytotoxic response without interfering factors, such as viral-induced cytopathicity or only being able to look at the cytotoxic response prior to peak antigen presentation. Indeed, our experimental model of RAL treatment in the presence and absence of CD8⁺ cells allowed us to determine a difference in the half-life of infected cells prior to viral integration compared to productively cells.

In section 3.0, we measured pVL differences in three groups of SIV-infected RMs: i) with CD8⁺ cell depletion only; ii) with CD8⁺ cell depletion plus RAL treatment; iii) with RAL monotherapy. We coupled the treatment strategies with a very frequent sampling schedule to aid in the subsequent mathematical modeling. In the CD8⁺ cell depletion and RAL monotherapy group, we reported an average decrease in pVL of 0.6 log₁₀ SIV RNA copies/mL plasma during treatment, while in the RAL monotherapy group, the average decrease in pVL was 1.99 log₁₀. These values by themselves are significant. In the previous studies, based on the use of NRTIs, no differences were observed between groups (141, 142). Upon fitting a model of viral dynamics in two steps to our data (the first step being a fit of the data from the RAL monotherapy group by itself and the second step being fitting the data from all twenty macaques simultaneously using the death rates estimated from the RAL monotherapy group), we concluded that the death rate of infected cells prior to integration was reduced 82% in the CD8⁺ cell depletion with RAL treatment group compared to the RAL monotherapy group. As such, our original hypothesis is correct. However, since our model tested multiple potential effector mechanisms simultaneously, we also found that CD8⁺ T cells exert a non-cytolytic effect on viral production. While not a part of the original hypothesis, this result agrees with the previously published conclusions conveying a non-cytolytic effect against replication, but goes beyond them by specifying the actual mechanism. The future steps for this study are to repeat the experiment, but take into consideration the potential effects cytotoxic CD4⁺ T cells may have on killing infected cells and reducing viral production (356). Analyzing the rebound of pVL following RAL interruption in

the study groups will need to be performed to confirm our data and add another level of support to our hypothesis.

In section 4.0, we expanded upon our analysis of the differences in pVL and looked at the effect of the three treatment groups on 2-LTR circle levels in PBMCs and LNs. 2-LTR circles have been reported to be useful as a surrogate of viral replication (337), and another study showed that cells containing virus prior to viral integration can represent a sizeable fraction of the total population of infected cells (308). 2-LTR circles are formed both by an inherent failure of viral integration and the presence of an InSTI, thus easily allowing us to look at the dynamics of 2-LTR circles in our already-established treatment groups. Further, they represent a unique aspect of the infection cycle whereby they are present either by themselves (as seen in previously uninfected cells) or alongside an already integrated viral genome (productively infected), which allows us to ask the question at which specific stage of 2-LTR presence do CD8⁺ T cells target for elimination? By looking at 2-LTR circle levels in PBMCs and LNs, we observed that RAL monotherapy does not increase the 2-LTR levels; CD8⁺ cell depletion significantly increased the 2-LTR levels; combined CD8⁺ cell depletion with RAL treatment further increased the 2-LTR levels and at a faster rate compared the CD8⁺ cell depletion group. By fitting a model of viral and 2-LTR dynamics to the data and using the same three assumptions from section 3.0, we showed that the best fits of the model occurred when there is an effect of CD8⁺ cells against infected cells prior to viral integration. Similar to our results from chapter one, we studied a model where CD8⁺ cells act non-cytolytically against 2-LTR⁺ cells, but this model had a lower AIC score than CD8⁺ cells exerting a cytotoxic response against infected cells prior to viral integration. As such, the results of this work represent a novel approach to monitor virus control by CD8⁺ T cells. This new interpretation of the 2-LTR circles may result in a new biomarker, as no one has thought of using 2-LTR dynamics in this manner previously. Further, since 2-LTR circles have different dynamics from circulating virus in the plasma and that our analysis was done in an extended viral dynamics model including 2-LTR circles, the data presented in this aim

provide somewhat independent support to our hypothesis, apart from the viral dynamics data. Alongside the future research endeavors from aim 1, the effects of 2-LTR dynamics following RAL interruption should be studied and fit in a similar model to corroborate these conclusions.

The third specific aim was intended to expand on the 2-LTR analysis from aim 2 with the intent of analyzing 2-LTR levels during RAL intensification. However, this experiment was not successful, as we observed rebound of virus during the RAL intensification phase. It is well-established that resistance mutations against HIV/SIV occurs frequently, even in the absence of pressures exerted by the drugs. This is attributed to the lack of proof-reading capabilities of viral RT and the very active and prolonged viral replication cycle (357). Resistance mutations occur at a faster rate in the presence of drug monotherapy and when the-ART regimen is not fully suppressive. As such, we were always concerned whether viral resistance will develop in our monkeys due to the study design. We attempted to prevent resistance by implementing a study design consisting of a short period of time prior to RAL intensification (four weeks of TFV/FTC followed by RAL intensification). However, the intensification was not successful, and we saw rebound of pVL during treatment. These results, though disappointing, prompted us to sequence circulating virus to monitor the resistance mutations. Indeed, upon sequencing, we saw both animals developed major and minor resistance mutations against both NRTIs and InSTIs. Though the development of resistance mutations is not novel, the observance of them in SIV-infected RMs during a triple ART regimen is something not previously reported. This data further serves as a reminder to researchers that rapid drug resistance will likely occur in SIV-infected NHPs treated with ART regimens, especially in protocols where non-suppressive virus replication may occur. These results are important as they stress the need to consider viral resistance when designing animal studies involving ART.

In summary, we have proven our hypothesis correct by showing in an *in vivo* model of SIV that CD8⁺ T cells both are cytolytic against infected cells prior to viral integration and are noncytolytic by reducing the overall viral production rate. We observed a similar outcome when

analyzing the effects of CD8⁺ T cells against 2-LTR⁺ cells, thus bolstering our hypothesis. Though we intended to analyze 2-LTR dynamics in a RAL intensification study, we were able to identify resistance mutations appearing in a triple ART regimen. These data will contribute to future vaccine and cure efforts by elucidating the true mechanisms of CD8⁺ T cells against HIV/SIV-infected cells.

7.0 PUBLIC HEALTH SIGNIFICANCE

Despite improved ART drugs and revised strategies for increasing awareness of HIV infection and promoting safer sex practices, HIV still remains one of the largest pandemics and currently affects over 36.7 million people worldwide, with 2.1 new infections occurring yearly (2). Further, efforts to develop a cure or a vaccine to prevent the infection continue to experience roadblocks and failures (358, 359). To develop an effective vaccine or cure, the immune response(s) against the virus needs to be fully understood and of these responses, the cytotoxic response (through CD8⁺ cells) is essential. While virus killing by the CD8⁺ T cells was shown to be essential for controlling viral replication, the exact mechanism of this control is not well understood. This gap in knowledge severely undermines our efforts in cure and vaccine research. Here, we sought to determine if CD8⁺ T cells exert a cytotoxic response against infected cells prior to integration (by both using 2-LTR circles as a surrogate for viral DNA and through modeling of pVL), against infected cells post-integration, or through non-cytolytic mechanisms. By utilizing complex study designs consisting of direct manipulation of major arms of the immune system (i.e. CD8 depletion *in vivo*) and InSTI monotherapy in SIV-infected RMs as a surrogate for HIV-infected humans, we concluded that CD8⁺ T cells exert a strong cytolytic response against infected cells prior to viral integration. This was supported in our work showing the same outcome using data on 2-LTR⁺ cells prior to integration.

One example of how my conclusions may further vaccine efforts is in the use of DTG as a pre-exposure prophylactic in a clinical trial to prevent HIV transmission in a cohort of high-risk individuals. The logic behind this type of clinical trial is DTG will act to prevent viral

infection by preventing viral integration in individuals who become exposed to the virus. As my studies show that CD8⁺ CTLs are able to target viral peptides presented on infected-cells' MHC-I prior to viral integration and kill these infected cells, the use of DTG will elongate the time that these peptides can be presented. This increased presence of viral peptides for removal may allow the host CTL response to more effectively kill these cells. If DTG is shown to act as efficiently as or more efficiently than TFV/FTC (most frequently administered pre-exposure prophylactic), this will increase the types and availabilities of pre-exposure prophylactics for preventing HIV infection.

Another example of how my conclusions may further cure research is in the use of DTG when developing cure strategies to stimulate the CTL response to remove infected cells. Though the majority of infected cells present in a chronic ART-treated HIV-infected contain virus in a latent state and unable to be targeted for removal by the immune system, the use of LRAs and CTL-stimulating drugs (commonly referred to as the “kick-and-kill” strategy”) alongside treatment with DTG may improve the CD8⁺ CTL killing capabilities by allowing viral peptides to be presented on MHC-I for an extended period of time. This may allow CTLs to better recognize and kill these infected cells while simultaneously preventing *de novo* infections.

Collectively, these findings emphasize that the host cytotoxic response against infected cells is essential to explore further and utilize when developing both vaccines against HIV and cures for those currently infected.

APPENDIX A: ABBREVIATIONS

Abbreviations are listed in order of appearance:

HIV – Human Immunodeficiency Virus

CTL – Cytotoxic T Lymphocyte

NRTI – Nucleotide/Nucleoside Reverse Transcriptase Inhibitor

SIV – Simian Immunodeficiency Virus

RM – Rhesus Macaque

RAL – Raltegravir

AIDS – Acquired immunodeficiency Syndrome

ARV – Antiretroviral

ART – Antiretroviral Treatment

NHP – Nonhuman Primate

VL – Viral Load

LN – Lymph Node

PIC – preintegration complex

LTR – Long Terminal Repeat

DC – Dendritic Cell

I.V. – intravenous

Dpi – Day Post-infection

FDA – Food and Drug Administration

MVC – Maraviroc

T20 – Enfuvirtide

TDF/TFV – Tenofovir Disoproxil Fumarate

FTC – Emtricitabine

ABC – Abacavir

AZT – Zidovudine

NNRTI – Non-nucleoside Reverse Transcriptase Inhibitor

EFV – Efavirenz

NVP – Nevirapine

RPV – Rilpivirine

ETR – Etravirine

InSTI – Integrase Strand-transfer Inhibitor

EVG – Elvitegravir

DTG – Dolutegravir

PI – Protease Inhibitor

SQV – Saquinavir

RTV – Ritonavir

DRV – Darunavir

LPV – Lopinavir

MHC-I – Major Histocompatibility Complex – I

TCR – T Cell Receptor

FasL – Fas Ligand

DISC – Death-inducing signaling complex

MIP-1 α – Macrophage inflammatory protein-1 α

RANTES – Regulated Upon Activation Normal T-cell Expressed And Secreted

CAF – T-cell Antiviral Factor

IFN- γ – Interferon- γ

TNF- α – Tumor Necrosis Factor- α

TNFR – TNF Receptor

MAPK- Mitogen-Activated Protein Kinase

ERK – Extracellular Signal-Regulated Kinase

JNK – c-Jun N-terminal Kinase

TRADD – TNFR-associated Death Domain

FADD – Fas-associated Death-domain

RT – Reverse Transcriptase

APOBEC3G – Apolipoprotein B mRNA-editing, Enzyme-catalytic, Polypeptide-like 3G

cDNA – Complementary DNA

dNTP – Deoxyribose Nucleoside Triphosphate

MTIT – Mother-to-infant Transmission

RTV – Ritonavir

CYP3A4 – Cytochrome p450 3A4

IAS – International AIDS Society

INT – Integrase inhibitor

pVL – Plasma Viral Load

qRT-PCR – quantitative real-time polymerase chain reaction

HLA – Human Leukocyte Antigen

RTI – Reverse Transcriptase Inhibitor

AAALAC – Association for Assessment and Accreditation of Laboratory Animal Care

IACUC – Institutional Animal Care and Use Committee

PBMC – Peripheral Blood Mononuclear Cell

AIC – Akaike Information Criteria

NK – Natural Killer

NKT – Natural Killer T

TCID-50 – Tissue Culture Infectious Dose-50

BCP – 1-bromo-3-chloropropane

qPCR – quantitative PCR

IDT – Integrated DNA Technologies

CRAN – The Comprehensive R Archive Network

Wpt – Weeks Post-treatment

APPENDIX B: PUBLICATIONS

The following is a compilation of all publications produced during my Ph.D. Though these studies do not directly relate to the testing of my dissertation hypothesis (as detailed in sections 3.0 and 4.0), the contributions I made to these studies were instrumental to my dissertation. Through them, I learned, practiced and perfected many of the essential experimental techniques implemented in my dissertation, including: animal work, viral load, flow cytometry, sequencing, analysis, data compilation, etc. As such, my participation in these studies contributed significantly to my learning experiencing during my Ph.D. training.

Inflammatory monocytes expressing tissue factor drive SIV and HIV coagulopathy.

Schechter ME; Andrade BB; He T; Richter GH; Tosh KW; Policicchio BB; Singh A; Raehtz KD; Sheikh V; Ma D; Brocca-Cofano E; Apetrei C; Tracey R; Ribeiro RM; Sher A; Francischetti IMB; Pandrea I; Sereti I.

Science Translational Medicine. 2017 August.

BBP performed pVL quantification and analysis.

In HIV infection, persistent inflammation despite effective antiretroviral therapy is linked to increased risk of noninfectious chronic complications such as cardiovascular and thromboembolic disease. A better understanding of inflammatory and coagulation pathways in HIV infection is needed to optimize clinical care. Markers of monocyte activation and coagulation independently predict morbidity and mortality associated with non-AIDS events. We identified a specific subset of monocytes that express tissue factor (TF), persist after virological suppression, and trigger the coagulation cascade by activating factor X. This subset of monocytes expressing TF had a distinct gene signature with up-regulated innate immune markers and evidence of robust production of multiple proinflammatory cytokines, including interleukin-1 β (IL-1 β), tumor necrosis factor- α (TNF- α), and IL-6, ex vivo and in vitro upon lipopolysaccharide stimulation. We validated our findings in a nonhuman primate model, showing that TF-expressing inflammatory monocytes were associated with simian immunodeficiency virus (SIV)-related coagulopathy in the progressive [pigtail macaques (PTMs)] but not in the nonpathogenic (African green monkeys) SIV infection model. Last, Ixolaris, an anticoagulant that inhibits the TF pathway, was tested and potently blocked functional TF activity in vitro in HIV and SIV infection without affecting monocyte responses to Toll-like receptor stimulation. Strikingly, in vivo treatment of SIV-infected PTMs with Ixolaris was associated with significant decreases in D-dimer and immune activation. These data suggest that TF-expressing monocytes are at the epicenter of inflammation and coagulation in chronic HIV and SIV infection and may represent a potential therapeutic target

Cutting Edge: T Regulatory Cell Depletion Reactivates Latent Simian Immunodeficiency Virus (SIV) in Controller Macaques While Boosting SIV-Specific T Lymphocytes.

He T*, Brocca-Cofano E*, Policicchio BB*, Sivanandham R, Gautam R, Raetz KD, Xu C, Pandrea I, Apetrei C

Immunology. 2016 December.

BBP prepared virus stocks to infect RMs; performed pVL quantification and analysis; performed analysis of flow cytometry data.

T regulatory cells (Tregs) are critical in shaping the latent HIV/SIV reservoir, as they are preferentially infected, reverse CD4⁺ T cell activation status, and suppress CTL responses. To reactivate latent virus and boost cell-mediated immune responses, we performed in vivo Treg depletion with Ontak (denileukin diftitox) in two SIV_{sub}-infected controller macaques. Ontak induced significant (>75%) Treg depletion and major CD4⁺ T cell activation, and only minimally depleted CD8⁺ T cells. The overall ability of Tregs to control immune responses was significantly impaired despite their incomplete depletion, resulting in both reactivation of latent virus (virus rebound to 10³ viral RNA copies/ml plasma in the absence of antiretroviral therapy) and a significant boost of SIV-specific CD8⁺ T cell frequency, with rapid clearance of reactivated virus. As none of the latency-reversing agents in development have such dual activity, our strategy holds great promise for cure research.

Multi-dose Romidepsin Reactivates Replication Competent SIV in Post-antiretroviral Rhesus Macaque Controllers.

Policicchio BB, Xu C, Brocca-Cofano E, Raetz KD, He T, Ma D, Li H, Sivanandham R, Haret-Richter GS, Dunsmore T, Trichel A, Mellors JW, Hahn BH, Shaw GM, Ribeiro RM, Pandrea I, Apetrei C.

PLoS Pathogens. 2016 September.

BBP performed pVL quantification and analysis; prepared drugs for administration; analyzed and compiled flow cytometry data; performed CTL assay; wrote and edited manuscript.

Viruses that persist despite seemingly effective antiretroviral treatment (ART) and can reinstate infection if treatment is stopped preclude definitive treatment of HIV-1 infected individuals, requiring lifelong ART. Among strategies proposed for targeting these viral reservoirs, the premise of the "shock and kill" strategy is to induce expression of latent proviruses [for example with histone deacetylase inhibitors (HDACis)] resulting in elimination of the affected cells through viral cytolysis or immune clearance mechanisms. Yet, *ex vivo* studies reported that HDACis have variable efficacy for reactivating latent proviruses, and hinder immune functions. We developed a nonhuman primate model of post-treatment control of SIV through early and prolonged administration of ART and performed *in vivo* reactivation experiments in controller RMs, evaluating the ability of the HDACi romidepsin (RMD) to reactivate SIV and the impact of RMD treatment on SIV-specific T cell responses. Ten RMs were IV-infected with a SIV_{smmFTq} transmitted-founder infectious molecular clone. Four RMs received conventional ART for >9 months, starting from 65 days post-infection. SIV_{smmFTq} plasma viremia was robustly controlled to <10 SIV RNA copies/mL with ART, without viral blips. At ART cessation, initial rebound viremia to ~10⁶ copies/mL was followed by a decline to < 10

copies/mL, suggesting effective immune control. Three post-treatment controller RMs received three doses of RMD every 35-50 days, followed by in vivo experimental depletion of CD8+ cells using monoclonal antibody M-T807R1. RMD was well-tolerated and resulted in a rapid and massive surge in T cell activation, as well as significant virus rebounds (~10⁴ copies/ml) peaking at 5-12 days post-treatment. CD8+ cell depletion resulted in a more robust viral rebound (10⁷ copies/ml) that was controlled upon CD8+ T cell recovery. Our results show that RMD can reactivate SIV in vivo in the setting of post-ART viral control. Comparison of the patterns of virus rebound after RMD administration and CD8+ cell depletion suggested that RMD impact on T cells is only transient and does not irreversibly alter the ability of SIV-specific T cells to control the reactivated virus.

Envelope residue 375 substitutions in simian-human immunodeficiency viruses enhance CD4 binding and replication in rhesus macaques.

Li H, Wang S, Kong R, Ding W, Lee FH, Parker Z, Kim E, Learn GH, Hahn P, Policicchio B, Brocca-Cofano E, Deleage C, Hao X, Chuang GY, Gorman J, Gardner M, Lewis MG, Hatziioannou T, Santra S, Apetrei C, Pandrea I, Alam SM, Liao HX, Shen X, Tomaras GD, Farzan M, Chertova E, Keele BF, Estes JD, Lifson JD, Doms RW, Montefiori DC, Haynes BF, Sodroski JG, Kwong PD, Hahn BH, Shaw GM

Proceedings of the National Academy of Science USA. 2016 June.

BBP prepared virus stock to infect RMs; performed pVL quantification and analysis.

Most simian-human immunodeficiency viruses (SHIVs) bearing envelope (Env) glycoproteins from primary HIV-1 strains fail to infect rhesus macaques (RMs). We hypothesized that inefficient Env binding to rhesus CD4 (rhCD4) limits virus entry and replication and could be enhanced by substituting naturally occurring simian immunodeficiency virus Env residues at position 375, which resides at a critical location in the CD4-binding pocket and is under strong positive evolutionary pressure across the broad spectrum of primate lentiviruses. SHIVs containing primary or transmitted/founder HIV-1 subtype A, B, C, or D Envs with genotypic variants at residue 375 were constructed and analyzed in vitro and in vivo. Bulky hydrophobic or basic amino acids substituted for serine-375 enhanced Env affinity for rhCD4, virus entry into cells bearing rhCD4, and virus replication in primary rhCD4 T cells without appreciably affecting antigenicity or antibody-mediated neutralization sensitivity. Twenty-four RMs inoculated with subtype A, B, C, or D SHIVs all became productively infected with different Env₃₇₅ variants-S, M, Y, H, W, or F-that were differentially selected in different Env backbones. Notably, SHIVs replicated persistently at titers comparable to HIV-1 in humans and elicited autologous neutralizing antibody responses typical of HIV-1. Seven animals succumbed to AIDS. These findings identify Env-rhCD4 binding as a critical determinant for productive

SHIV infection in RMs and validate a novel and generalizable strategy for constructing SHIVs with Env glycoproteins of interest, including those that in humans elicit broadly neutralizing antibodies or bind particular Ig germ-line B-cell receptors.

Antibiotic and Antiinflammatory Therapy Transiently Reduces Inflammation and Hypercoagulation in Acutely SIV-infected Pigtailed Macaques.

Pandrea I, Xu C, Stock JL, Frank DN, Ma D, Policicchio BB, He T, Kristoff J, Cornell E, Haret-Richter GS, Trichel A, Ribeiro RM, Tracy R, Wilson C, Landay AL, Apetrei C.

PLoS Pathogens. 2016 January.

BBP prepared virus stock to infect pigtailed macaques; performed pVL quantification and analysis.

Increased chronic immune activation and inflammation are hallmarks of HIV/SIV infection and are highly correlated with progression to AIDS and development of non-AIDS comorbidities, such as hypercoagulability and cardiovascular disease. Intestinal dysfunction resulting in microbial translocation has been proposed as a lead cause of systemic immune activation and hypercoagulability in HIV/SIV infection. Our goal was to assess the biological and clinical impact of a therapeutic strategy designed to reduce microbial translocation through reduction of the microbial content of the intestine (Rifaximin-RFX) and of gut inflammation (Sulfasalazine-SFZ). RFX is an intraluminal antibiotic that was successfully used in patients with hepatic encephalopathy. SFZ is an antiinflammatory drug successfully used in patients with mild to moderate inflammatory bowel disease. Both these clinical conditions are associated with increased microbial translocation, similar to HIV-infected patients. Treatment was administered for 90 days to five acutely SIV-infected pigtailed macaques (PTMs) starting at the time of infection; seven untreated SIVsab-infected PTMs were used as controls. RFX+SFZ were also administered for 90 days to three chronically SIVsab-infected PTMs. RFX+SFZ administration during acute SIVsab infection of PTMs resulted in: significantly lower microbial translocation, lower systemic immune activation, lower viral replication, better preservation of mucosal CD4+

T cells and significantly lower levels of hypercoagulation biomarkers. This effect was clear during the first 40 days of treatment and was lost during the last stages of treatment. Administration of RFX+SFZ to chronically SIV_{sub}-infected PTMs had no discernible effect on infection. Our data thus indicate that early RFX+SFZ administration transiently improves the natural history of acute and postacute SIV infection, but has no effect during chronic infection.

Animal Models for HIV Cure Research.

Policicchio BB; Pandrea I; Apetrei C.

Frontiers in Immunology. 2016 January.

BBP performed an extensive literature search, wrote and edited the manuscript.

The HIV-1/AIDS pandemic continues to spread unabated worldwide, and no vaccine exists within our grasp. Effective antiretroviral therapy (ART) has been developed, but ART cannot clear the virus from the infected patient. A cure for HIV-1 is badly needed to stop both the spread of the virus in human populations and disease progression in infected individuals. A safe and effective cure strategy for human immunodeficiency virus (HIV) infection will require multiple tools, and appropriate animal models are tools that are central to cure research. An ideal animal model should recapitulate the essential aspects of HIV pathogenesis and associated immune responses, while permitting invasive studies, thus allowing a thorough evaluation of strategies aimed at reducing the size of the reservoir (functional cure) or eliminating the reservoir altogether (sterilizing cure). Since there is no perfect animal model for cure research, multiple models have been tailored and tested to address specific quintessential questions of virus persistence and eradication. The development of new non-human primate and mouse models, along with a certain interest in the feline model, has the potential to fuel cure research. In this review, we highlight the major animal models currently utilized for cure research and the contributions of each model to this goal.

Critical Role for the Adenosine Pathway in Controlling Simian Immunodeficiency Virus-Related Immune Activation and Inflammation in Gut Mucosal Tissues.

He T, Brocca-Cofano E, Gillespie DG, Xu C, Stock JL, Ma D, Policicchio BB, Raetz KD, Rinaldo CR, Apetrei C, Jackson EK, Macatangay BJ, Pandrea I

Journal of Virology. September 2015.

BBP prepared virus stock to infected NHPs; performed pVL quantification and analysis.

The role of the adenosine (ADO) pathway in human immunodeficiency virus type 1/simian immunodeficiency virus (HIV-1/SIV) infection remains unclear. We compared SIVsub-induced changes of markers related to ADO production (CD39 and CD73) and breakdown (CD26 and adenosine deaminase) on T cells from blood, lymph nodes, and intestine collected from pigtailed macaques (PTMs) and African green monkeys (AGMs) that experience different SIVsub infection outcomes. We also measured ADO and inosine (INO) levels in tissues by mass spectrometry. Finally, we assessed the suppressive effect of ADO on proinflammatory cytokine production after T cell receptor stimulation. The baseline level of both CD39 and CD73 coexpression on regulatory T cells and ADO levels were higher in AGMs than in PTMs. Conversely, high INO levels associated with dramatic increases in CD26 expression and adenosine deaminase activity were observed in PTMs during chronic SIV infection. Immune activation and inflammation markers in the gut and periphery inversely correlated with ADO and directly correlated with INO. Ex vivo administration of ADO significantly suppressed proinflammatory cytokine production by T cells in both species. In conclusion, the opposite dynamics of ADO pathway-related markers and contrasting ADO/INO levels in species with divergent proinflammatory responses to SIV infection support a key role of ADO in controlling immune activation/inflammation in nonprogressive SIV infections. Changes in ADO levels

predominately occurred in the gut, suggesting that the ADO pathway may be involved in sparing natural hosts of SIVs from developing SIV-related gut dysfunction. Focusing studies of the ADO pathway on mucosal sites of viral replication is warranted.

Population Bottlenecks and Pathogen Extinction: “Make This Everyone’s Mission to Mars, Including Yours.

Policicchio BB, Pandrea I, Apetrei C

Journal of Virology. 2015 August.

BBP performed literature search, wrote and edited manuscript.

Kapusinszky et al. (J Virol 89:8152-8161, 2015, <http://dx.doi.org/10.1128/JVI.00671-15>) report that host population bottlenecks may result in pathogen extinction, which provides a compelling argument for an alternative approach to vaccination for the control of virus spread. By comparing the prevalence levels of three viral **pathogens** in two populations of African green monkeys (AGMs) (*Chlorocebus sabaeus*) from Africa and two Caribbean Islands, they convincingly show that a major host bottleneck resulted in the eradication of select **pathogens** from a given host.

Simian Immunodeficiency Virus SIVsab Infection of Rhesus Macaques as a Model of Complete Immunological Suppression with Persistent Reservoirs of Replication-Competent Virus: Implications for Cure Research.

Ma D, Xu C, Cillo AR, Policicchio B, Kristoff J, Haret-Richter G, Mellors JW, Pandrea I, Apetrei C

Journal of Virology. 2015 June.

BBP performed pVL quantification and analysis; assisted in flow cytometry analysis and compilation.

Simian immunodeficiency virus SIVsab infection is completely controlled in rhesus macaques (RMs) through functional immune responses. We report that in SIVsab-infected RMs, (i) viral replication is controlled to <0 to 3 copies/ml, (ii) about one-third of the virus strains in reservoirs are replication incompetent, and (iii) rebounding virus after CD8(+) cell depletion is replication competent and genetically similar to the original virus stock, suggesting early reservoir seeding. This model permits assessment of strategies aimed at depleting the reservoir without multidrug antiretroviral therapy.

Kinetics of myeloid dendritic cell trafficking and activation: impact on progressive, nonprogressive and controlled SIV infections.

Wijewardana V, Kristoff J, Xu C, Ma D, Haret-Richter G, Stock JL, Policicchio BB, Mobley AD, Nusbaum R, Aamer H, Trichel A, Ribeiro RM, Apetrei C, Pandrea I.

PLoS Pathogens. 2013 October.

BBP performed flow sorting and subsequent analysis.

We assessed the role of myeloid dendritic cells (mDCs) in the outcome of SIV infection by comparing and contrasting their frequency, mobilization, phenotype, cytokine production and apoptosis in pathogenic (pigtailed macaques, PTMs), nonpathogenic (African green monkeys, AGMs) and controlled (rhesus macaques, RMs) SIV_{agmSab} infection. Through the identification of recently replicating cells, we demonstrated that mDC mobilization from the bone marrow occurred in all species postinfection, being most prominent in RMs. Circulating mDCs were depleted with disease progression in PTMs, recovered to baseline values after the viral peak in AGMs, and significantly increased at the time of virus control in RMs. Rapid disease progression in PTMs was associated with low baseline levels and incomplete recovery of circulating mDCs during chronic infection. mDC recruitment to the intestine occurred in all pathogenic scenarios, but loss of mucosal mDCs was associated only with progressive infection. Sustained mDC immune activation occurred throughout infection in PTMs and was associated with increased bystander apoptosis in blood and intestine. Conversely, mDC activation occurred only during acute infection in nonprogressive and controlled infections. Postinfection, circulating mDCs rapidly became unresponsive to TLR7/8 stimulation in all species. Yet, stimulation with LPS, a bacterial product translocated in circulation only in SIV-infected PTMs, induced mDC hyperactivation, apoptosis and excessive production of proinflammatory cytokines. After

infection, spontaneous production of proinflammatory cytokines by mucosal mDCs increased only in progressor PTMs. We thus propose that mDCs promote tolerance to SIV in the biological systems that lack intestinal dysfunction. In progressive infections, mDC loss and excessive activation of residual mDCs by SIV and additional stimuli, such as translocated microbial products, enhance generalized immune activation and inflammation. Our results thus provide a mechanistic basis for the role of mDCs in the pathogenesis of AIDS and elucidate the causes of mDC loss during progressive HIV/SIV infections.

BIBLIOGRAPHY

1. Joint United Nations Program on HIV/AIDS. 2013. UNAIDS reports a 52% reduction in new HIV infections among children and a combined 33% reduction among adults and children since 2001 | UNAIDS. <http://www.unaids.org/en/resources/presscentre/pressreleaseandstatementarchive/2013/september/20130923prunga/>.
2. Joint United Nations Program on HIV/AIDS. 2017. Fact sheet - Latest statistics on the status of the AIDS epidemic. Accessed
3. Shaw GM, Hunter E. 2012. HIV transmission. *Cold Spring Harb Perspect Med* 2.
4. United Nations Program on HIV/AIDS. 2007. 2007 AIDS Epidemic Update.
5. Antiretroviral Therapy Cohort Collaboration. 2008. Life expectancy of individuals on combination antiretroviral therapy in high-income countries: a collaborative analysis of 14 cohort studies. *Lancet* 372:293-299.
6. Fischer M, Hafner R, Schneider C, Trkola A, Joos B, Joller H, Hirschel B, Weber R, Gunthard HF. 2003. HIV RNA in plasma rebounds within days during structured treatment interruptions. *AIDS* 17:195-9.
7. Genesca M. 2011. Characterization of an effective CTL response against HIV and SIV infections. *J Biomed Biotechnol* 2011:103924.
8. Rosenberg ZF, Fauci AS. 1991. Immunopathogenesis of HIV infection. *Faseb j* 5:2382-90.
9. Patterson S, Knight SC. 1987. Susceptibility of human peripheral blood dendritic cells to infection by human immunodeficiency virus. *J Gen Virol* 68 (Pt 4):1177-81.
10. Koenig S, Gendelman HE, Orenstein JM, Dal Canto MC, Pezeshkpour GH, Yungbluth M, Janotta F, Aksamit A, Martin MA, Fauci AS. 1986. Detection of AIDS virus in macrophages in brain tissue from AIDS patients with encephalopathy. *Science* 233:1089-93.
11. Freed EO. 2015. HIV-1 assembly, release and maturation. *Nat Rev Microbiol* 13:484-96.
12. Lehmann-Che J, Saib A. 2004. Early stages of HIV replication: how to hijack cellular functions for a successful infection. *AIDS Rev* 6:199-207.
13. Marx PA, Li Y, Lerche NW, Sutjipto S, Gettie A, Yee JA, Brotman BH, Prince AM, Hanson A, Webster RG, et al. 1991. Isolation of a simian immunodeficiency virus related to human immunodeficiency virus type 2 from a west African pet sooty mangabey. *J Virol* 65:4480-5.
14. Gao F, Bailes E, Robertson DL, Chen Y, Rodenburg CM, Michael SF, Cummins LB, Arthur LO, Peeters M, Shaw GM, Sharp PM, Hahn BH. 1999. Origin of HIV-1 in the chimpanzee *Pan troglodytes troglodytes*. *Nature* 397:436-41.

15. Gao F, Yue L, White AT, Pappas PG, Barchue J, Hanson AP, Greene BM, Sharp PM, Shaw GM, Hahn BH. 1992. Human infection by genetically diverse SIVSM-related HIV-2 in west Africa. *Nature* 358:495-9.
16. Fauci AS, Desrosiers RC. 1997. Pathogenesis of HIV and SIV. *In* Coffin JM, Hughes SH, Varmus HE (ed), *Retroviruses*. Cold Spring Harbor Laboratory Press, Cold Spring Harbor (NY).
17. Sui Y, Gordon S, Franchini G, Berzofsky JA. 2013. Non-human primate models for HIV/AIDS vaccine development. *Current Protocols in Immunology* 102:1-30.
18. Del Prete GQ, Lifson JD. 2013. Considerations in the development of nonhuman primate models of combination antiretroviral therapy for studies of AIDS virus suppression, residual virus, and curative strategies. *Current Opinion in HIV and AIDS* 8:262-272.
19. Evans DT, Silvestri G. 2013. Non-human primate models in AIDS research. *Current opinion in HIV and AIDS* 8:255-261.
20. Haase AT. 2011. Early Events in Sexual Transmission of HIV and SIV and Opportunities for Interventions. *Annual Review of Medicine* 62:127-139.
21. Lackner AA, Veazey RS. 2007. Current concepts in AIDS pathogenesis: insights from the SIV/macaque model. *Annual Review of Medicine* 58:461-476.
22. Hirsch VM, Fuerst TR, Sutter G, Carroll MW, Yang LC, Goldstein S, Piatak M, Jr., Elkins WR, Alvord WG, Montefiori DC, Moss B, Lifson JD. 1996. Patterns of viral replication correlate with outcome in simian immunodeficiency virus (SIV)-infected macaques: effect of prior immunization with a trivalent SIV vaccine in modified vaccinia virus Ankara. *J Virol* 70:3741-52.
23. Hirsch VM, Santra S, Goldstein S, Plishka R, Buckler-White A, Seth A, Ourmanov I, Brown CR, Engle R, Montefiori D, Glowczwskie J, Kunstman K, Wolinsky S, Letvin NL. 2004. Immune failure in the absence of profound CD4+ T-lymphocyte depletion in simian immunodeficiency virus-infected rapid progressor macaques. *J Virol* 78:275-84.
24. Pandrea I, Gaufin T, Gautam R, Kristoff J, Mandell D, Montefiori D, Keele BF, Ribeiro RM, Veazey RS, Apetrei C. 2011. Functional Cure of SIVagm Infection in Rhesus Macaques Results in Complete Recovery of CD4+ T Cells and Is Reverted by CD8+ Cell Depletion. *PLoS Pathogens* 7.
25. Crise B, Li Y, Yuan C, Morcock DR, Whitby D, Munroe DJ, Arthur LO, Wu X. 2005. Simian Immunodeficiency Virus Integration Preference Is Similar to That of Human Immunodeficiency Virus Type 1. *Journal of Virology* 79:12199-12204.
26. Nishimura Y, Sadjadpour R, Mattapallil JJ, Igarashi T, Lee W, Buckler-White A, Roederer M, Chun TW, Martin MA. 2009. High frequencies of resting CD4+ T cells containing integrated viral DNA are found in rhesus macaques during acute lentivirus infections. *Proceedings of the National Academy of Sciences* 106:8015-8020.
27. Shen A, Zink MC, Mankowski JL, Chadwick K, Margolick JB, Carruth LM, Li M, Clements JE, Siliciano RF. 2003. Resting CD4+ T Lymphocytes but Not Thymocytes Provide a Latent Viral Reservoir in a Simian Immunodeficiency Virus-Macaca nemestrina Model of Human Immunodeficiency Virus Type 1-Infected Patients on Highly Active Antiretroviral Therapy. *Journal of Virology* 77:4938-4949.
28. Barber SA, Gama L, Dudaronek JM, Voelker T, Tarwater PM, Clements JE. 2006. Mechanism for the Establishment of Transcriptional HIV Latency in the Brain in a Simian Immunodeficiency Virus-Macaque Model. *Journal of Infectious Diseases* 193:963-970.

29. Shen A, Yang HC, Zhou Y, Chase AJ, Boyer JD, Zhang H, Margolick JB, Zink MC, Clements JE, Siliciano RF. 2007. Novel Pathway for Induction of Latent Virus from Resting CD4+ T Cells in the Simian Immunodeficiency Virus/Macaque Model of Human Immunodeficiency Virus Type 1 Latency. *Journal of Virology* 81:1660-1670.
30. Bourry O, Mannioui A, Sellier P, Roucairol C, Durand-Gasselin L, Dereuddre-Bosquet N, Benech H, Roques P, Le Grand R. 2010. Effect of a short-term HAART on SIV load in macaque tissues is dependent on time of initiation and antiviral diffusion. *Retrovirology* 7:78.
31. Mannioui A, Bourry O, Sellier P, Delache B, Brochard P, Andrieu T, Vaslin B, Karlsson I, Roques P, Le Grand R. 2009. Dynamics of viral replication in blood and lymphoid tissues during SIVmac251 infection of macaques. *Retrovirology* 6:106.
32. Sellier P, Mannioui A, Bourry O, Dereuddre-Bosquet N, Delache B, Brochard P, Calvo J, Prévot S, Roques P. 2010. Antiretroviral Treatment Start-Time during Primary SIVmac Infection in Macaques Exerts a Different Impact on Early Viral Replication and Dissemination. *PLoS ONE* 5.
33. Shytaj IL, Norelli S, Chirullo B, Della Corte A, Collins M, Yalley-Ogunro J, Greenhouse J, Iraci N, Acosta EP, Barreca ML, Lewis MG, Savarino A. 2012. A Highly Intensified ART Regimen Induces Long-Term Viral Suppression and Restriction of the Viral Reservoir in a Simian AIDS Model. *PLoS Pathog* 8:e1002774.
34. Del Prete GQ, Smedley J, Macallister R, Jones GS, Li B, Hattersley J, Zheng J, Piatak M, Keele BF, Hesselgesser J, Geleziunas R, Lifson JD. 2015. Short communication: comparative evaluation of coformulated injectable combination antiretroviral therapy regimens in simian immunodeficiency virus-infected rhesus macaques. *AIDS Research and Human Retroviruses* 32:163-168.
35. Moore JP, Kitchen SG, Pugach P, Zack JA. 2004. The CCR5 and CXCR4 coreceptors--central to understanding the transmission and pathogenesis of human immunodeficiency virus type 1 infection. *AIDS Res Hum Retroviruses* 20:111-26.
36. Suzuki Y, Craigie R. 2007. The road to chromatin - nuclear entry of retroviruses. *Nat Rev Microbiol* 5:187-96.
37. Lukic Z, Dharan A, Fricke T, Diaz-Griffero F, Campbell EM. 2014. HIV-1 uncoating is facilitated by dynein and kinesin 1. *J Virol* 88:13613-25.
38. Lusic M, Siliciano RF. 2017. Nuclear landscape of HIV-1 infection and integration. *Nat Rev Micro* 15:69-82.
39. Gelderblom HC, Vatakis DN, Burke SA, Lawrie SD, Bristol GC, Levy DN. 2008. Viral complementation allows HIV-1 replication without integration. *Retrovirology* 5:60.
40. Chan CN, Trinite B, Lee CS, Mahajan S, Anand A, Wodarz D, Sabbaj S, Bansal A, Goepfert PA, Levy DN. 2016. HIV-1 latency and virus production from unintegrated genomes following direct infection of resting CD4 T cells. *Retrovirology* 13:1.
41. Trinite B, Ohlson EC, Voznesensky I, Rana SP, Chan CN, Mahajan S, Alster J, Burke SA, Wodarz D, Levy DN. 2013. An HIV-1 replication pathway utilizing reverse transcription products that fail to integrate. *J Virol* 87:12701-20.
42. Kelly J, Beddall MH, Yu D, Iyer SR, Marsh JW, Wu Y. 2008. Human macrophages support persistent transcription from unintegrated HIV-1 DNA. *Virology* 372:300-12.
43. Musinova YR, Sheval EV, Dib C, Germini D, Vassetzky YS. 2016. Functional roles of HIV-1 Tat protein in the nucleus. *Cell Mol Life Sci* 73:589-601.

44. Rausch JW, Le Grice SF. 2015. HIV Rev Assembly on the Rev Response Element (RRE): A Structural Perspective. *Viruses* 7:3053-75.
45. Kula A, Marcello A. 2012. Dynamic Post-Transcriptional Regulation of HIV-1 Gene Expression. *Biology (Basel)* 1:116-33.
46. Meng B, Lever AM. 2013. Wrapping up the bad news: HIV assembly and release. *Retrovirology* 10:5.
47. Mohammadi P, Desfarges S, Bartha I, Joos B, Zangger N, Munoz M, Gunthard HF, Beerenwinkel N, Telenti A, Ciuffi A. 2013. 24 hours in the life of HIV-1 in a T cell line. *PLoS Pathog* 9:e1003161.
48. Keele BF, Giorgi EE, Salazar-Gonzalez JF, Decker JM, Pham KT, Salazar MG, Sun C, Grayson T, Wang S, Li H, Wei X, Jiang C, Kirchherr JL, Gao F, Anderson JA, Ping LH, Swanstrom R, Tomaras GD, Blattner WA, Goepfert PA, Kilby JM, Saag MS, Delwart EL, Busch MP, Cohen MS, Montefiori DC, Haynes BF, Gaschen B, Athreya GS, Lee HY, Wood N, Seoighe C, Perelson AS, Bhattacharya T, Korber BT, Hahn BH, Shaw GM. 2008. Identification and characterization of transmitted and early founder virus envelopes in primary HIV-1 infection. *Proc Natl Acad Sci U S A* 105:7552-7.
49. Haaland RE, Hawkins PA, Salazar-Gonzalez J, Johnson A, Tichacek A, Karita E, Manigart O, Mulenga J, Keele BF, Shaw GM, Hahn BH, Allen SA, Derdeyn CA, Hunter E. 2009. Inflammatory genital infections mitigate a severe genetic bottleneck in heterosexual transmission of subtype A and C HIV-1. *PLoS Pathog* 5:e1000274.
50. Chen HY, Di Mascio M, Perelson AS, Ho DD, Zhang L. 2007. Determination of virus burst size in vivo using a single-cycle SIV in rhesus macaques. *Proc Natl Acad Sci U S A* 104:19079-84.
51. Hu J, Gardner MB, Miller CJ. 2000. Simian Immunodeficiency Virus Rapidly Penetrates the Cervicovaginal Mucosa after Intravaginal Inoculation and Infects Intraepithelial Dendritic Cells. *Journal of Virology* 74:6087.
52. Amerongen HM, Weltzin R, Farnet CM, Michetti P, Haseltine WA, Neutra MR. 1991. Transepithelial transport of HIV-1 by intestinal M cells: a mechanism for transmission of AIDS. *J Acquir Immune Defic Syndr* 4:760-5.
53. Barreto-de-Souza V, Arakelyan A, Margolis L, Vanpouille C. 2014. HIV-1 vaginal transmission: cell-free or cell-associated virus? *Am J Reprod Immunol* 71:589-99.
54. Ribeiro Dos Santos P, Rancez M, Pretet JL, Michel-Salzat A, Messent V, Bogdanova A, Couedel-Courteille A, Souil E, Cheynier R, Butor C. 2011. Rapid dissemination of SIV follows multisite entry after rectal inoculation. *PLoS One* 6:e19493.
55. Miller CJ, Li Q, Abel K, Kim E-Y, Ma Z-M, Wietgreffe S, Franco-Scheuch LL, Compton L, Duan L, Shore MD, Zupancic M, Busch M, Carlis J, Wolinsky S, Haase AT. 2005. Propagation and Dissemination of Infection after Vaginal Transmission of Simian Immunodeficiency Virus. *Journal of Virology* 79:9217-9227.
56. Li Q, Duan L, Estes JD, Ma Z-M, Rourke T, Wang Y, Reilly C, Carlis J, Miller CJ, Haase AT. 2005. Peak SIV replication in resting memory CD4+ T cells depletes gut lamina propria CD4+ T cells. *Nature* 434:1148-1152.
57. Little SJ, McLean AR, Spina CA, Richman DD, Havlir DV. 1999. Viral dynamics of acute HIV-1 infection. *J Exp Med* 190:841-50.
58. McMichael AJ, Borrow P, Tomaras GD, Goonetilleke N, Haynes BF. 2009. The immune response during acute HIV-1 infection: clues for vaccine development. *Nature Reviews Immunology* 10:11-23.

59. Finkel TH, Tudor-Williams G, Banda NK, Cotton MF, Curiel T, Monks C, Baba TW, Ruprecht RM, Kupfer A. 1995. Apoptosis occurs predominantly in bystander cells and not in productively infected cells of HIV- and SIV-infected lymph nodes. *Nat Med* 1:129-134.
60. McCune JM. 2001. The dynamics of CD4+ T-cell depletion in HIV disease. *Nature* 410:974-979.
61. Moanna A, Dunham R, Paiardini M, Silvestri G. 2005. CD4+ T-cell depletion in HIV infection: killed by friendly fire? *Curr HIV/AIDS Rep* 2:16-23.
62. Davenport MP, Zhang L, Shiver JW, Casmiro DR, Ribeiro RM, Perelson AS. 2006. Influence of peak viral load on the extent of CD4+ T-cell depletion in simian HIV infection. *J Acquir Immune Defic Syndr* 41:259-65.
63. Zhou Y, Shen L, Yang HC, Siliciano RF. 2008. Preferential cytolysis of peripheral memory CD4+ T cells by in vitro X4-tropic human immunodeficiency virus type 1 infection before the completion of reverse transcription. *J Virol* 82:9154-63.
64. Mehandru S, Poles MA, Tenner-Racz K, Horowitz A, Hurley A, Hogan C, Boden D, Racz P, Markowitz M. 2004. Primary HIV-1 infection is associated with preferential depletion of CD4+ T lymphocytes from effector sites in the gastrointestinal tract. *J Exp Med* 200:761-70.
65. Brenchley JM, Schacker TW, Ruff LE, Price DA, Taylor JH, Beilman GJ, Nguyen PL, Khoruts A, Larson M, Haase AT, Douek DC. 2004. CD4+ T cell depletion during all stages of HIV disease occurs predominantly in the gastrointestinal tract. *J Exp Med* 200:749-59.
66. Muro-Cacho CA, Pantaleo G, Fauci AS. 1995. Analysis of apoptosis in lymph nodes of HIV-infected persons. Intensity of apoptosis correlates with the general state of activation of the lymphoid tissue and not with stage of disease or viral burden. *J Immunol* 154:5555-66.
67. Hurtrel B, Petit F, Arnoult D, Muller-Trutwin M, Silvestri G, Estaquier J. 2005. Apoptosis in SIV infection. *Cell Death Differ* 12 Suppl 1:979-90.
68. Koup RA, Safrit JT, Cao Y, Andrews CA, McLeod G, Borkowsky W, Farthing C, Ho DD. 1994. Temporal association of cellular immune responses with the initial control of viremia in primary human immunodeficiency virus type 1 syndrome. *Journal of Virology* 68:4650-4655.
69. Wilson JD, Ogg GS, Allen RL, Davis C, Shaunak S, Downie J, Dyer W, Workman C, Sullivan S, McMichael AJ, Rowland-Jones SL. 2000. Direct visualization of HIV-1-specific cytotoxic T lymphocytes during primary infection. *Aids* 14:225-33.
70. Borrow P, Lewicki H, Hahn BH, Shaw GM, Oldstone MB. 1994. Virus-specific CD8+ cytotoxic T-lymphocyte activity associated with control of viremia in primary human immunodeficiency virus type 1 infection. *Journal of Virology* 68:6103.
71. Mattapallil JJ, Douek DC, Hill B, Nishimura Y, Martin M, Roederer M. 2005. Massive infection and loss of memory CD4+ T cells in multiple tissues during acute SIV infection. *Nature* 434:1093-1097.
72. Veazey RS, DeMaria M, Chalifoux LV, Shvetz DE, Pauley DR, Knight HL, Rosenzweig M, Johnson RP, Desrosiers RC, Lackner AA. 1998. Gastrointestinal tract as a major site of CD4+ T cell depletion and viral replication in SIV infection. *Science* 280:427-31.
73. Turnbull EL, Wong M, Wang S, Wei X, Jones NA, Conrod KE, Aldam D, Turner J, Pellegrino P, Keele BF, Williams I, Shaw GM, Borrow P. 2009. Kinetics of expansion of

- epitope-specific T cell responses during primary HIV-1 infection. *J Immunol* 182:7131-45.
74. Goonetilleke N, Liu MK, Salazar-Gonzalez JF, Ferrari G, Giorgi E, Ganusov VV, Keele BF, Learn GH, Turnbull EL, Salazar MG, Weinhold KJ, Moore S, Letvin N, Haynes BF, Cohen MS, Hraber P, Bhattacharya T, Borrow P, Perelson AS, Hahn BH, Shaw GM, Korber BT, McMichael AJ. 2009. The first T cell response to transmitted/founder virus contributes to the control of acute viremia in HIV-1 infection. *J Exp Med* 206:1253-72.
 75. U.S. Department of Health and Human Services, Centers for Disease Control and Prevention (CDC). Morbidity and Mortality Weekly Report. 1993. Revised classification system for HIV infection and expanded surveillance case definition for AIDS among adolescents and adults. <https://www.cdc.gov/mmwr/preview/mmwrhtml/00018871.htm>.
 76. Thompson MA, Aberg JA, Hoy JF, et al. 2012. Antiretroviral treatment of adult hiv infection: 2012 recommendations of the international antiviral society–usa panel. *JAMA* 308:387-402.
 77. Hogg RS, Yip B, Kully C, Craib KJ, O'Shaughnessy MV, Schechter MT, Montaner JS. 1999. Improved survival among HIV-infected patients after initiation of triple-drug antiretroviral regimens. *Cmaj* 160:659-65.
 78. Graham NM, Hoover DR, Park LP, Stein DS, Phair JP, Mellors JW, Detels R, Saah AJ. 1996. Survival in HIV-infected patients who have received zidovudine: comparison of combination therapy with sequential monotherapy and continued zidovudine monotherapy. Multicenter AIDS Cohort Study Group. *Ann Intern Med* 124:1031-8.
 79. Merigan TC. 1991. Treatment of AIDS with combinations of antiretroviral agents. *Am J Med* 90:8s-17s.
 80. Trickey A, May MT, Vehreschild J-J, Obel N, Gill MJ, Crane HM, Boesecke C, Patterson S, Grabar S, Cazanave C, Cavassini M, Shepherd L, Monforte AdA, van Sighem A, Saag M, Lampe F, Hernando V, Montero M, Zangerle R, Justice AC, Sterling T, Ingle SM, Sterne JAC. 2017. Survival of HIV-positive patients starting antiretroviral therapy between 1996 and 2013: a collaborative analysis of cohort studies. *The Lancet HIV* 4:e349-e356.
 81. Mannheimer S, Friedland G, Matts J, Child C, Chesney M. 2002. The consistency of adherence to antiretroviral therapy predicts biologic outcomes for human immunodeficiency virus-infected persons in clinical trials. *Clin Infect Dis* 34:1115-21.
 82. Dybul M, Fauci AS, Bartlett JG, Kaplan JE, Pau AK. 2002. Guidelines for using antiretroviral agents among HIV-infected adults and adolescents. *Ann Intern Med* 137:381-433.
 83. Hogg RS, Heath K, Bangsberg D, Yip B, Press N, O'Shaughnessy MV, Montaner JS. 2002. Intermittent use of triple-combination therapy is predictive of mortality at baseline and after 1 year of follow-up. *Aids* 16:1051-8.
 84. Egger M, May M, Chene G, Phillips AN, Ledergerber B, Dabis F, Costagliola D, D'Arminio Monforte A, de Wolf F, Reiss P, Lundgren JD, Justice AC, Staszewski S, Leport C, Hogg RS, Sabin CA, Gill MJ, Salzberger B, Sterne JA. 2002. Prognosis of HIV-1-infected patients starting highly active antiretroviral therapy: a collaborative analysis of prospective studies. *Lancet* 360:119-29.
 85. Boyd MA, Moore CL, Molina JM, Wood R, Madero JS, Wolff M, Ruxrungtham K, Losso M, Renjifo B, Tepler H, Kelleher AD, Amin J, Emery S, Cooper DA. 2015.

- Baseline HIV-1 resistance, virological outcomes, and emergent resistance in the SECOND-LINE trial: an exploratory analysis. *Lancet HIV* 2:e42-51.
86. Montaner JS, Harrigan PR, Jahnke N, Raboud J, Castillo E, Hogg RS, Yip B, Harris M, Montessori V, O'Shaughnessy MV. 2001. Multiple drug rescue therapy for HIV-infected individuals with prior virologic failure to multiple regimens. *Aids* 15:61-9.
 87. Miller V, Cozzi-Lepri A, Hertogs K, Gute P, Larder B, Bloor S, Klauke S, Rabenau H, Phillips A, Staszewski S. 2000. HIV drug susceptibility and treatment response to mega-HAART regimen in patients from the Frankfurt HIV cohort. *Antivir Ther* 5:49-55.
 88. Perelson AS, Neumann AU, Markowitz M, Leonard JM, Ho DD. 1996. HIV-1 dynamics in vivo: virion clearance rate, infected cell life-span, and viral generation time. *Science* 271:1582-1586.
 89. Zhang LQ, Dailey PJ, He T, Gettie A, Bonhoeffer S, Perelson AS, Ho DD. 1999. Rapid clearance of simian immunodeficiency virus particles from plasma of rhesus macaques. *Journal of Virology* 73:855-860.
 90. Wei XP, Ghosh SK, Taylor ME, Johnson VA, Emini EA, Deutsch P, Lifson JD, Bonhoeffer S, Nowak MA, Hahn BH, Saag MS, Shaw GM. 1995. Viral Dynamics in Human-Immunodeficiency-Virus Type-1 Infection. *Nature* 373:117-122.
 91. Perelson AS, Essunger P, Cao Y, Vesanen M, Hurley A, Saksela K, Markowitz M, Ho DD. 1997. Decay characteristics of HIV-1 infected compartments during combination therapy. *387:188-191*.
 92. Hlavacek WS, Stilianakis NI, Notermans DW, Danner SA, Perelson AS. 2000. Influence of follicular dendritic cells on decay of HIV during antiretroviral therapy. *Proceedings of the National Academy of Sciences of the United States of America* 97:10966-10971.
 93. Hlavacek WS, Stilianakis NI, Perelson AS. 2000. Influence of follicular dendritic cells on HIV dynamics. *Philosophical Transactions of the Royal Society of London Series B, Biological Sciences* 355:1051-1058.
 94. Andrade A, Rosenkranz SL, Cillo AR, Lu D, Daar ES, Jacobson JM, Lederman M, Acosta EP, Campbell T, Feinberg J, Flexner C, Mellors JW, Kuritzkes DR. 2013. Three Distinct Phases of HIV-1 RNA Decay in Treatment-Naive Patients Receiving Raltegravir-Based Antiretroviral Therapy: ACTG A5248. *The Journal of Infectious Diseases* 208:884-891.
 95. Palmer S, Maldarelli F, Wiegand A, Bernstein B, Hanna GJ, Brun SC, Kempf DJ, Mellors JW, Coffin JM, King MS. 2008. Low-level viremia persists for at least 7 years in patients on suppressive antiretroviral therapy. *Proceedings of the National Academy of Sciences* 105:3879-3884.
 96. Siliciano JD, Kajdas J, Finzi D, Quinn TC, Chadwick K, Margolick JB, Kovacs C, Gange SJ, Siliciano RF. 2003. Long-term follow-up studies confirm the stability of the latent reservoir for HIV-1 in resting CD4+ T cells. *Nature Medicine* 9:727-728.
 97. Stöhr W, Fidler S, McClure M, Weber J, Cooper D, Ramjee G, Kaleebu P, Tambussi G, Schechter M, Babiker A, Phillips RE, Porter K, Frater J. 2013. Duration of HIV-1 viral suppression on cessation of antiretroviral therapy in primary infection correlates with time on therapy. *PLoS ONE* 8:e78287.
 98. Hamlyn E, Ewings FM, Porter K, Cooper DA, Tambussi G, Schechter M, Pedersen C, Okulicz JF, McClure M, Babiker A, Weber J, Fidler S, on behalf of the IS, Investigators S. 2012. Plasma HIV viral rebound following protocol-indicated cessation of ART commenced in primary and chronic HIV infection. *PLoS ONE* 7:e43754.

99. Calin R, Hamimi C, Lambert-Niclot S, Carcelain G, Bellet J, Assoumou L, Tubiana R, Calvez V, Dudoit Y, Costagliola D, Autran B, Katlama C, Group US. 2016. Treatment interruption in chronically HIV-infected patients with an ultralow HIV reservoir. *AIDS (London, England)* 30:761-9.
100. Ruiz L, Martinez-Picado J, Romeu J, Paredes R, Zayat MK, Marfil S, Negredo E, Sirera G, Tural C, Clotet B. 2000. Structured treatment interruption in chronically HIV-1 infected patients after long-term viral suppression. *AIDS (London, England)* 14:397-403.
101. Sáez-Cirión A, Bacchus C, Hocqueloux L, Avettand-Fenoel V, Girault I, Lecuroux C, Potard V, Versmisse P, Melard A, Prazuck T, Descours B, Guergnon J, Viard J-P, Boufassa F, Lambotte O, Goujard C, Meyer L, Costagliola D, Venet A, Pancino G, Autran B, Rouzioux C. 2013. Post-Treatment HIV-1 Controllers with a Long-Term Virological Remission after the Interruption of Early Initiated Antiretroviral Therapy ANRS VISCONTI Study. *PLoS Pathogens* 9.
102. Ho DD, Neumann AU, Perelson AS, Chen W, Leonard JM, Markowitz M. 1995. Rapid turnover of plasma virions and CD4 lymphocytes in HIV-1 infection. *Nature* 373:123-6.
103. Wei X, Ghosh SK, Taylor ME, Johnson VA, Emini EA, Deutsch P, Lifson JD, Bonhoeffer S, Nowak MA, Hahn BH, et al. 1995. Viral dynamics in human immunodeficiency virus type 1 infection. *Nature* 373:117-22.
104. Gartner S, Markovits P, Markovitz DM, Kaplan MH, Gallo RC, Popovic M. 1986. The role of mononuclear phagocytes in HTLV-III/LAV infection. *Science* 233:215-9.
105. Maldarelli F, Palmer S, King MS, Wiegand A, Polis MA, Mican J, Kovacs JA, Davey RT, Rock-Kress D, Dewar R, Liu S, Metcalf JA, Rehm C, Brun SC, Hanna GJ, Kempf DJ, Coffin JM, Mellors JW. 2007. ART suppresses plasma HIV-1 RNA to a stable set point predicted by pretherapy viremia. *PLoS Pathog* 3:e46.
106. Blanco JL, Martinez-Picado J. 2012. HIV integrase inhibitors in ART-experienced patients. *Curr Opin HIV AIDS* 7:415-21.
107. Hazuda DJ, Felock P, Witmer M, Wolfe A, Stillmock K, Grobler JA, Espeseth A, Gabryelski L, Schleif W, Blau C, Miller MD. 2000. Inhibitors of strand transfer that prevent integration and inhibit HIV-1 replication in cells. *Science (New York, NY)* 287:646-650.
108. Murray JM, Emery S, Kelleher AD, Law M, Chen J, Hazuda DJ, Nguyen B-YT, Teppler H, Cooper DA. 2007. Antiretroviral therapy with the integrase inhibitor raltegravir alters decay kinetics of HIV, significantly reducing the second phase. *Aids* 21:2315-2321.
109. Pauza CD, Trivedi P, McKechnie TS, Richman DD, Graziano FM. 1994. 2-LTR Circular Viral DNA as a Marker for Human Immunodeficiency Virus Type 1 Infection in Vivo. *Virology* 205:470-478.
110. Morlese J, Teo IA, Choi J-w, Gazzard B, Shaunak S. 2003. Identification of two mutually exclusive groups after long-term monitoring of HIV DNA 2-LTR circle copy number in patients on HAART. *AIDS (London, England)* 17:679-683.
111. Zhu W, Jiao Y, Lei R, Hua W, Wang R, Ji Y, Liu Z, Wei F, Zhang T, Shi X, Wu H, Zhang L. 2011. Rapid Turnover of 2-LTR HIV-1 DNA during Early Stage of Highly Active Antiretroviral Therapy. *PLoS ONE* 6.
112. Thierry S, Munir S, Thierry E, Subra F, Leh H, Zamborlini A, Saenz D, Levy DN, Lesbats P, Saïb A, Parissi V, Poeschla E, Deprez E, Delelis O. 2015. Integrase inhibitor reversal dynamics indicate unintegrated HIV-1 dna initiate de novo integration. *Retrovirology* 12:24.

113. Delelis O, Petit C, Leh H, Mbemba G, Mouscadet J-F, Sonigo P. 2005. A novel function for spumaretrovirus integrase: an early requirement for integrase-mediated cleavage of 2 LTR circles. *Retrovirology* 2:31.
114. Buzón M, Massanella M, Llibre JM, Esteve A, Dahl V, Puertas MC, Gatell JM, Domingo P, Paredes R, Sharkey M, Palmer S, Stevenson M, Clotet B, Blanco J, Martinez-Picado J. 2010. HIV-1 replication and immune dynamics are affected by raltegravir intensification of HAART-suppressed subjects. *Nature Medicine* 16:460-465.
115. Hatano H, Strain MC, Scherzer R, Bacchetti P, Wentworth D, Hoh R, Martin JN, McCune JM, Neaton JD, Tracy RP, Hsue PY, Richman DD, Deeks SG. 2013. Increase in 2-Long Terminal Repeat Circles and Decrease in D-dimer After Raltegravir Intensification in Patients With Treated HIV Infection: A Randomized, Placebo-Controlled Trial. *The Journal of Infectious Diseases* 208:1436-1442.
116. Llibre JM, Buzón MJ, Massanella M, Esteve A, Dahl V, Puertas MC, Domingo P, Gatell JM, Larrouse M, Gutierrez M, Palmer S, Stevenson M, Blanco J, Martinez-Picado J, Clotet B. 2012. Treatment intensification with raltegravir in subjects with sustained HIV-1 viraemia suppression: a randomized 48-week study. *Antiviral Therapy* 17:355-364.
117. Luo R, Cardozo EF, Piovoso MJ, Wu H, Buzon MJ, Martinez-Picado J, Zurakowski R. 2013. Modelling HIV-1 2-LTR dynamics following raltegravir intensification. *Journal of the Royal Society Interface* 10.
118. Gandhi RT, Coombs RW, Chan ES, Bosch RJ, Zheng L, Margolis DM, Read S, Kallungal B, Chang M, Goecker EA, Wiegand A, Kearney M, Jacobson JM, D'Aquila R, Lederman MM, Mellors JW, Eron JJ. 2012. No Effect of Raltegravir Intensification on Viral Replication Markers in the Blood of HIV-1-Infected Patients Receiving Antiretroviral Therapy. *JAIDS Journal of Acquired Immune Deficiency Syndromes* 59:229-235.
119. Besson GJ, McMahon D, Maldarelli F, Mellors JW. 2012. Short-course raltegravir intensification does not increase 2 long terminal repeat episomal HIV-1 DNA in patients on effective antiretroviral therapy. *Clin Infect Dis* 54:451-3.
120. Delaugerre C, Charreau I, Braun J, Nere ML, de Castro N, Yeni P, Ghosn J, Aboulker JP, Molina JM, Simon F. 2010. Time course of total HIV-1 DNA and 2-long-terminal repeat circles in patients with controlled plasma viremia switching to a raltegravir-containing regimen. *AIDS* 24:2391-5.
121. Vallejo A, Gutierrez C, Hernandez-Novoa B, Diaz L, Madrid N, Abad-Fernandez M, Dronda F, Perez-Elias MJ, Zamora J, Munoz E, Munoz-Fernandez MA, Moreno S. 2012. The effect of intensification with raltegravir on the HIV-1 reservoir of latently infected memory CD4 T cells in suppressed patients. *AIDS* 26:1885-94.
122. Pantaleo G, Graziosi C, Butini L, Pizzo PA, Schnittman SM, Kotler DP, Fauci AS. 1991. Lymphoid organs function as major reservoirs for human immunodeficiency virus. *Proc Natl Acad Sci U S A* 88:9838-42.
123. Lafeuillade A, Khiri H, Chadapaud S, Hittinger G, Halfon P. 2001. Persistence of HIV-1 resistance in lymph node mononuclear cell RNA despite effective HAART. *Aids* 15:1965-9.
124. Popovic M, Tenner-Racz K, Pelsler C, Stellbrink HJ, van Lunzen J, Lewis G, Kalyanaraman VS, Gallo RC, Racz P. 2005. Persistence of HIV-1 structural proteins and glycoproteins in lymph nodes of patients under highly active antiretroviral therapy. *Proc Natl Acad Sci U S A* 102:14807-12.

125. Horiike M, Iwami S, Kodama M, Sato A, Watanabe Y, Yasui M, Ishida Y, Kobayashi T, Miura T, Igarashi T. 2012. Lymph nodes harbor viral reservoirs that cause rebound of plasma viremia in SIV-infected macaques upon cessation of combined antiretroviral therapy. *Virology* 423:107-118.
126. Cardozo EF, Luo R, Piovoso MJ, Zurakowski R. 2014. Spatial modeling of HIV cryptic viremia and 2-LTR formation during raltegravir intensification. *Journal of Theoretical Biology* 345:61-69.
127. Altfeld M, Gale Jr M. 2015. Innate immunity against HIV-1 infection. *Nat Immunol* 16:554-562.
128. Overbaugh J, Morris L. 2012. The Antibody Response against HIV-1. *Cold Spring Harb Perspect Med* 2:a007039.
129. Gulzar N, Copeland KF. 2004. CD8+ T-cells: function and response to HIV infection. *Curr HIV Res* 2:23-37.
130. Brumme ZL, Harrigan PR. 2006. The impact of human genetic variation on HIV disease in the era of HAART. *AIDS reviews* 8:78-87.
131. Borrow P, Lewicki H, Wei X, Horwitz MS, Peffer N, Meyers H, Nelson JA, Gairin JE, Hahn BH, Oldstone MB, Shaw GM. 1997. Antiviral pressure exerted by HIV-1-specific cytotoxic T lymphocytes (CTLs) during primary infection demonstrated by rapid selection of CTL escape virus. *Nature Medicine* 3:205-211.
132. Chen ZW, Craiu A, Shen L, Kuroda MJ, Iroku UC, Watkins DI, Voss G, Letvin NL. 2000. Simian Immunodeficiency Virus Evades a Dominant Epitope-Specific Cytotoxic T Lymphocyte Response Through a Mutation Resulting in the Accelerated Dissociation of Viral Peptide and MHC Class I. *The Journal of Immunology* 164:6474-6479.
133. McMichael AJ, Phillips RE. 1997. Escape of human immunodeficiency virus from immune control. *Annual Review of Immunology* 15:271-296.
134. Phillips RE, Rowland-Jones S, Nixon DF, Gotch FM, Edwards JP, Ogunlesi AO, Elvin JG, Rothbard JA, Bangham CRM, Rizza CR, McMichael AJ. 1991. Human immunodeficiency virus genetic variation that can escape cytotoxic T cell recognition. *Nature* 354:453-459.
135. Goulder PJR, Phillips RE, Colbert RA, McAdam S, Ogg G, Nowak MA, Giangrande P, Luzzi G, Morgana B, Edwards A, McMichael AJ, Rowland-Jones S. 1997. Late escape from an immunodominant cytotoxic T-lymphocyte response associated with progression to AIDS. *Nature Medicine* 3:212-217.
136. Policicchio BB, Pandrea I, Apetrei C. 2016. Animal models for HIV cure research. *Frontiers in Immunology* 7.
137. Gaufin T, Ribeiro RM, Gautam R, Dufour J, Mandell D, Apetrei C, Pandrea I. 2010. Experimental depletion of CD8+ cells in acutely SIVagm-infected African Green Monkeys results in increased viral replication. *Retrovirology* 7:42.
138. Chowdhury A, Hayes TL, Bosinger SE, Lawson BO, Vanderford T, Schmitz JE, Paiardini M, Betts M, Chahroudi A, Estes JD, Silvestri G. 2015. Differential Impact of In Vivo CD8+ T Lymphocyte Depletion in Controller versus Progressor Simian Immunodeficiency Virus-Infected Macaques. *Journal of Virology* 89:8677-8686.
139. Schmitz JE, Zahn RC, Brown CR, Rett MD, Li M, Tang H, Pryputniewicz S, Byrum RA, Kaur A, Montefiori DC, Allan JS, Goldstein S, Hirsch VM. 2009. Inhibition of adaptive immune responses leads to a fatal clinical outcome in SIV-infected pigtailed macaques but not vervet African green monkeys. *PLoS pathogens* 5:e1000691.

140. Cartwright EK, Spicer L, Smith SA, Lee D, Fast R, Paganini S, Lawson BO, Nega M, Easley K, Schmitz JE, Bosinger SE, Paiardini M, Chahroudi A, Vanderford TH, Estes JD, Lifson JD, Derdeyn CA, Silvestri G. 2016. CD8(+) Lymphocytes Are Required for Maintaining Viral Suppression in SIV-Infected Macaques Treated with Short-Term Antiretroviral Therapy. *Immunity* 45:656-668.
141. Wong JK, Strain MC, Porrata R, Reay E, Sankaran-Walters S, Ignacio CC, Russell T, Pillai SK, Looney DJ, Dandekar S. 2010. In Vivo CD8+ T-Cell Suppression of SIV Viremia Is Not Mediated by CTL Clearance of Productively Infected Cells. *PLoS Pathogens* 6.
142. Klatt NR, Shudo E, Ortiz AM, Engram JC, Paiardini M, Lawson B, Miller MD, Else J, Pandrea I, Estes JD, Apetrei C, Schmitz JE, Ribeiro RM, Perelson AS, Silvestri G. 2010. CD8+ Lymphocytes Control Viral Replication in SIVmac239-Infected Rhesus Macaques without Decreasing the Lifespan of Productively Infected Cells, *PLoS Pathog*, vol 6.
143. Schmitz JE, Kuroda MJ, Santra S, Sasseville VG, Simon MA, Lifton MA, Racz P, Tenner-Racz K, Dalesandro M, Scallon BJ, Ghayeb J, Forman MA, Montefiori DC, Rieber EP, Letvin NL, Reimann KA. 1999. Control of Viremia in Simian Immunodeficiency Virus Infection by CD8+ Lymphocytes. *Science* 283:857-860.
144. Schmitz JE, Simon MA, Kuroda MJ, Lifton MA, Ollert MW, Vogel CW, Racz P, Tenner-Racz K, Scallon BJ, Dalesandro M, Ghayeb J, Rieber EP, Sasseville VG, Reimann KA. 1999. A nonhuman primate model for the selective elimination of CD8+ lymphocytes using a mouse-human chimeric monoclonal antibody. *The American Journal of Pathology* 154:1923-1932.
145. Matano T, Shibata R, Siemon C, Connors M, Lane HC, Martin MA. 1998. Administration of an Anti-CD8 Monoclonal Antibody Interferes with the Clearance of Chimeric Simian/Human Immunodeficiency Virus during Primary Infections of Rhesus Macaques. *Journal of Virology* 72:164-169.
146. Jin X, Bauer DE, Tuttleton SE, Lewin S, Gettie A, Blanchard J, Irwin CE, Safrit JT, Mittler J, Weinberger L. 1999. Dramatic rise in plasma viremia after CD8+ T cell depletion in simian immunodeficiency virus-infected macaques. *The Journal of experimental medicine* 189:991-998.
147. Madden LJ, Zandonatti MA, Flynn CT, Taffe MA, Marcondes MCG, Schmitz JE, Reimann KA, Henriksen SJ, Fox HS. 2004. CD8+ cell depletion amplifies the acute retroviral syndrome. *Journal of Neurovirology* 10 Suppl 1:58-66.
148. Walker CM, Moody DJ, Stites DP, Levy JA. 1986. CD8+ lymphocytes can control HIV infection in vitro by suppressing virus replication. *Science (New York, NY)* 234:1563-1566.
149. Kannagi M, Chalifoux LV, Lord CI, Letvin NL. 1988. Suppression of simian immunodeficiency virus replication in vitro by CD8+ lymphocytes. *Journal of Immunology (Baltimore, Md: 1950)* 140:2237-2242.
150. Addo MM, Yu XG, Rathod A, Cohen D, Eldridge RL, Strick D, Johnston MN, Corcoran C, Wurcel AG, Fitzpatrick CA, Feeney ME, Rodriguez WR, Basgoz N, Draenert R, Stone DR, Brander C, Goulder PJ, Rosenberg ES, Altfeld M, Walker BD. 2003. Comprehensive epitope analysis of human immunodeficiency virus type 1 (HIV-1)-specific T-cell responses directed against the entire expressed HIV-1 genome demonstrate broadly directed responses, but no correlation to viral load. *J Virol* 77:2081-92.

151. Andersen MH, Schrama D, Thor Straten P, Becker JC. 2006. Cytotoxic T Cells. *Journal of Investigative Dermatology* 126:32-41.
152. Pawelec G, Schneider EM, Wernet P. 1986. Acquisition of suppressive activity and natural killer-like cytotoxicity by human alloproliferative "helper" T cell clones. *J Immunol* 136:402-11.
153. Gillespie GM, Wills MR, Appay V, O'Callaghan C, Murphy M, Smith N, Sissons P, Rowland-Jones S, Bell JI, Moss PA. 2000. Functional heterogeneity and high frequencies of cytomegalovirus-specific CD8(+) T lymphocytes in healthy seropositive donors. *J Virol* 74:8140-50.
154. Guidotti LG, Ishikawa T, Hobbs MV, Matzke B, Schreiber R, Chisari FV. 1996. Intracellular inactivation of the hepatitis B virus by cytotoxic T lymphocytes. *Immunity* 4:25-36.
155. Lechner F, Wong DK, Dunbar PR, Chapman R, Chung RT, Dohrenwend P, Robbins G, Phillips R, Klenerman P, Walker BD. 2000. Analysis of successful immune responses in persons infected with hepatitis C virus. *J Exp Med* 191:1499-512.
156. Callan MF. 2003. The evolution of antigen-specific CD8+ T cell responses after natural primary infection of humans with Epstein-Barr virus. *Viral Immunol* 16:3-16.
157. Hersperger AR, Pereyra F, Nason M, Demers K, Sheth P, Shin LY, Kovacs CM, Rodriguez B, Sieg SF, Teixeira-Johnson L, Gudonis D, Goepfert PA, Lederman MM, Frank I, Makedonas G, Kaul R, Walker BD, Betts MR. 2010. Perforin expression directly ex vivo by HIV-specific CD8 T-cells is a correlate of HIV elite control. *PLoS Pathog* 6:e1000917.
158. Ferrari G, Korber B, Goonetilleke N, Liu MK, Turnbull EL, Salazar-Gonzalez JF, Hawkins N, Self S, Watson S, Betts MR, Gay C, McGhee K, Pellegrino P, Williams I, Tomaras GD, Haynes BF, Gray CM, Borrow P, Roederer M, McMichael AJ, Weinhold KJ. 2011. Relationship between functional profile of HIV-1 specific CD8 T cells and epitope variability with the selection of escape mutants in acute HIV-1 infection. *PLoS Pathog* 7:e1001273.
159. Betts MR, Harari A. 2008. Phenotype and function of protective T cell immune responses in HIV. *Curr Opin HIV AIDS* 3:349-55.
160. Keefe D, Shi L, Feske S, Massol R, Navarro F, Kirchhausen T, Lieberman J. 2005. Perforin triggers a plasma membrane-repair response that facilitates CTL induction of apoptosis. *Immunity* 23:249-62.
161. Cullen SP, Martin SJ. 2008. Mechanisms of granule-dependent killing. *Cell Death Differ* 15:251-62.
162. Alimonti JB, Shi L, Baijal PK, Greenberg AH. 2001. Granzyme B induces BID-mediated cytochrome c release and mitochondrial permeability transition. *J Biol Chem* 276:6974-82.
163. Fan Z, Beresford PJ, Oh DY, Zhang D, Lieberman J. 2003. Tumor suppressor NM23-H1 is a granzyme A-activated DNase during CTL-mediated apoptosis, and the nucleosome assembly protein SET is its inhibitor. *Cell* 112:659-72.
164. Zhao T, Zhang H, Guo Y, Zhang Q, Hua G, Lu H, Hou Q, Liu H, Fan Z. 2007. Granzyme K cleaves the nucleosome assembly protein SET to induce single-stranded DNA nicks of target cells. *Cell Death Differ* 14:489-99.

165. Guo Y, Chen J, Zhao T, Fan Z. 2008. Granzyme K degrades the redox/DNA repair enzyme Apel to trigger oxidative stress of target cells leading to cytotoxicity. *Mol Immunol* 45:2225-35.
166. Johnson H, Scorrano L, Korsmeyer SJ, Ley TJ. 2003. Cell death induced by granzyme C. *Blood* 101:3093-101.
167. Bovenschen N, de Koning PJ, Quadir R, Broekhuizen R, Damen JM, Froelich CJ, Slijper M, Kummer JA. 2008. NK cell protease granzyme M targets alpha-tubulin and disorganizes the microtubule network. *J Immunol* 180:8184-91.
168. Cullen SP, Brunet M, Martin SJ. 2010. Granzymes in cancer and immunity. *Cell Death Differ* 17:616-623.
169. Rouvier E, Luciani MF, Golstein P. 1993. Fas involvement in Ca(2+)-independent T cell-mediated cytotoxicity. *J Exp Med* 177:195-200.
170. Kischkel FC, Hellbardt S, Behrmann I, Germer M, Pawlita M, Krammer PH, Peter ME. 1995. Cytotoxicity-dependent APO-1 (Fas/CD95)-associated proteins form a death-inducing signaling complex (DISC) with the receptor. *Embo j* 14:5579-88.
171. Lavrik IN, Krammer PH. 2012. Regulation of CD95/Fas signaling at the DISC. *Cell Death Differ* 19:36-41.
172. O' Reilly L, Tai L, Lee L, Kruse EA, Grabow S, Fairlie WD, Haynes NM, Tarlinton DM, Zhang JG, Belz GT, Smyth MJ, Bouillet P, Robb L, Strasser A. 2009. Membrane-bound Fas ligand only is essential for Fas-induced apoptosis. *Nature* 461:659-63.
173. Shankar P, Xu Z, Lieberman J. 1999. Viral-specific cytotoxic T lymphocytes lyse human immunodeficiency virus-infected primary T lymphocytes by the granule exocytosis pathway. *Blood* 94:3084-93.
174. Katsikis PD, Wunderlich ES, Smith CA, Herzenberg LA, Herzenberg LA. 1995. Fas antigen stimulation induces marked apoptosis of T lymphocytes in human immunodeficiency virus-infected individuals. *J Exp Med* 181:2029-36.
175. Streeck H, Brumme ZL, Anastario M, Cohen KW, Jolin JS, Meier A, Brumme CJ, Rosenberg ES, Alter G, Allen TM, Walker BD, Altfeld M. 2008. Antigen load and viral sequence diversification determine the functional profile of HIV-1-specific CD8+ T cells. *PLoS Med* 5:e100.
176. Betts MR, Nason MC, West SM, De Rosa SC, Migueles SA, Abraham J, Lederman MM, Benito JM, Goepfert PA, Connors M, Roederer M, Koup RA. 2006. HIV nonprogressors preferentially maintain highly functional HIV-specific CD8+ T cells. *Blood* 107:4781-9.
177. Catalfamo M, Karpova T, McNally J, Costes SV, Lockett SJ, Bos E, Peters PJ, Henkart PA. 2004. Human CD8+ T cells store RANTES in a unique secretory compartment and release it rapidly after TcR stimulation. *Immunity* 20:219-30.
178. Wagner L, Yang OO, Garcia-Zepeda EA, Ge Y, Kalams SA, Walker BD, Pasternack MS, Luster AD. 1998. Beta-chemokines are released from HIV-1-specific cytolytic T-cell granules complexed to proteoglycans. *Nature* 391:908-11.
179. Cocchi F, DeVico AL, Garzino-Demo A, Arya SK, Gallo RC, Lusso P. 1995. Identification of RANTES, MIP-1 alpha, and MIP-1 beta as the major HIV-suppressive factors produced by CD8+ T cells. *Science (New York, NY)* 270:1811-1815.
180. Coffey MJ, Woffendin C, Phare SM, Strieter RM, Markovitz DM. 1997. RANTES inhibits HIV-1 replication in human peripheral blood monocytes and alveolar macrophages. *Am J Physiol* 272:L1025-9.

181. Copeland KF. 2002. The role of CD8+ T cell soluble factors in human immunodeficiency virus infection. *Curr Med Chem* 9:1781-90.
182. Moriuchi H, Moriuchi M, Combadiere C, Murphy PM, Fauci AS. 1996. CD8+ T-cell-derived soluble factor(s), but not beta-chemokines RANTES, MIP-1 alpha, and MIP-1 beta, suppress HIV-1 replication in monocyte/macrophages. *Proc Natl Acad Sci U S A* 93:15341-5.
183. Trkola A, Gordon C, Matthews J, Maxwell E, Ketas T, Czaplewski L, Proudfoot AE, Moore JP. 1999. The CC-chemokine RANTES increases the attachment of human immunodeficiency virus type 1 to target cells via glycosaminoglycans and also activates a signal transduction pathway that enhances viral infectivity. *J Virol* 73:6370-9.
184. Mackewicz CE, Barker E, Greco G, Reyes-Teran G, Levy JA. 1997. Do beta-chemokines have clinical relevance in HIV infection? *J Clin Invest* 100:921-30.
185. Walker CM, Moody DJ, Stites DP, Levy JA. 1986. CD8+ lymphocytes can control HIV infection in vitro by suppressing virus replication. *Science* 234:1563-6.
186. Mackewicz CE, Ortega H, Levy JA. 1994. Effect of cytokines on HIV replication in CD4+ lymphocytes: lack of identity with the CD8+ cell antiviral factor. *Cell Immunol* 153:329-43.
187. Copeland KF, Leith JG, McKay PJ, Rosenthal KL. 1997. CD8+ T cell supernatants of HIV type 1-infected individuals have opposite effects on long terminal repeat-mediated transcription in T cells and monocytes. *AIDS Res Hum Retroviruses* 13:71-7.
188. Vella C, Daniels RS. 2003. CD8+ T-cell-mediated non-cytolytic suppression of human immunodeficiency viruses. *Curr Drug Targets Infect Disord* 3:97-113.
189. Mackewicz CE, Patterson BK, Lee SA, Levy JA. 2000. CD8(+) cell noncytotoxic anti-human immunodeficiency virus response inhibits expression of viral RNA but not reverse transcription or provirus integration. *J Gen Virol* 81:1261-4.
190. Chang TL-Y, François F, Mosoian A, Klotman ME. 2003. CAF-Mediated Human Immunodeficiency Virus (HIV) Type 1 Transcriptional Inhibition Is Distinct from α -Defensin-1 HIV Inhibition. *Journal of Virology* 77:6777-6784.
191. Le Borgne S, Fevrier M, Callebaut C, Lee SP, Riviere Y. 2000. CD8(+)-Cell antiviral factor activity is not restricted to human immunodeficiency virus (HIV)-specific T cells and can block HIV replication after initiation of reverse transcription. *J Virol* 74:4456-64.
192. Epperson DE, Arnold D, Spies T, Cresswell P, Poher JS, Johnson DR. 1992. Cytokines increase transporter in antigen processing-1 expression more rapidly than HLA class I expression in endothelial cells. *J Immunol* 149:3297-301.
193. Cramer LA, Nelson SL, Klemsz MJ. 2000. Synergistic induction of the Tap-1 gene by IFN-gamma and lipopolysaccharide in macrophages is regulated by STAT1. *J Immunol* 165:3190-7.
194. Wallach D, Fellous M, Revel M. 1982. Preferential effect of gamma interferon on the synthesis of HLA antigens and their mRNAs in human cells. *Nature* 299:833-6.
195. Johnson DR, Poher JS. 1990. Tumor necrosis factor and immune interferon synergistically increase transcription of HLA class I heavy- and light-chain genes in vascular endothelium. *Proc Natl Acad Sci U S A* 87:5183-7.
196. Groettrup M, Soza A, Eggers M, Kuehn L, Dick TP, Schild H, Rammensee HG, Koszinowski UH, Kloetzel PM. 1996. A role for the proteasome regulator PA28alpha in antigen presentation. *Nature* 381:166-8.

197. Xu X, Fu XY, Plate J, Chong AS. 1998. IFN-gamma induces cell growth inhibition by Fas-mediated apoptosis: requirement of STAT1 protein for up-regulation of Fas and FasL expression. *Cancer Res* 58:2832-7.
198. Tsujimoto M, Yip YK, Vilcek J. 1986. Interferon-gamma enhances expression of cellular receptors for tumor necrosis factor. *J Immunol* 136:2441-4.
199. Ruggiero V, Tavernier J, Fiers W, Baglioni C. 1986. Induction of the synthesis of tumor necrosis factor receptors by interferon-gamma. *J Immunol* 136:2445-50.
200. Biswas P, Poli G, Kinter AL, Justement JS, Stanley SK, Maury WJ, Bressler P, Orenstein JM, Fauci AS. 1992. Interferon gamma induces the expression of human immunodeficiency virus in persistently infected promonocytic cells (U1) and redirects the production of virions to intracytoplasmic vacuoles in phorbol myristate acetate-differentiated U1 cells. *J Exp Med* 176:739-50.
201. Kull FC, Jr. 1988. The TNF receptor in TNF-mediated cytotoxicity. *Nat Immun Cell Growth Regul* 7:254-65.
202. Lazdins JK, Grell M, Walker MR, Woods-Cook K, Scheurich P, Pfizenmaier K. 1997. Membrane tumor necrosis factor (TNF) induced cooperative signaling of TNFR60 and TNFR80 favors induction of cell death rather than virus production in HIV-infected T cells. *J Exp Med* 185:81-90.
203. Kumar A, Abbas W, Herbein G. 2013. TNF and TNF receptor superfamily members in HIV infection: new cellular targets for therapy? *Mediators Inflamm* 2013:484378.
204. DiDonato JA, Hayakawa M, Rothwarf DM, Zandi E, Karin M. 1997. A cytokine-responsive I κ B kinase that activates the transcription factor NF- κ B. *Nature* 388:548-54.
205. Hsu H, Shu HB, Pan MG, Goeddel DV. 1996. TRADD-TRAF2 and TRADD-FADD interactions define two distinct TNF receptor 1 signal transduction pathways. *Cell* 84:299-308.
206. Di Marzio P, Tse J, Landau NR. 1998. Chemokine receptor regulation and HIV type 1 tropism in monocyte-macrophages. *AIDS Res Hum Retroviruses* 14:129-38.
207. Simmons G, Clapham PR, Picard L, Offord RE, Rosenkilde MM, Schwartz TW, Buser R, Wells TN, Proudfoot AE. 1997. Potent inhibition of HIV-1 infectivity in macrophages and lymphocytes by a novel CCR5 antagonist. *Science* 276:276-9.
208. McManus CM, Brosnan CF, Berman JW. 1998. Cytokine induction of MIP-1 alpha and MIP-1 beta in human fetal microglia. *J Immunol* 160:1449-55.
209. Duh EJ, Maury WJ, Folks TM, Fauci AS, Rabson AB. 1989. Tumor necrosis factor alpha activates human immunodeficiency virus type 1 through induction of nuclear factor binding to the NF- κ B sites in the long terminal repeat. *Proc Natl Acad Sci U S A* 86:5974-8.
210. Osborn L, Kunkel S, Nabel GJ. 1989. Tumor necrosis factor alpha and interleukin 1 stimulate the human immunodeficiency virus enhancer by activation of the nuclear factor kappa B. *Proc Natl Acad Sci U S A* 86:2336-40.
211. Griffin GE, Leung K, Folks TM, Kunkel S, Nabel GJ. 1989. Activation of HIV gene expression during monocyte differentiation by induction of NF- κ B. *Nature* 339:70-3.
212. Elemans M, Basatena N-KSa, Klatt NR, Gkekas C, Silvestri G, Asquith B. 2011. Why Don't CD8+ T Cells Reduce the Lifespan of SIV-Infected Cells In Vivo? *PLoS Computational Biology* 7:e1002200.

213. Wick WD, Yang OO. 2012. Biologically-directed modeling reflects cytolytic clearance of SIV-infected cells in vivo in macaques. *PLoS One* 7:e44778.
214. Chun T-W, Carruth LM, Finzi D, Shen X, DiGiuseppe JA, Taylor H, Hermankova M, Chadwick K, Margolick J, Quinn TC, Kuo Y-H, Brookmeyer R, Zeiger MA, Barditch-Crovo P, Siliciano RF. 1997. Quantification of latent tissue reservoirs and total body VL in HIV-1 infection. *Nature* 387:183-188.
215. Cuevas JM, Geller R, Garijo R, Lopez-Aldeguer J, Sanjuan R. 2015. Extremely High Mutation Rate of HIV-1 In Vivo. *PLoS Biol* 13:e1002251.
216. Jung A, Maier R, Vartanian JP, Bocharov G, Jung V, Fischer U, Meese E, Wain-Hobson S, Meyerhans A. 2002. Recombination: Multiply infected spleen cells in HIV patients. *Nature* 418:144.
217. Eigen M. 1996. On the nature of virus quasispecies. *Trends Microbiol* 4:216-8.
218. Mansky LM. 1998. Retrovirus mutation rates and their role in genetic variation. *J Gen Virol* 79 (Pt 6):1337-45.
219. Roberts JD, Bebenek K, Kunkel TA. 1988. The accuracy of reverse transcriptase from HIV-1. *Science* 242:1171-3.
220. Preston BD, Poiesz BJ, Loeb LA. 1988. Fidelity of HIV-1 reverse transcriptase. *Science* 242:1168-71.
221. O'Neil PK, Sun G, Yu H, Ron Y, Dougherty JP, Preston BD. 2002. Mutational analysis of HIV-1 long terminal repeats to explore the relative contribution of reverse transcriptase and RNA polymerase II to viral mutagenesis. *J Biol Chem* 277:38053-61.
222. Chiu YL, Greene WC. 2008. The APOBEC3 cytidine deaminases: an innate defensive network opposing exogenous retroviruses and endogenous retroelements. *Annu Rev Immunol* 26:317-53.
223. Harris RS, Liddament MT. 2004. Retroviral restriction by APOBEC proteins. *Nat Rev Immunol* 4:868-77.
224. Mangeat B, Turelli P, Caron G, Friedli M, Perrin L, Trono D. 2003. Broad antiretroviral defence by human APOBEC3G through lethal editing of nascent reverse transcripts. *Nature* 424:99-103.
225. Weil AF, Ghosh D, Zhou Y, Seiple L, McMahon MA, Spivak AM, Siliciano RF, Stivers JT. 2013. Uracil DNA glycosylase initiates degradation of HIV-1 cDNA containing misincorporated dUTP and prevents viral integration. *Proceedings of the National Academy of Sciences* 110:E448-E457.
226. Conticello SG, Harris RS, Neuberger MS. 2003. The Vif protein of HIV triggers degradation of the human antiretroviral DNA deaminase APOBEC3G. *Curr Biol* 13:2009-13.
227. Ramirez BC, Simon-Loriere E, Galetto R, Negroni M. 2008. Implications of recombination for HIV diversity. *Virus Res* 134:64-73.
228. Zhang J, Tang LY, Li T, Ma Y, Sapp CM. 2000. Most retroviral recombinations occur during minus-strand DNA synthesis. *J Virol* 74:2313-22.
229. Hu WS, Temin HM. 1990. Retroviral recombination and reverse transcription. *Science* 250:1227-33.
230. Zhuang J, Jetzt AE, Sun G, Yu H, Klarmann G, Ron Y, Preston BD, Dougherty JP. 2002. Human immunodeficiency virus type 1 recombination: rate, fidelity, and putative hot spots. *J Virol* 76:11273-82.

231. Charpentier C, Nora T, Tenaillon O, Clavel F, Hance AJ. 2006. Extensive recombination among human immunodeficiency virus type 1 quasispecies makes an important contribution to viral diversity in individual patients. *J Virol* 80:2472-82.
232. Nora T, Charpentier C, Tenaillon O, Hoede C, Clavel F, Hance AJ. 2007. Contribution of recombination to the evolution of human immunodeficiency viruses expressing resistance to antiretroviral treatment. *J Virol* 81:7620-8.
233. Bretscher MT, Althaus CL, Muller V, Bonhoeffer S. 2004. Recombination in HIV and the evolution of drug resistance: for better or for worse? *Bioessays* 26:180-8.
234. Althaus CL, Bonhoeffer S. 2005. Stochastic interplay between mutation and recombination during the acquisition of drug resistance mutations in human immunodeficiency virus type 1. *J Virol* 79:13572-8.
235. Dorr P, Westby M, Dobbs S, Griffin P, Irvine B, Macartney M, Mori J, Rickett G, Smith-Burchnell C, Napier C, Webster R, Armour D, Price D, Stammen B, Wood A, Perros M. 2005. Maraviroc (UK-427,857), a potent, orally bioavailable, and selective small-molecule inhibitor of chemokine receptor CCR5 with broad-spectrum anti-human immunodeficiency virus type 1 activity. *Antimicrob Agents Chemother* 49:4721-32.
236. Dragic T, Trkola A, Thompson DA, Cormier EG, Kajumo FA, Maxwell E, Lin SW, Ying W, Smith SO, Sakmar TP, Moore JP. 2000. A binding pocket for a small molecule inhibitor of HIV-1 entry within the transmembrane helices of CCR5. *Proc Natl Acad Sci U S A* 97:5639-44.
237. Moore JP, Kuritzkes DR. 2009. A piece de resistance: how HIV-1 escapes small molecule CCR5 inhibitors. *Curr Opin HIV AIDS* 4:118-24.
238. Berro R, Klasse PJ, Jakobsen MR, Gorry PR, Moore JP, Sanders RW. 2012. V3 determinants of HIV-1 escape from the CCR5 inhibitors Maraviroc and Vicriviroc. *Virology* 427:158-65.
239. Yuan Y, Maeda Y, Terasawa H, Monde K, Harada S, Yusa K. 2011. A combination of polymorphic mutations in V3 loop of HIV-1 gp120 can confer noncompetitive resistance to maraviroc. *Virology* 413:293-9.
240. Kilby JM, Hopkins S, Venetta TM, DiMassimo B, Cloud GA, Lee JY, Alldredge L, Hunter E, Lambert D, Bolognesi D, Matthews T, Johnson MR, Nowak MA, Shaw GM, Saag MS. 1998. Potent suppression of HIV-1 replication in humans by T-20, a peptide inhibitor of gp41-mediated virus entry. *Nat Med* 4:1302-7.
241. Matthews T, Salgo M, Greenberg M, Chung J, DeMasi R, Bolognesi D. 2004. Enfuvirtide: the first therapy to inhibit the entry of HIV-1 into host CD4 lymphocytes. *Nat Rev Drug Discov* 3:215-25.
242. Rimsky LT, Shugars DC, Matthews TJ. 1998. Determinants of human immunodeficiency virus type 1 resistance to gp41-derived inhibitory peptides. *J Virol* 72:986-93.
243. Nameki D, Kodama E, Ikeuchi M, Mabuchi N, Otaka A, Tamamura H, Ohno M, Fujii N, Matsuoka M. 2005. Mutations conferring resistance to human immunodeficiency virus type 1 fusion inhibitors are restricted by gp41 and Rev-responsive element functions. *J Virol* 79:764-70.
244. Menzo S, Castagna A, Monchetti A, Hasson H, Danise A, Carini E, Bagnarelli P, Lazzarin A, Clementi M. 2004. Genotype and phenotype patterns of human immunodeficiency virus type 1 resistance to enfuvirtide during long-term treatment. *Antimicrob Agents Chemother* 48:3253-9.

245. Mink M, Mosier SM, Janumpalli S, Davison D, Jin L, Melby T, Sista P, Erickson J, Lambert D, Stanfield-Oakley SA, Salgo M, Cammack N, Matthews T, Greenberg ML. 2005. Impact of human immunodeficiency virus type 1 gp41 amino acid substitutions selected during enfuvirtide treatment on gp41 binding and antiviral potency of enfuvirtide in vitro. *J Virol* 79:12447-54.
246. Mehellou Y, De Clercq E. 2010. Twenty-six years of anti-HIV drug discovery: where do we stand and where do we go? *J Med Chem* 53:521-38.
247. Meyer PR, Matsuura SE, So AG, Scott WA. 1998. Unblocking of chain-terminated primer by HIV-1 reverse transcriptase through a nucleotide-dependent mechanism. *Proc Natl Acad Sci U S A* 95:13471-6.
248. Huang H, Chopra R, Verdine GL, Harrison SC. 1998. Structure of a covalently trapped catalytic complex of HIV-1 reverse transcriptase: implications for drug resistance. *Science* 282:1669-75.
249. Iyidogan P, Anderson KS. 2014. Current Perspectives on HIV-1 Antiretroviral Drug Resistance. *Viruses* 6:4095-4139.
250. Deval J, White KL, Miller MD, Parkin NT, Courcambek J, Halfon P, Selmi B, Boretto J, Canard B. 2004. Mechanistic basis for reduced viral and enzymatic fitness of HIV-1 reverse transcriptase containing both K65R and M184V mutations. *J Biol Chem* 279:509-16.
251. Feng JY, Myrick FT, Margot NA, Mulamba GB, Rimsky L, Borroto-Esoda K, Selmi B, Canard B. 2006. Virologic and enzymatic studies revealing the mechanism of K65R- and Q151M-associated HIV-1 drug resistance towards emtricitabine and lamivudine. *Nucleosides Nucleotides Nucleic Acids* 25:89-107.
252. Menendez-Arias L. 2008. Mechanisms of resistance to nucleoside analogue inhibitors of HIV-1 reverse transcriptase. *Virus Res* 134:124-46.
253. Marcelin AG, Delaugerre C, Wirden M, Viegas P, Simon A, Katlama C, Calvez V. 2004. Thymidine analogue reverse transcriptase inhibitors resistance mutations profiles and association to other nucleoside reverse transcriptase inhibitors resistance mutations observed in the context of virological failure. *J Med Virol* 72:162-5.
254. Wensing AM, Calvez V, Gunthard HF, Johnson VA, Paredes R, Pillay D, Shafer RW, Richman DD. 2017. 2017 Update of the Drug Resistance Mutations in HIV-1. *Top Antivir Med* 24:132-133.
255. Das K, Arnold E. 2013. HIV-1 reverse transcriptase and antiviral drug resistance. Part 1. *Curr Opin Virol* 3:111-8.
256. Sarafianos SG, Marchand B, Das K, Himmel DM, Parniak MA, Hughes SH, Arnold E. 2009. Structure and function of HIV-1 reverse transcriptase: molecular mechanisms of polymerization and inhibition. *J Mol Biol* 385:693-713.
257. Xia Q, Radzio J, Anderson KS, Sluis-Cremer N. 2007. Probing nonnucleoside inhibitor-induced active-site distortion in HIV-1 reverse transcriptase by transient kinetic analyses. *Protein Sci* 16:1728-37.
258. Rittinger K, Divita G, Goody RS. 1995. Human immunodeficiency virus reverse transcriptase substrate-induced conformational changes and the mechanism of inhibition by nonnucleoside inhibitors. *Proc Natl Acad Sci U S A* 92:8046-9.
259. Spence RA, Kati WM, Anderson KS, Johnson KA. 1995. Mechanism of inhibition of HIV-1 reverse transcriptase by nonnucleoside inhibitors. *Science* 267:988-93.

260. Martins S, Ramos MJ, Fernandes PA. 2008. The current status of the NNRTI family of antiretrovirals used in the HAART regime against HIV infection. *Curr Med Chem* 15:1083-95.
261. World Health Organization. 2010. WHO Guidelines Approved by the Guidelines Review Committee, Antiretroviral Drugs for Treating Pregnant Women and Preventing HIV Infection in Infants: Recommendations for a Public Health Approach: 2010 Version. World Health Organization
Copyright (c) World Health Organization 2010., Geneva.
262. World Health Organization. 2006. Antiretroviral Drugs for Treating Pregnant Women and Preventing HIV Infection in Infants: Towards Universal Access: Recommendations for a public health approach - 2006 version.
263. Tambuyzer L, Azijn H, Rimsky LT, Vingerhoets J, Lecocq P, Kraus G, Picchio G, de Bethune MP. 2009. Compilation and prevalence of mutations associated with resistance to non-nucleoside reverse transcriptase inhibitors. *Antivir Ther* 14:103-9.
264. Das K, Bauman JD, Clark AD, Jr., Frenkel YV, Lewi PJ, Shatkin AJ, Hughes SH, Arnold E. 2008. High-resolution structures of HIV-1 reverse transcriptase/TMC278 complexes: strategic flexibility explains potency against resistance mutations. *Proc Natl Acad Sci U S A* 105:1466-71.
265. Vingerhoets J, Azijn H, Fransen E, De Baere I, Smeulders L, Jochmans D, Andries K, Pauwels R, de Bethune MP. 2005. TMC125 displays a high genetic barrier to the development of resistance: evidence from in vitro selection experiments. *J Virol* 79:12773-82.
266. Ludovici DW, De Corte BL, Kukla MJ, Ye H, Ho CY, Lichtenstein MA, Kavash RW, Andries K, de Bethune MP, Azijn H, Pauwels R, Lewi PJ, Heeres J, Koymans LM, de Jonge MR, Van Aken KJ, Daeyaert FF, Das K, Arnold E, Janssen PA. 2001. Evolution of anti-HIV drug candidates. Part 3: Diarylpyrimidine (DAPY) analogues. *Bioorg Med Chem Lett* 11:2235-9.
267. Vingerhoets J, Tambuyzer L, Azijn H, Hoogstoel A, Nijs S, Peeters M, de Bethune MP, De Smedt G, Woodfall B, Picchio G. 2010. Resistance profile of etravirine: combined analysis of baseline genotypic and phenotypic data from the randomized, controlled Phase III clinical studies. *Aids* 24:503-14.
268. Towner WJ, Casseti I, Domingo P, Nijs S, Kakuda TN, Vingerhoets J, Woodfall B. 2010. Etravirine: clinical review of a treatment option for HIV type-1-infected patients with non-nucleoside reverse transcriptase inhibitor resistance. *Antivir Ther* 15:803-16.
269. Xu HT, Colby-Germinario SP, Asahchop EL, Oliveira M, McCallum M, Schader SM, Han Y, Quan Y, Sarafianos SG, Wainberg MA. 2013. Effect of mutations at position E138 in HIV-1 reverse transcriptase and their interactions with the M184I mutation on defining patterns of resistance to nonnucleoside reverse transcriptase inhibitors rilpivirine and etravirine. *Antimicrob Agents Chemother* 57:3100-9.
270. Sharma M, Saravolatz LD. 2013. Rilpivirine: a new non-nucleoside reverse transcriptase inhibitor. *J Antimicrob Chemother* 68:250-6.
271. Craigie R. 2012. The molecular biology of HIV integrase. *Future Virol* 7:679-686.
272. Hazuda D, Iwamoto M, Wenning L. 2009. Emerging pharmacology: inhibitors of human immunodeficiency virus integration. *Annu Rev Pharmacol Toxicol* 49:377-94.
273. Shah BM, Schafer JJ, Desimone JA, Jr. 2014. Dolutegravir: a new integrase strand transfer inhibitor for the treatment of HIV. *Pharmacotherapy* 34:506-20.

274. Hicks C, Gulick RM. 2009. Raltegravir: the first HIV type 1 integrase inhibitor. *Clin Infect Dis* 48:931-9.
275. Hurt CB, Sebastian J, Hicks CB, Eron JJ. 2014. Resistance to HIV integrase strand transfer inhibitors among clinical specimens in the United States, 2009-2012. *Clin Infect Dis* 58:423-31.
276. Cooper DA, Steigbigel RT, Gatell JM, Rockstroh JK, Katlama C, Yeni P, Lazzarin A, Clotet B, Kumar PN, Eron JE, Schechter M, Markowitz M, Loutfy MR, Lennox JL, Zhao J, Chen J, Ryan DM, Rhodes RR, Killar JA, Gilde LR, Strohmaier KM, Meibohm AR, Miller MD, Hazuda DJ, Nessly ML, DiNubile MJ, Isaacs RD, Tepler H, Nguyen BY. 2008. Subgroup and resistance analyses of raltegravir for resistant HIV-1 infection. *N Engl J Med* 359:355-65.
277. Goethals O, Clayton R, Van Ginderen M, Vereycken I, Wagemans E, Geluykens P, Dockx K, Strijbos R, Smits V, Vos A, Meersseman G, Jochmans D, Vermeire K, Schols D, Hallenberger S, Hertogs K. 2008. Resistance mutations in human immunodeficiency virus type 1 integrase selected with elvitegravir confer reduced susceptibility to a wide range of integrase inhibitors. *J Virol* 82:10366-74.
278. Shimura K, Kodama E, Sakagami Y, Matsuzaki Y, Watanabe W, Yamataka K, Watanabe Y, Ohata Y, Doi S, Sato M, Kano M, Ikeda S, Matsuoka M. 2008. Broad antiretroviral activity and resistance profile of the novel human immunodeficiency virus integrase inhibitor elvitegravir (JTK-303/GS-9137). *J Virol* 82:764-74.
279. Kobayashi M, Yoshinaga T, Seki T, Wakasa-Morimoto C, Brown KW, Ferris R, Foster SA, Hazen RJ, Miki S, Suyama-Kagitani A, Kawauchi-Miki S, Taishi T, Kawasuji T, Johns BA, Underwood MR, Garvey EP, Sato A, Fujiwara T. 2011. In Vitro antiretroviral properties of S/GSK1349572, a next-generation HIV integrase inhibitor. *Antimicrob Agents Chemother* 55:813-21.
280. Hightower KE, Wang R, Deanda F, Johns BA, Weaver K, Shen Y, Tomberlin GH, Carter HL, 3rd, Broderick T, Sigethy S, Seki T, Kobayashi M, Underwood MR. 2011. Dolutegravir (S/GSK1349572) exhibits significantly slower dissociation than raltegravir and elvitegravir from wild-type and integrase inhibitor-resistant HIV-1 integrase-DNA complexes. *Antimicrob Agents Chemother* 55:4552-9.
281. Quashie PK, Mesplede T, Han YS, Oliveira M, Singhroy DN, Fujiwara T, Underwood MR, Wainberg MA. 2012. Characterization of the R263K mutation in HIV-1 integrase that confers low-level resistance to the second-generation integrase strand transfer inhibitor dolutegravir. *J Virol* 86:2696-705.
282. Quashie PK, Mesplede T, Han YS, Veres T, Osman N, Hassounah S, Sloan RD, Xu HT, Wainberg MA. 2013. Biochemical analysis of the role of G118R-linked dolutegravir drug resistance substitutions in HIV-1 integrase. *Antimicrob Agents Chemother* 57:6223-35.
283. Llibre JM, Pulido F, Garcia F, Garcia Deltoro M, Blanco JL, Delgado R. 2015. Genetic barrier to resistance for dolutegravir. *AIDS Rev* 17:56-64.
284. Louis JM, Ishima R, Torchia DA, Weber IT. 2007. HIV-1 protease: structure, dynamics, and inhibition. *Adv Pharmacol* 55:261-98.
285. Huff JR, Kahn J. 2001. Discovery and clinical development of HIV-1 protease inhibitors. *Adv Protein Chem* 56:213-51.
286. Kempf DJ, Marsh KC, Kumar G, Rodrigues AD, Denissen JF, McDonald E, Kukulka MJ, Hsu A, Granneman GR, Baroldi PA, Sun E, Pizzuti D, Plattner JJ, Norbeck DW, Leonard JM. 1997. Pharmacokinetic enhancement of inhibitors of the human

- immunodeficiency virus protease by coadministration with ritonavir. *Antimicrob Agents Chemother* 41:654-60.
287. Mahalingam B, Louis JM, Reed CC, Adomat JM, Krouse J, Wang YF, Harrison RW, Weber IT. 1999. Structural and kinetic analysis of drug resistant mutants of HIV-1 protease. *Eur J Biochem* 263:238-45.
 288. Gulnik SV, Suvorov LI, Liu B, Yu B, Anderson B, Mitsuya H, Erickson JW. 1995. Kinetic characterization and cross-resistance patterns of HIV-1 protease mutants selected under drug pressure. *Biochemistry* 34:9282-7.
 289. Markowitz M, Conant M, Hurley A, Schluger R, Duran M, Peterkin J, Chapman S, Patick A, Hendricks A, Yuen GJ, Hoskins W, Clendeninn N, Ho DD. 1998. A preliminary evaluation of nelfinavir mesylate, an inhibitor of human immunodeficiency virus (HIV)-1 protease, to treat HIV infection. *J Infect Dis* 177:1533-40.
 290. Rhee SY, Taylor J, Fessel WJ, Kaufman D, Towner W, Troia P, Ruane P, Hellinger J, Shirvani V, Zolopa A, Shafer RW. 2010. HIV-1 protease mutations and protease inhibitor cross-resistance. *Antimicrob Agents Chemother* 54:4253-61.
 291. López M, Soriano V, Benito JM. 2007. Escape mutations in HIV infection and its impact on CD8+ T cell responses. *Current Molecular Medicine* 7:446-458.
 292. Collins KL, Chen BK, Kalams SA, Walker BD, Baltimore D. 1998. HIV-1 Nef protein protects infected primary cells against killing by cytotoxic T lymphocytes. *Nature* 391:397-401.
 293. Walker BD, Burton DR. 2008. Toward an AIDS Vaccine. *Science* 320:760-764.
 294. Wodarz D, Klenerman P, Nowak MA. 1998. Dynamics of cytotoxic T-lymphocyte exhaustion. *Proceedings Biological Sciences* 265:191-203.
 295. Yang OO, Lin H, Dagarag M, Ng HL, Effros RB, Uittenbogaart CH. 2005. Decreased perforin and granzyme B expression in senescent HIV-1-specific cytotoxic T lymphocytes. *Virology* 332:16-19.
 296. Yagita Y, Kuse N, Kuroki K, Gatanaga H, Carlson JM, Chikata T, Brumme ZL, Murakoshi H, Akahoshi T, Pfeifer N, Mallal S, John M, Ose T, Matsubara H, Kanda R, Fukunaga Y, Honda K, Kawashima Y, Ariumi Y, Oka S, Maenaka K, Takiguchi M. 2013. Distinct HIV-1 escape patterns selected by cytotoxic T cells with identical epitope specificity. *J Virol* 87:2253-63.
 297. Akahoshi T, Chikata T, Tamura Y, Gatanaga H, Oka S, Takiguchi M. 2012. Selection and accumulation of an HIV-1 escape mutant by three types of HIV-1-specific cytotoxic T lymphocytes recognizing wild-type and/or escape mutant epitopes. *J Virol* 86:1971-81.
 298. Policicchio BB, Xu C, Brocca-Cofano E, Raetz KD, He T, Ma D, Li H, Sivanandham R, Haret-Richter GS, Dunsmore T, Trichel A, Mellors JW, Hahn BH, Shaw GM, Ribeiro RM, Pandrea I, Apetrei C. 2016. Multi-dose Romidepsin Reactivates Replication Competent SIV in Post-antiretroviral Rhesus Macaque Controllers. *PLoS pathogens* 12:e1005879.
 299. Lifson JD, Rossio JL, Piatak M, Parks T, Li L, Kiser R, Coalter V, Fisher B, Flynn BM, Czajak S, Hirsch VM, Reimann KA, Schmitz JE, Ghayeb J, Bischofberger N, Nowak MA, Desrosiers RC, Wodarz D. 2001. Role of CD8+ Lymphocytes in Control of Simian Immunodeficiency Virus Infection and Resistance to Rechallenge after Transient Early Antiretroviral Treatment. *Journal of Virology* 75:10187-10199.
 300. Catalfano M, Henkart PA. 2003. Perforin and the granule exocytosis cytotoxicity pathway. *Current Opinion in Immunology* 15:522-527.

301. Nagata S, Suda T. 1995. Fas and Fas ligand: lpr and gld mutations. *Immunology Today* 16:39-43.
302. Levy JA. 2003. The search for the CD8+ cell anti-HIV factor (CAF). *Trends in Immunology* 24:628-632.
303. Spits HB, Mudrikova T, Schellens IM, Wensing AM, Prins JM, Feuth T, Spierings E, Nijhuis M, van Baarle D, Borghans JA. 2016. The presence of protective cytotoxic T lymphocytes does not correlate with shorter lifespans of productively infected cells in HIV-1 infection. *Aids* 30:9-17.
304. Seich al Basatena N-K, Chatzimichalis K, Graw F, Frost SDW, Regoes RR, Asquith B. 2013. Can Non-lytic CD8+ T Cells Drive HIV-1 Escape? *PLoS Pathogens* 9.
305. National Research Council. Guide for the care and use of laboratory animals, 8th edition.
306. Pandrea I, Apetrei C, Dufour J, Dillon N, Barbercheck J, Metzger M, Jacquelin B, Bohm R, Marx PA, Barre-Sinoussi F, Hirsch VM, Müller-Trutwin MC, Lackner AA, Veazey RS. 2006. Simian immunodeficiency virus SIV_{agm.sab} infection of caribbean African green monkeys: a new model for the study of SIV pathogenesis in natural hosts. *Journal of Virology* 80:4858-4867.
307. Mandy FF, Nicholson JKA, McDougal JS, Cdc. 2003. Guidelines for performing single-platform absolute CD4+ T-cell determinations with CD45 gating for persons infected with human immunodeficiency virus. Centers for Disease Control and Prevention. *MMWR Recommendations and reports: Morbidity and mortality weekly report Recommendations and reports / Centers for Disease Control* 52:1-13.
308. Cardozo EF, Andrade A, Mellors JW, Kuritzkes DR, Perelson AS, Ribeiro RM. 2017. Treatment with integrase inhibitor suggests a new interpretation of HIV RNA decay curves that reveals a subset of cells with slow integration. *PLoS Pathog* 13:e1006478.
309. Perelson AS, Ribeiro RM. 2013. Modeling the within-host dynamics of HIV infection. *BMC Biol* 11:96.
310. Burnham K, Anderson D. 2004. *Model Selection and Multimodel Inference*. Springer, New York, New York.
311. Mackewicz CE, Blackbourn DJ, Levy JA. 1995. CD8+ T cells suppress human immunodeficiency virus replication by inhibiting viral transcription. *Proc Natl Acad Sci U S A* 92:2308-12.
312. Althaus CL, De Boer RJ. 2011. Implications of CTL-Mediated Killing of HIV-Infected Cells during the Non-Productive Stage of Infection. *PLoS ONE* 6:e16468.
313. Gadhamsetty S, Coorens T, de Boer RJ. 2016. Notwithstanding Circumstantial Alibis, Cytotoxic T Cells Can Be Major Killers of HIV-1-Infected Cells. *J Virol* 90:7066-83.
314. Andrade A, Guedj J, Rosenkranz SL, Lu D, Mellors J, Kuritzkes DR, Perelson AS, Ribeiro RM. 2015. Early HIV RNA decay during raltegravir-containing regimens exhibits two distinct subphases (1a and 1b). *AIDS (London, England)* 29:2419-2426.
315. Goulder PJR, Watkins DI. 2004. HIV and SIV CTL escape: implications for vaccine design. *Nature Reviews Immunology* 4:630-640.
316. Freel SA, Saunders KO, Tomaras GD. 2011. CD8(+)T-cell-mediated control of HIV-1 and SIV infection. *Immunol Res* 49:135-46.
317. Tsubota H, Lord CI, Watkins DI, Morimoto C, Letvin NL. 1989. A cytotoxic T lymphocyte inhibits acquired immunodeficiency syndrome virus replication in peripheral blood lymphocytes. *J Exp Med* 169:1421-34.

318. Walker CM, Levy JA. 1989. A diffusible lymphokine produced by CD8+ T lymphocytes suppresses HIV replication. *Immunology* 66:628-30.
319. Klenerman P, Phillips RE, Rinaldo CR, Wahl LM, Ogg G, May RM, McMichael AJ, Nowak MA. 1996. Cytotoxic T lymphocytes and viral turnover in HIV type 1 infection. *Proceedings of the National Academy of Sciences of the United States of America* 93:15323-15328.
320. Sacha JB, Chung C, Rakasz EG, Spencer SP, Jonas AK, Bean AT, Lee W, Burwitz BJ, Stephany JJ, Loffredo JT. 2007. Gag-specific CD8+ T lymphocytes recognize infected cells before AIDS-virus integration and viral protein expression. *The Journal of Immunology* 178:2746-2754.
321. Kloverpris HN, Payne RP, Sacha JB, Rasaiyaah JT, Chen F, Takiguchi M, Yang OO, Towers GJ, Goulder P, Prado JG. 2013. Early antigen presentation of protective HIV-1 KF11Gag and KK10Gag epitopes from incoming viral particles facilitates rapid recognition of infected cells by specific CD8+ T cells. *J Virol* 87:2628-38.
322. Perelson AS. 2002. Modelling viral and immune system dynamics. *Nature Reviews Immunology* 2:28-36.
323. Alter G, Malenfant JM, Delabre RM, Burgett NC, Yu XG, Lichterfeld M, Zaunders J, Altfeld M. 2004. Increased natural killer cell activity in viremic HIV-1 infection. *J Immunol* 173:5305-11.
324. Alter G, Altfeld M. 2009. NK cells in HIV-1 infection: evidence for their role in the control of HIV-1 infection. *J Intern Med* 265:29-42.
325. Kottlilil S, Shin K, Planta M, McLaughlin M, Hallahan CW, Ghany M, Chun TW, Sneller MC, Fauci AS. 2004. Expression of chemokine and inhibitory receptors on natural killer cells: effect of immune activation and HIV viremia. *J Infect Dis* 189:1193-8.
326. Mavilio D, Lombardo G, Benjamin J, Kim D, Follman D, Marcenaro E, O'Shea MA, Kinter A, Kovacs C, Moretta A, Fauci AS. 2005. Characterization of CD56-/CD16+ natural killer (NK) cells: a highly dysfunctional NK subset expanded in HIV-infected viremic individuals. *Proc Natl Acad Sci U S A* 102:2886-91.
327. Johnson S, Eller M, Teigler JE, Maloveste SM, Schultz BT, Soghoian DZ, Lu R, Oster AF, Chenine AL, Alter G, Dittmer U, Marovich M, Robb ML, Michael NL, Bolton D, Streeck H. 2015. Cooperativity of HIV-Specific Cytolytic CD4 T Cells and CD8 T Cells in Control of HIV Viremia. *J Virol* 89:7494-505.
328. Sacha JB, Giraldo-Vela JP, Buechler MB, Martins MA, Maness NJ, Chung C, Wallace LT, Leon EJ, Friedrich TC, Wilson NA, Hiraoka A, Watkins DI. 2009. Gag- and Nef-specific CD4+ T cells recognize and inhibit SIV replication in infected macrophages early after infection. *Proc Natl Acad Sci U S A* 106:9791-6.
329. Nemes E, Bertonecelli L, Lugli E, Pinti M, Nasi M, Manzini L, Manzini S, Prati F, Borghi V, Cossarizza A, Mussini C. 2010. Cytotoxic granule release dominates gag-specific CD4+ T-cell response in different phases of HIV infection. *Aids* 24:947-57.
330. Soghoian DZ, Streeck H. 2010. Cytolytic CD4(+) T cells in viral immunity. *Expert Rev Vaccines* 9:1453-63.
331. Muraro E, Merlo A, Martorelli D, Cangemi M, Dalla Santa S, Dolcetti R, Rosato A. 2017. Fighting Viral Infections and Virus-Driven Tumors with Cytotoxic CD4+ T Cells. *Front Immunol* 8:197.
332. Chun T-W, Davey RT, Ostrowski M, Shawn Justement J, Engel D, Mullins JI, Fauci AS. 2000. Relationship between pre-existing viral reservoirs and the re-emergence of plasma

- viremia after discontinuation of highly active anti-retroviral therapy. *Nature Medicine* 6:757-761.
333. Chun T-W, Davey RT, Engel D, Lane HC, Fauci AS. 1999. AIDS: Re-emergence of HIV after stopping therapy. *Nature* 401:874-875.
 334. Wong JK, Hezareh M, Günthard HF, Havlir DV, Ignacio CC, Spina CA, Richman DD. 1997. Recovery of Replication-Competent HIV Despite Prolonged Suppression of Plasma Viremia. *Science* 278:1291-1295.
 335. Middleton T, Lim HB, Montgomery D, Rockway T, Tang H, Cheng X, Lu L, Mo H, Kohlbrenner WE, Molla A, Kati WM. 2004. Inhibition of human immunodeficiency virus type I integrase by naphthamidines and 2-aminobenzimidazoles. *Antiviral Research* 64:35-45.
 336. Sharkey ME, Teo I, Greenough T, Sharova N, Luzuriaga K, Sullivan JL, Bucy RP, Kostrikis LG, Haase A, Veryard C, Davaro RE, Cheeseman SH, Daly JS, Bova C, Ellison RT, Mady B, Lai KK, Moyle G, Nelson M, Gazzard B, Shaunak S, Stevenson M. 2000. Persistence of episomal HIV-1 infection intermediates in patients on highly active anti-retroviral therapy. *Nature Medicine* 6:76-81.
 337. Pierson TC, Kieffer TL, Ruff CT, Buck C, Gange SJ, Siliciano RF. 2002. Intrinsic stability of episomal circles formed during human immunodeficiency virus type 1 replication. *J Virol* 76:4138-44.
 338. Gilmore JB, Kelleher AD, Cooper DA, Murray JM. 2013. Explaining the determinants of first phase HIV decay dynamics through the effects of stage-dependent drug action. *PLoS Comput Biol* 9:e1002971.
 339. Wang S, Hottz P, Schechter M, Rong L. 2015. Modeling the Slow CD4+ T Cell Decline in HIV-Infected Individuals. *PLoS Comput Biol* 11:e1004665.
 340. Svarovskaia ES, Cheslock SR, Zhang WH, Hu WS, Pathak VK. 2003. Retroviral mutation rates and reverse transcriptase fidelity. *Front Biosci* 8:d117-34.
 341. Pennings PS. 2013. HIV drug resistance: Problems and perspectives. *Infect Dis Rep* 5:e5.
 342. Sluis-Cremer N, Wainberg MA, Schinazi RF. 2015. Resistance to reverse transcriptase inhibitors used in the treatment and prevention of HIV-1 infection. *Future Microbiol* 10:1773-82.
 343. Pandrea I, Apetrei C, Dufour J, Dillon N, Barbercheck J, Metzger M, Jacquelin B, Bohm R, Marx PA, Barre-Sinoussi F, Hirsch VM, Muller-Trutwin MC, Lackner AA, Veazey RS. 2006. Simian immunodeficiency virus SIVagm.sab infection of Caribbean African green monkeys: a new model for the study of SIV pathogenesis in natural hosts. *J Virol* 80:4858-67.
 344. Policicchio BB, Pandrea I, Apetrei C. 2016. Animal models for HIV cure research. *Front Immunol* 7:12.
 345. Hassounah SA, Mesplede T, Quashie PK, Oliveira M, Sandstrom PA, Wainberg MA. 2014. Effect of HIV-1 integrase resistance mutations when introduced into SIVmac239 on susceptibility to integrase strand transfer inhibitors. *J Virol* 88:9683-92.
 346. Lloyd SB, Lichtfuss M, Amarasena TH, Alcantara S, De Rose R, Tachedjian G, Alinejad-Rokny H, Venturi V, Davenport MP, Winnall WR, Kent SJ. 2016. High fidelity simian immunodeficiency virus reverse transcriptase mutants have impaired replication in vitro and in vivo. *Virology* 492:1-10.
 347. Hassounah SA, Liu Y, Quashie PK, Oliveira M, Moisi D, Brenner BG, Sandstrom PA, Mesplede T, Wainberg MA. 2015. Characterization of the drug resistance profiles of

- integrase strand transfer inhibitors in simian immunodeficiency virus SIVmac239. *J Virol* 89:12002-13.
348. Hazuda DJ, Young SD, Guare JP, Anthony NJ, Gomez RP, Wai JS, Vacca JP, Handt L, Motzel SL, Klein HJ, Dornadula G, Danovich RM, Witmer MV, Wilson KA, Tussey L, Schleif WA, Gabryelski LS, Jin L, Miller MD, Casimiro DR, Emini EA, Shiver JW. 2004. Integrase inhibitors and cellular immunity suppress retroviral replication in rhesus macaques. *Science* 305:528-32.
349. Van Rompay KK, Johnson JA, Blackwood EJ, Singh RP, Lipscomb J, Matthews TB, Marthas ML, Pedersen NC, Bischofberger N, Heneine W, North TW. 2007. Sequential emergence and clinical implications of viral mutants with K70E and K65R mutation in reverse transcriptase during prolonged tenofovir monotherapy in rhesus macaques with chronic RT-SHIV infection. *Retrovirology* 4:25.
350. Van Rompay KK, Singh RP, Pahar B, Sodora DL, Wingfield C, Lawson JR, Marthas ML, Bischofberger N. 2004. CD8+-cell-mediated suppression of virulent simian immunodeficiency virus during tenofovir treatment. *J Virol* 78:5324-37.
351. National Research Council. 1996. Guide for the care and use of laboratory animals. National Academy Press, Washington, DC.
352. Mandy FF, Nicholson JK, McDougal JS, Centers for Disease Control. 2003. Guidelines for performing single-platform absolute CD4+ T-cell determinations with CD45 gating for persons infected with human immunodeficiency virus. Centers for Disease Control and Prevention. *MMWR Recomm Rep* 52:1-13.
353. Andreatta KN, Miller MD, White KL. 2016. Drug Susceptibility and Viral Fitness of HIV-1 with Integrase Strand Transfer Inhibitor Resistance Substitution Q148R or N155H in Combination with Nucleoside/Nucleotide Reverse Transcriptase Inhibitor Resistance Substitutions. *Antimicrob Agents Chemother* 60:757-65.
354. Collins SE, Grant PM, Shafer RW. 2016. Modifying antiretroviral therapy in virologically suppressed HIV-1-infected patients. *Drugs* 76:75-98.
355. Del Prete GQ, Smedley J, Macallister R, Jones GS, Li B, Hattersley J, Zheng J, Piatak M, Jr., Keele BF, Hesselgesser J, Geleziunas R, Lifson JD. 2016. Short Communication: Comparative evaluation of coformulated injectable combination antiretroviral therapy regimens in simian immunodeficiency virus-infected rhesus macaques. *AIDS Res Hum Retroviruses* 32:163-8.
356. Micci L, Alvarez X, Iriete RI, Ortiz AM, Ryan ES, McGary CS, Deleage C, McAtee BB, He T, Apetrei C, Easley K, Pahwa S, Collman RG, Derdeyn CA, Davenport MP, Estes JD, Silvestri G, Lackner AA, Paiardini M. 2014. CD4 Depletion in SIV-Infected Macaques Results in Macrophage and Microglia Infection with Rapid Turnover of Infected Cells. *PLoS Pathog* 10:e1004467.
357. Svarovskaia ES, Cheslock SR, Zhang W-H, Hu W-S, Pathak VK. 2003. Retroviral mutation rates and reverse transcriptase fidelity. *Frontiers in Bioscience: A Journal and Virtual Library* 8:d117-134.
358. Wang HB, Mo QH, Yang Z. 2015. HIV vaccine research: the challenge and the way forward. *J Immunol Res* 2015:503978.
359. Thorlund K, Horwitz MS, Fife BT, Lester R, Cameron DW. 2017. Landscape review of current HIV 'kick and kill' cure research - some kicking, not enough killing. *BMC Infect Dis* 17:595.